

Development and Characterization of Novel Mcl-1 Inhibitors for Treatment of Cancer

by

Ahmed Samir Ahmed Mady

A dissertation submitted in partial fulfillment
of the requirements for the degree of
Doctor of Philosophy
(Medicinal Chemistry)
in the University of Michigan
2016

Doctoral Committee:

Associate Professor Zaneta Nikolovska-Coleska, Chair
Research Professor Hollis D. Showalter
Professor Duxin Sun
Professor Shaomeng Wang

© Ahmed Samir Mady 2016

DEDICATION

All Praise is due to Allah (SWT), the most graceful, the most merciful.

I dedicate this thesis to my dear **Father; Samir Mady** and **Mother; Marwa Ahmed** for their limitless love, encouragement and being the reason for what I have become today. I also dedicate it to my life partner, soulmate and beloved **Wife; Asma Oral** for her continuous support and her patience throughout my PhD journey

ACKNOWLEDGEMENTS

The journey to this point in my life has been very exciting: from finishing my Bachelor's degree at Ain-Shams University in Egypt, to obtaining my Master's at Utrecht University in the Netherlands, and ending with my PhD at Michigan. I have gained a lot of knowledge throughout this journey, not only on the scientific level, but also on the personal level. This dissertation would not be possible without the help and support of many people.

First and foremost, I would like to express my ultimate gratitude to Dr. Zaneta Nikolovska-Coleska for being my mentor during my PhD journey. I have learned many lessons from her mentorship which will stay with me for the rest of my life. Sharing a not-so-different scientific track, having both trained as pharmacists, helped us develop very mind-stimulating discussions in the area of drug discovery. I learned from her how to be a successful scientist; to always think critically and to never miss the details. Her limitless support and advice to me, as a student and a future independent scientist, is much appreciated.

I would like to thank Dr. Hollis Showalter, Dr. Duxin Sun, and Dr. Shaomeng Wang for being my committee members during this journey. Their input and advice was of great importance in completing this thesis work. I would like to specially thank Dr. Shaomeng Wang and his lab members for providing instruments, reagents, and cell lines that were important to my thesis work. I also appreciate the help of Dr. Duxin Sun and his lab members in testing our compounds for liver microsomal stability and doing pharmacokinetics studies which were crucial to the progress of my research.

I would like to thank all my committee members for their patience and for spending time writing recommendation letters for me, especially Dr. Hollis Showalter.

I had the opportunity to work with very intelligent and helpful lab members. I would like to thank past lab members who trained me during my starting period in the lab. I specially thank Dr. Garrett Gibbons and Dr. Chenxi Chen for helping me in the beginning with several biochemical and biological techniques that I needed for the progress of my project. I would like to thank Dr. Julie Di Bernardo for her help in learning cell culture techniques and tricks for some difficult

model cell lines. I would like to thank Dr. Naval Bajwa, Dr. Chenzhong Liao and Dr. Fardokht Abulwerdi. Their work was very critical in chapter 2 of my thesis. I would like also to thank the current members for their help in polishing my thesis research and for our fruitful discussions about our different projects. I would like to specially thank Dr. Lei Miao for his significant contribution to my thesis, especially chapters 3 and with the synthesis of more than one hundred and fifty compounds. I would also like to thank Sierrah Grigsby for her help and the interesting discussions about our projects, as well as for talking about all our ups and downs during our research journey. I would like to thank Karson Kump and Katherine Lev for their hard work and contributions to the overall Mcl-1 project. Special thanks to our visiting scholar, Dr. Andrej Perdih, for his crucial molecular modeling efforts that were very critical for chapter 3 in my thesis and for his help in revising and polishing my manuscripts for publications.

I had the opportunity to collaborate with many bright researchers at the University of Michigan. Their help and discussions were very important in the progress of my research project. I would like to specially thank Dr. Malathi Kandarpa and Dr. Luke Peterson for their help in the multiple myeloma part of my studies by providing cell lines and performing the *in vivo* efficacy studies. I would like to thank Dr. Thomas Carey, Dr. Chad Brenner, and his lab members Susan Foltin and Nicole Michmerhuizen for collaborating in the Head and Neck cancer part of my studies.

I would like to acknowledge the Medicinal Chemistry department for giving me this fortunate opportunity to do my PhD. I specially thank Dr. Sylvie Garneau-Tsodikova for supporting my PhD application to the department and allowing me to do research in her lab before joining the program. I also would like to thank the current department chair, Dr. George Garcia, and the past chair Dr. Ronald Woodard for their continuous support and help to me and all other Medicinal Chemistry students. I have also spent three beautiful semesters teaching under the supervision of Dr. Mustapha Beleh, who was a model teacher and presenter. I would like to thank Dr. Garry Dotson for his help and guidance as an advisor for first year graduate students. I would like to thank all former and current Medicinal Chemistry graduate students for all the nice times and fruitful discussions. I especially thank my small Medicinal Chemistry class; Andrew Pratt, Aubrie Harland, Anthony Emanuele, and Frank Kwarcinski.

I would like to thank all my Ann Arbor friends, who are still here or who have left, for their help and support during moving to Ann Arbor and the nice times we spent together. I specially

thank Khaled Alashmouny for being the first to meet me in Ann Arbor and to help me settle during my first days. I would like to thank my friends Amjad Abu-Jbara, Ahmed Awadallah, Ahmed Al-Sabbagh, Ahmed Almuhtady, Amr Alaa, Samer Kadous, Mahmoud Elazzouny, Dr. Mohamed El-Sayed, and their families.

I am very thankful to have the opportunity to be a co-founder of Egypt Scholars Inc. with a handful of University of Michigan graduate students. Now we are registered as a non-profit organization in USA with more than 300 volunteers, all-over the world, and we have helped hundreds of thousands of people worldwide with our career counseling services, published books, and scientific research webinars and workshops.

I would like to thank my parents for their continuous support and endless love and care. Special thanks to my dear father Dr. Samir Mady, for encouraging me during my journey and being my role model for steadfastness and perseverance; my dear mother, Marwa Ahmed, for her encouraging words to me daily on the phone and making dua for me day and night. I am very thankful to have my dear brother, Muhammad Mady, with whom I shared my dreams and plans in life. Special thanks are extended to my beloved wife, Asma Oral, for her support during my journey and her patience with my PhD lifestyle; with the long working hours and late night experiments. I am very thankful to have her as my life partner and mother to our son, Ibrahim Mady, and our soon-to-come second son, Idris Mady. I am also thankful to have my in-laws in my life, as they are a very big help and support to me. I specially thank my mother-in-law, Hamidah Kaufman, for her care and love, as well as my late grandmother-in-law Joyce Seward for believing in me and encouraging me during my PhD journey. I am very thankful to having a big and caring family of in-laws including my father-in-law, Dr. Hamid Oral; my sisters-in-law, Halima Oral, Rabia Oral, Sabire Oral, and Munire Oral; and my brothers-in-law, Buraq Oral and Jason Kaufman.

Last but not least, I would like to thank Dr. Abdullah Mohammed at the Al-Jahra hospital in Kuwait, who was the first person to introduce the idea of drug discovery research to me in my first year of pharmacy school and ignited the spark that led me to take this interesting and exciting journey.

Finally, I thank Allah (may He be exalted) every day, for all the blessings and grace He is bestowing upon me and I hope that I spend this life journey in the way that pleases Him.

TABLE OF CONTENTS

DEDICATION.....	ii
ACKNOWLEDGEMENTS	iii
LIST OF FIGURES	ix
ABSTRACT.....	xii
CHAPTER 1.Introduction	1
1.1 Hallmarks of cancer	1
1.2 Apoptosis and regulation of cell death.....	3
1.3 Bcl-2 family proteins.....	4
1.4 Bcl-2 family proteins as therapeutic targets for cancer.....	7
1.5 Efforts to develop small-molecule Mcl-1 inhibitors	9
1.6 References	11
CHAPTER 2.Utilization of PubChem’s BioAssay Database for drug discovery: Integrated HTS and virtual screening for identification of novel small-molecule Mcl-1 inhibitors.....	15
2.1 Introduction	15
2.2 Approaches and strategies to identify inhibitors of PPIs	16
2.2.1 High-throughput screening (HTS).....	16
2.2.2 Virtual screening.....	16
2.3 Reported Mcl-1 inhibitors	17
2.4 Results	19
2.4.1 Integrated screening for identification of novel small-molecule Mcl-1 inhibitors .	19
2.4.2 Biochemical assays and ¹ H, ¹⁵ N HSQC NMR validation experiments	21
2.4.3 SAR investigation of the validated hit compound 20	29
2.4.4 Using model cell lines to better understand the cellular activity of E305	34
2.5 Conclusions	35
2.6 Materials and methods	37
2.7 Contributions.....	42
2.8 Appendix	43

2.9	References	46
CHAPTER 3. Structure-based design of novel potent and selective small-molecule Mcl-1 inhibitors..... 50		
3.1	Introduction	50
3.2	Structure-based design approach to develop protein-protein interactions modulators ..	51
3.3	Results	51
3.3.1	Structure based design of novel Mcl-1 inhibitors based on validated HTS hit	51
3.3.2	SAR investigation of new class of Mcl-1 inhibitors	53
3.3.3	Structural studies of novel Mcl-1 inhibitors	59
3.3.4	Structure-based optimization of Mcl-1 inhibitors.....	62
3.3.5	Selectivity Profile.....	69
3.3.6	Pulldown Experiment.....	70
3.3.7	483LM and 487LM antagonize Mcl-1 function	71
3.3.8	483LM has on-target cellular activity	71
3.4	Materials and methods	72
3.5	Contributions	78
3.6	Appendix	79
3.7	References	83
CHAPTER 4. Functional genomics to predict response to cancer therapies..... 85		
4.1	Introduction	85
4.1.1	Promise and limitations of genetic markers for patient stratification	85
4.1.2	BH3 profiling assay	86
4.1.3	Cancers that show dependence on the Bcl-2 family proteins for survival.....	90
4.2	Results	92
4.2.1	BH3 profiling determines anti-apoptotic survival dependence	92
4.2.2	Pharmacological approach for confirmation of cancer cell survival dependence	96
4.2.3	Selective Mcl-1 inhibitors activate the hallmarks of apoptosis in Mcl-1 dependent cancers	98
4.2.4	<i>In Vivo</i> efficacy of 483LM in mouse xenograft models with Mcl-1 sensitive cell line	100
4.2.5	483LM causes cell death in Mcl-1 and Bcl-2/Bcl-xL codependent cell lines in combination with ABT 263.	100
4.3	Conclusions	101

4.4	Materials and Methods	102
4.5	Contributions	106
4.6	References	107
CHAPTER 5. Summary and future directions		110
5.1	Summary	110
5.2	Impact and significance of the dissertation studies	112
5.3	Future directions.....	113
5.4	References	114

LIST OF FIGURES

Figure 1.1. Hallmarks of cancer and the potential therapeutic targeting mechanisms.	2
Figure 1.2. Simplified illustration of the intrinsic and extrinsic pathways of apoptosis.....	4
Figure 1.3. Structure of Bcl-2 family proteins and conserved interactions between BH3-only and anti-apoptotic proteins.	5
Figure 1.4. Selectivity of interactions among the Bcl-2 family of proteins.....	6
Figure 1.5. Proposed models of interactions of Bcl-2 family proteins.	7
Figure 1.6. Structure of small-molecule inhibitors of Bcl-2 family proteins.....	9
Figure 1.7. Structure of small-molecules selective Mcl-1 inhibitors.....	10
Figure 2.1. Reported scaffolds of small-molecule Mcl-1 inhibitors.	18
Figure 2.2. Interaction of conserved residues of pro-apoptotic proteins with anti-apoptotic proteins.....	19
Figure 2.3. Workflow of the validation of the Mcl-1 inhibitors and further optimization of compound 20.....	20
Figure 2.4. Mcl-1 inhibitor E305 induce Bax/Bak-dependent cell death to MEFS and on-target Mcl-1 cell activity.	35
Figure 2.5. Predicted binding poses and the HSQC NMR analysis of the confirmed compounds 1,2,3,4 and 5.....	43
Figure 2.6. Predicted binding poses and the HSQC NMR analysis of the confirmed compounds 5,6,7,8, and 10.....	44
Figure 2.7. Predicted binding poses and the HSQC NMR analysis of the confirmed compounds 12,13,17,18, and 19.....	45
Figure 3.1. Binding models of E238 and 368LM in the BH3 binding pocket of Mcl-1 based on HSQC NMR data.	54
Figure 3.2. Co-crystal structures of 382LM, 496LM and 462LM with Mcl-1.....	60
Figure 3.3. Alignment of 382LM co-crystal structure with reported co-crystal structures and predicted binding mode of 483LM.	64

Figure 3.4. Developed inhibitors exhibits on-target activity towards Mcl-1 in invitro and cell-based assays	72
Figure 3.5. Omit electron density maps for the bound ligands of Mcl-1.....	79
Figure 3.6. Binding affinity of 483LM, 487LM and Noxa using competitive SPR-based assay.	80
Figure 3.7. Selectivity profile of 483LM and 480LM using Competitive FP-based assay	80
Figure 3.8. Mitochondrial functional assay showing the inability of 483LM to inhibit the function of Bcl-xL like Bad peptide.....	81
Figure 3.9. Using Eu-myc lymphoma cell lines to confirm the selectivity of ABT-263 and inactivity of 486LM.	81
Figure 4.1. Bcl-2 family regulation of apoptosis. Cellular stress leads to the activation of BIM and BID leading to the activation of effectors and ultimately cell death.....	87
Figure 4.2. BH3 profiling distinguishes between three classes of apoptosis evasion.....	88
Figure 4.3. Selectivity profile of synthetic BH3 peptides and small-molecule BH3 mimetics.	89
Figure 4.4. Whole cell BH3 profiling.	90
Figure 4.5. BH3 profiling distinguishes between Mcl-1 and Bcl-2/Bcl-xL dependence.....	93
Figure 4.6. Plots between percentage of mitochondrial depolarization by MS1 in multiple myeloma cell lines and RPKM expression levels.	95
Figure 4.7. The sensitivity of MM cell lines correlates with percentage of mitochondrial depolarization by MS1.....	95
Figure 4.8. BH3 profiling using 483LM and ABT263 resembles the selectivity of NOXA and BAD respectively.....	96
Figure 4.9. Detection of apoptosis induction after treatment with 483LM and ABT-263	97
Figure 4.10. BH3 mimetics induce apoptosis in HNSCC UM-49 and UM-110 cell lines	97
Figure 4.11. Mcl-1 siRNA knockdown induces cell death to UM-49 but not to UM110.	98
Figure 4.12. 483LM disrupts the interaction between Mcl-1 and BAK inducing mitochondrial membrane depolarization and Smac release.	99
Figure 4.13. 483LM induces caspase 3 activation and PARP cleavage.	99
Figure 4.14. <i>In vivo</i> efficacy of 483LM in mouse xenograft model with Mcl-1 dependent H929.	100
Figure 4.15. 483LM exhibits synergism with ABT263 in PANC-1 and Mia Paca2 cell lines that depends on Mcl-1 and Bcl-2/Bcl-xL for survival.	101

LIST OF TABLES

Table 2.1. Binding results of the assayed 38 selected compounds.	22
Table 2.2. Exploring the influence of substituting the two five-membered furan moieties R1 and R2 in the initial hit compound E238.	30
Table 2.3. Measured Mcl-1 inhibition properties for the series of compounds that explore the influence of variation of the R3 group interacting with the Mcl-1 p2 pocket.	31
Table 2.4. Determining the effect of variation of the R3 and R4 groups on binding to Mcl-1.....	33
Table 2.5. Selectivity profile of E238 and other analogs.	34
Table 3.1. Exploring the SAR of substituted benzoic acid scaffold	55
Table 3.2. SAR of the phenethylthio benzoic acid derivatives for binding to Mcl-1 determined by FP and for selected compounds with TR-FRET binding assays.....	57
Table 3.3. SAR of the second-generation benzoic acid derivatives for binding to Mcl-1 determined by FP and for selected compounds with TR-FRET binding assays.....	66
Table 3.4. Selectivity of selected inhibitors against Bcl-2 anti-apoptotic proteins.....	70
Table 3.5. Crystallography data collection and refinement statistics.....	81
Table 4.1. RPKM expression levels of anti-apoptotic proteins based on RNA-Seq data.	94

ABSTRACT

Myeloid cell leukemia-1 (Mcl-1) is a potent anti-apoptotic protein, member of the anti-apoptotic Bcl-2 family. Overexpression of Mcl-1 is associated with high tumor grade, resistance to chemotherapy, and poor prognosis in many types of cancers. Thus, Mcl-1 is emerging as a critical survival factor in a broad range of human cancers and represents an attractive molecular target for the development of a new class of cancer therapy.

Applying an integrated screening strategy through combining high throughput and virtual screenings, multiple hit compounds with structural diversity were validated as Mcl-1 inhibitors using biochemical and biophysical methods. Based on the confirmed hit molecule and analyzing structure activity relationship (SAR) together with computational docking predicted binding poses supported by HSQC NMR studies, we have designed and optimized a novel class of selective small-molecule inhibitors of Mcl-1 using a 2,4,5 substituted benzoic acid as a scaffold. Several co-crystal structures of this class of inhibitors in complex with Mcl-1 have provided a basis for their further optimization, which ultimately led to the discovery of nanomolar potent and selective ligands that bind to the BH3 hydrophobic groove of the Mcl-1 protein. Mechanistic studies performed in genetically engineered cell lines revealed that our inhibitors have on-target activity and induce Bax/Bak dependent apoptosis; selectively antagonizing Mcl-1 function leading to the induction of the hallmarks of apoptosis. Using functional BH3 profiling assay, we identified heterogeneous dependency on Bcl-2 family members for survival in hematologic malignancies, as well as in solid human cancers. The mitochondrial response to selective Mcl-1 BH3 peptides (Noxa and MS1) predicted the *in vitro* sensitivity to Mcl-1 inhibitors of several cell lines found to be Mcl-1 dependent, including multiple myeloma cell line H929. **483LM**, one of the most potent developed Mcl-1 inhibitors, inhibited the cell growth and induced mechanism-based apoptotic cell death in the H929 cells. Intraperitoneal treatment of the H929 cancer xenograft model with **483LM** led to significant dose-dependent tumor regression. Collectively, our data demonstrates that the

new class of Mcl-1 inhibitors has promising *in vitro* and *in vivo* efficacy, warranting further development toward clinical use in the treatment of human cancers.

CHAPTER 1

Introduction

1.1 Hallmarks of cancer

Cancer is major worldwide disease that is considered the second most common cause of death after cardiovascular diseases.[1] Globally, there are tens of millions of people who are diagnosed with cancer. More than half of the diagnosed cancer patients die eventually from the disease. The increased aging population is of high risk of developing cancer, causing the disease to be a worldwide health issue.

The debilitating health problems of cancer led to extensive researches to be conducted in order to understand the disease, its risk factors, and the means of treatment. There is now a fundamental change in the way cancer research is conducted. Cancer research is becoming a logical science with a tendency to break down disease complexity into simple underlying principles.

It is evident that the transformation of normal cells to tumors is a process that includes several steps of genetic changes. Based on the suggestions of Hanahan and Weinberg, tumorigenesis is a result of six alterations or traits in cell physiology which are collectively named “Hallmarks of Cancer” (Figure 1.1).[2] The six hallmarks are 1) Sustained growth signals, 2) Evading anti-growth signals, 3) Activated invasiveness and metastasis, 4) Evading apoptosis, 5) Limitless replication potential, and 6) Angiogenesis. These six core hallmarks are acquired during tumorigenesis through various mechanisms which are enabled through two major characteristics. The first is genetic instability and mutations which lead to changes in the genetic makeup of cells driving tumorigenesis, and the second is the inflammatory state of the tumor where inflammation provides the tumor with sustaining bioactive molecules to promote its proliferation, limitless growth, and cell death resistance.[3, 4]

In the recent decade, some other characteristics in tumors are suggested to be important in tumorigenesis. There are two emerging hallmarks that could be added to the six hallmarks mentioned above. The first one is the alteration of the cellular energy metabolism of cancers compared to normal tissues, and the second is ability of tumor to evade immune cells and avoid detection by the immune system and consequent eradication. Further studies are required to understand those two emerging hallmarks in order to confirm their generality in all types of cancer and subsequently considering them part of the core hallmarks of cancer.

The great progress in understanding cancer resulted in the emergence of mechanism-based cancer therapeutics. These types of therapeutics possess the advantage of having, in principle, less side effects compared to chemotherapy. However, there are still challenges in mechanism-based therapeutics since tumors can still survive and adapt to the selective pressure imposed by the therapy. As a result, targeting several cancer hallmarks and drug combinations might be the best approach to overcome tumor resistance. In this thesis study, we are interested in the ability of cancer to evade cell death; particularly apoptosis, and the development and characterization of novel small molecules that block this cancer hallmark.

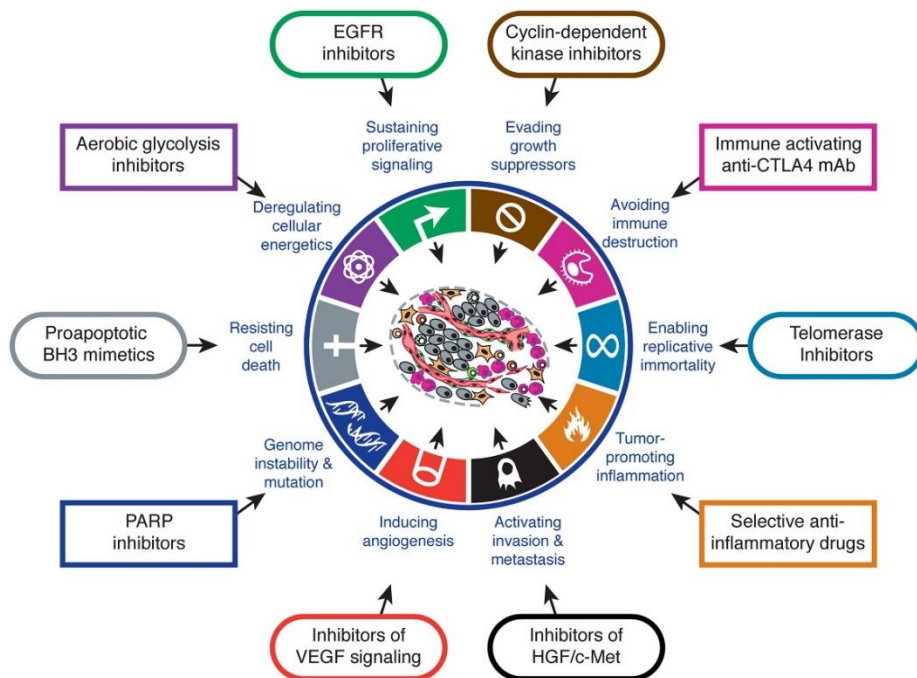


Figure 1.1. Hallmarks of cancer and the potential therapeutic targeting mechanisms. The figure is adapted from Hanahan, D.; Weinberg, R. A., *Cell* 2011, 144 (5), 646-74.

1.2 Apoptosis and regulation of cell death

Apoptosis (programmed cell death) is a controlled cell death mechanism that provides a way to degrade damaged cells via a non-inflammatory process. It is a normal process that occurs during development and aging and as a homeostatic mechanism in order to maintain cell populations in tissues. The term “apoptosis” was first introduced and described in a paper by Kerr et al 1972.[5] Apoptosis is characterized by nuclear condensation, shrinking of cells, blebbing of cell membrane, and DNA fragmentation. Consequently, the cells break down their components to be eventually engulfed by white blood cells. This process is different from necrosis where the cells release cellular contents to the surrounding tissues and cause damage. [6] Any dysregulation in the process of apoptosis can lead to development of diseases. Excessive apoptosis can cause degenerative disorders while increased cell survival can lead to cancer, which is the focus of my thesis study.[7] Apoptosis is activated in response to intracellular signals such as DNA lesions, defects in mitosis, oxidative stress, or other stresses e.g. certain drugs or UV light (intrinsic apoptotic pathway). Activation can also be due to extracellular signals emitted by other cells (extrinsic apoptotic pathway) (Figure 1.2).[8, 9]

The activation of the intrinsic apoptotic pathway leads to the activation of B-cell lymphoma-2 (BCL-2) family proteins. Consequently, the mitochondria undergo mitochondrial outer membrane permeabilization (MOMP), causing the efflux of cytochrome c as well as the second mitochondrial activator of caspases (Smac). Cytochrome c binds to the apoptotic protease activating factor 1 (APAF1), and recruits procaspase 9 for the apoptosome. Apoptosomes cleave procaspase 9 to caspase 9 which in turn activates caspases 3 and 7, inducing the cleavage of poly ADP ribose polymerase (PARP) and ultimately apoptosis. Several ubiquitin ligases are involved in the inhibition of cell death, e.g. X-linked Inhibitor of Apoptosis Proteins; (XIAP). Smac indirectly promotes apoptosis by blocking the effects of XIAP.

The extrinsic apoptotic pathway is activated when the death ligands, such as FASL, TNF-related apoptosis-inducing ligand (TRAIL), or tumor necrosis factor- α (TNF α) bind to their corresponding death receptors FASR, TNFR and DR4/5 respectively. The binding forms the death-inducing signaling complex (DISC) which activates caspase 8 and 10, leading to the subsequent activation of caspases 3 and 7. The extrinsic apoptotic pathway activation mediates the truncation

of the pro-apoptotic protein Bid to the truncated form (tBid) by caspase 8, which in turn translocate to mitochondria and activates MOMP through the intrinsic apoptotic pathway.[10]

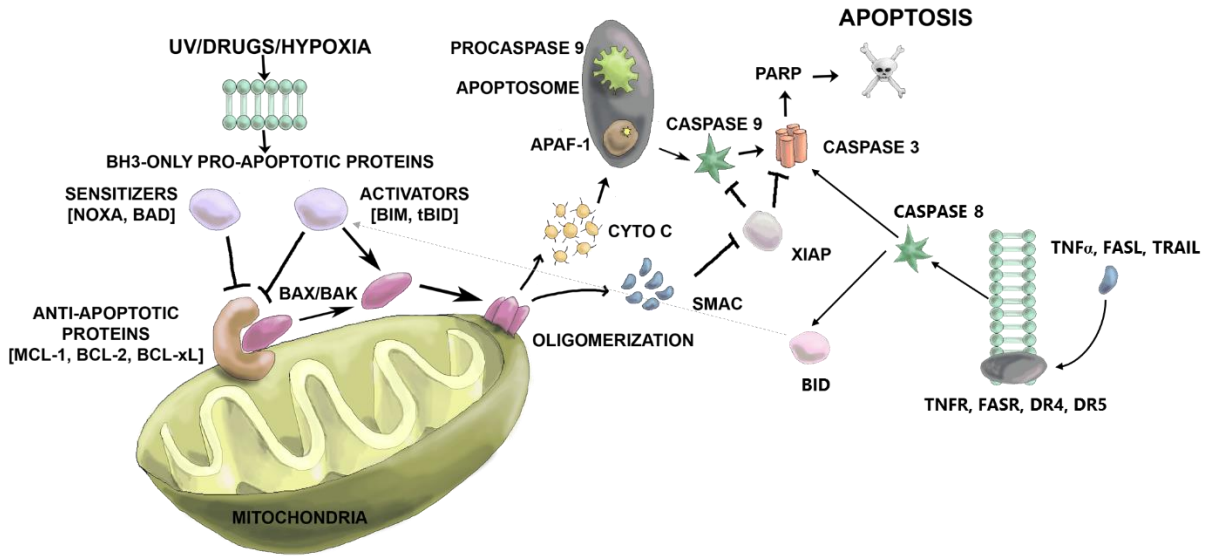


Figure 1.2. Simplified illustration of the intrinsic and extrinsic pathways of apoptosis.

1.3 Bcl-2 family proteins

Bcl-2 (B-cell lymphoma-2) proto-oncogene was discovered at the chromosomal breakpoint of t(14;18) bearing human B-cell follicular lymphomas.[11] The number of Bcl-2 family members has expanded significantly and included both pro-apoptotic (promoting apoptosis) and anti-apoptotic (inhibiting apoptosis) proteins. The ratio between the two groups of proteins regulates the ability of cells to respond to the death signal.[12] The members of have the ability to form homodimers as well as heterodimers, suggesting neutralizing competition between these proteins. Proteins of the Bcl-2 family possess blocks of sequence homology known as Bcl-2 homology (BH) domains. There are six anti-apoptotic proteins Bcl-2, Bcl-xL, Bcl-w, Bcl-b, A1, and myeloid cell leukemia sequence 1 (Mcl-1), and three pro-apoptotic effector proteins Bax, Bak, and Bok and they all share four BH domains (BH1-4).[13] They have similar globular structures; several α -helices where a hydrophobic pocket is formed by α -helices 2,3,4 and 5.[14] This pocket interacts with the BH3 domain of pro-apoptotic BH3-only proteins (Bim, tBid, Puma, Bad, Noxa, Bik, Hrk and Bmf) (Figure 1.3a).

BH3-only proteins contain only the BH3 amphipathic α -helix, which mediate their interaction with the groove of multi-domain Bcl-2 family members. The BH3-only proteins bind to the BH3 binding hydrophobic groove of anti-apoptotic proteins through interactions between four conserved hydrophobic residues (h1-4) and four hydrophobic pockets (P1-4) of anti-apoptotic proteins, and the conserved hydrogen bond between Asp residue of BH3-only protein and Arg residue in anti-apoptotic proteins BH1 domain (Figure 1.3b). [15, 16]

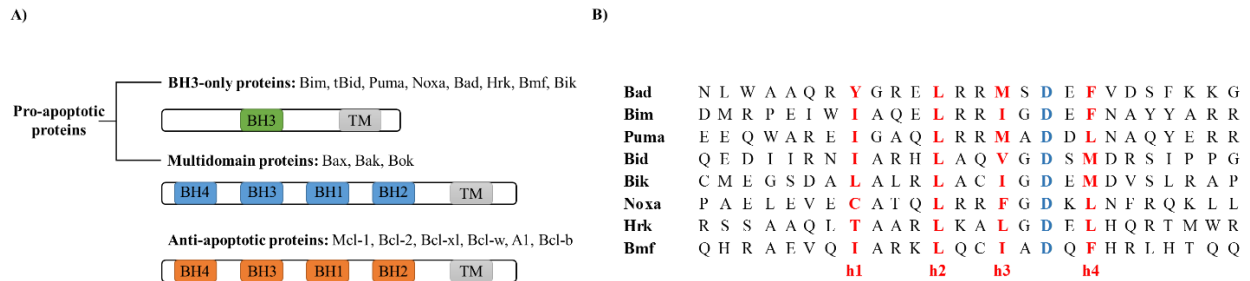


Figure 1.3. Structure of Bcl-2 family proteins and conserved interactions between BH3-only and anti-apoptotic proteins.

BH3-only proteins have different binding profiles to the anti-apoptotic proteins. Some show selective binding, for example, Noxa interacts only with Mcl-1 and A1, while Bad interacts with Bcl-2, Bcl-xL and Bcl-w (Figure 1.4). However, some BH3-only proteins show promiscuity and bind to all anti-apoptotic proteins including tBid, Bim, and Puma. The flexibility of the BH3 binding pocket contributes to the ability of anti-apoptotic proteins to bind to several pro-apoptotic partners.[17] In addition to BH domains, most family members have a transmembrane (TM) domain for anchoring to organelles including the mitochondria and endoplasmic reticulum.[18]

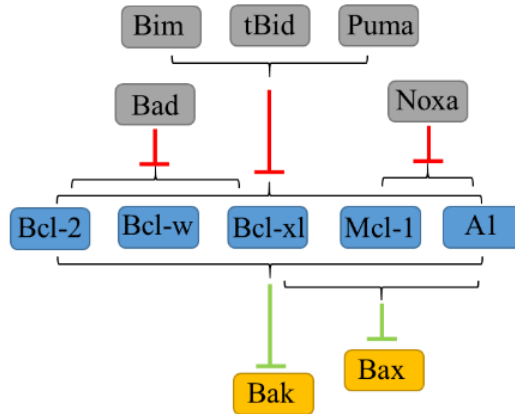


Figure 1.4. Selectivity of interactions among the Bcl-2 family of proteins.

When the intrinsic apoptotic pathway is activated, pro-apoptotic BH3-only proteins are induced transcriptionally or post-translationally.[19] There are two proposed mechanisms by which the BH3-only proteins carry out their pro-apoptotic function. [20, 21] The first is neutralization of the anti-apoptotic proteins and indirect activation of effectors Bax and Bak (Figure 1.5a). This mechanism has been well studied on structural and functional levels, encouraging the development of novel therapeutics that target the anti-apoptotic proteins. When the intrinsic pathway is activated, the BH3-only proteins bind to anti-apoptotic proteins and cause the release of activated Bax and Bak, triggering the apoptosis cascade.

The second proposed mechanism suggests the direct activation of Bax and Bak. In this mechanism the BH3-only proteins are subdivided into activators which directly activate Bax and Bak (tBid, Bim, or Puma), and sensitizers which are not able to directly activate Bak or Bax (Noxa, Bad, etc.). On activation of the intrinsic pathway, sensitizers bind to anti-apoptotic proteins and release the activators which in turn activate Bax and Bak (Figure 1.5b). The current consensus is that both models play a role in the pathway. In the unified model, sensitizers bind to anti-apoptotic proteins, displacing activated Bax and Bak (indirect) as well as activators (direct).[22]

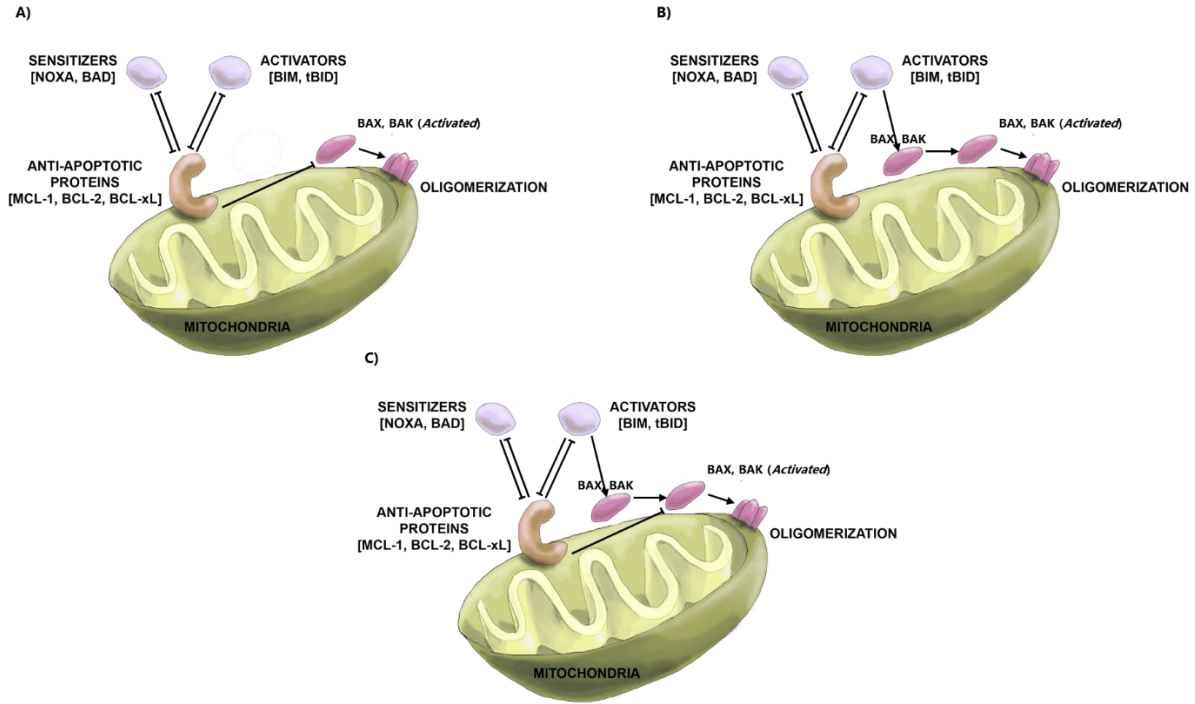


Figure 1.5. Proposed models of interactions of Bcl-2 family proteins. (A) Indirect activation model, **(B)** Direct activation model, and **(C)** Unified model.

It seems that some cells display predominantly a certain model over the other and that could be attributed to the types of cells under investigation or the types of stimuli that triggers activation of the intrinsic apoptotic pathway (Figure 1.5c). When the intrinsic apoptotic pathway is triggered, Bak is activated and homo-oligomerizes to induce MOMP. Although Bak resides on the mitochondria, Bax is a cytosolic protein which accumulates on the mitochondria and homo-oligomerize when apoptosis is triggered (Figure 1.2).[23, 24]

1.4 Bcl-2 family proteins as therapeutic targets for cancer

Understanding the apoptosis mechanisms and the immense structural knowledge of the Bcl-2 family of proteins introduces the idea of developing inhibitors that can inhibit the function of anti-apoptotic proteins. These inhibitors could be crucial in the fight against cancer. Many studies have shown that elevated levels of anti-apoptotic proteins are frequently observed in cancer.[25] This usually leads to resistance to various chemotherapeutics. In the past years, the anti-apoptotic protein families have been targeted in cancer treatment strategies. Several types of inhibitors of anti-apoptotic proteins have been developed, including peptidomimetics [26, 27] and

antisense oligonucleotides.[28] Consequently, the development of small-molecule BH3 mimetics that block anti-apoptotic proteins became a promising approach to disrupt the interaction with the bound pro-apoptotic proteins and force cancer cells to undergo apoptosis. Developing small molecules targeting these protein-protein interactions is a challenging process. However, there are number of BH3 mimetics reported to trigger apoptosis undergoing extensive clinical and preclinical studies. Obatoclax (GX015-070), which is derived from prodiginines, is a pan-inhibitor of Bcl-2 family proteins.[29, 30] Several studies on Obatoclax suggest that it is effective as a single agent or in combination therapy (Figure 1.6). It is under phase III clinical trials, but the development of neurotoxicity as a side effect might hinder its progress as a drug.[31] Gossypol (AT-101) is another anticancer agent that has shown inhibition of Bcl-2, Bcl-xL and Mcl-1.[32] Gossypol is currently in clinical trials.[33] A derivative of Gossypol, TW-37, is another pan-inhibitor that shows promising results as a single agent and in combination with other agents. [34-36] Abbvie team spearheaded the drug discovery efforts to develop BH3 mimetics that target anti-apoptotic proteins. The team developed ABT-737 as a potent inhibitor of Bcl-2, Bcl-xL and Bcl-w. [37] This compound and its orally available analog ABT-263 (Navitoclax) have been extensively studied to confirm their modes of action.[38, 39] Clinical trials of ABT-263 were carried out for treatment of lymphoid malignancies and chronic lymphocytic leukemia.[40, 41] Significant thrombocytopenia was reported in clinical trials which was attributed to inhibiting Bcl-xL protein from circulating platelets. This led to the development of ABT-199 (Venetoclax) which shows selective binding to Bcl-2.[42] ABT-199 progressed to clinical trials.[43] The U.S. Food and Drug Administration (FDA) approved Venetoclax for the treatment of patients who have chronic lymphocytic leukemia (CLL) with a chromosomal abnormality called 17p. Venetoclax is the first FDA-approved treatment that targets Bcl-2 family proteins. However, Mcl-1 mediates resistance to Bcl-2 and Bcl-xL inhibitors, including ABT-199, because they fail to inhibit Mcl-1.[44] This raises the need for Mcl-1 inhibitors as a future therapeutic intervention.

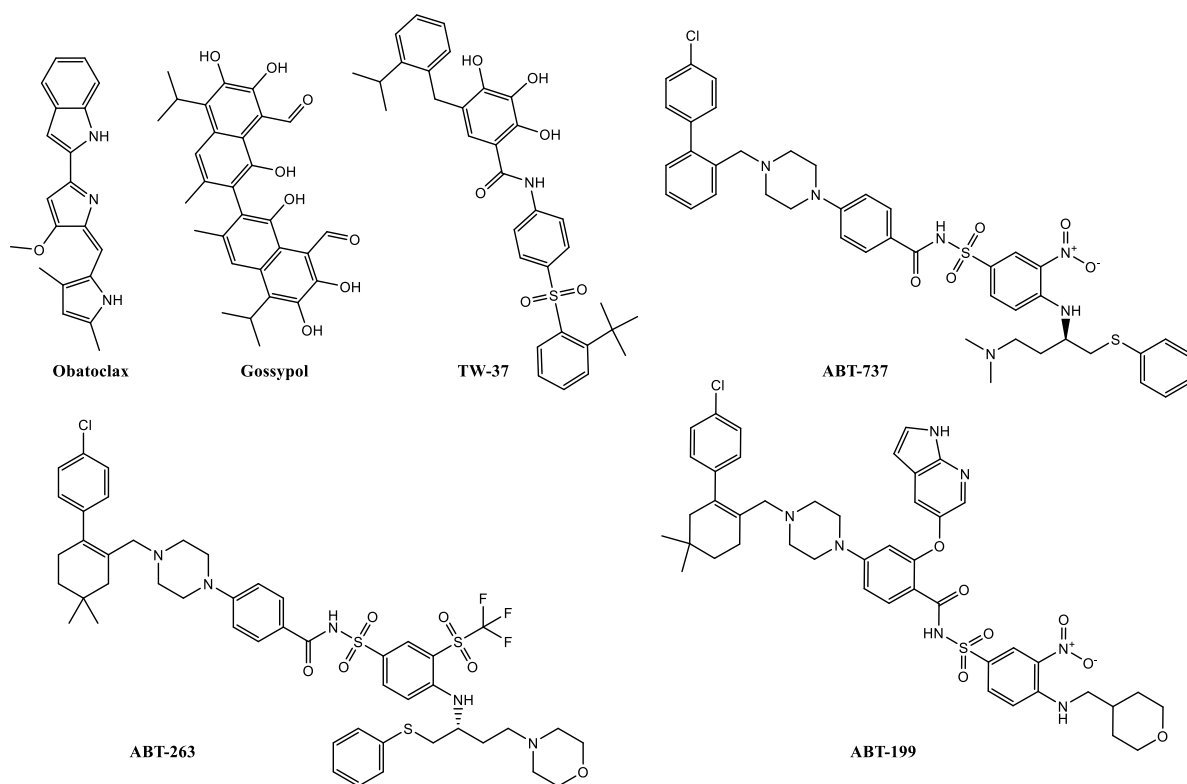


Figure 1.6. Structure of small-molecule inhibitors of Bcl-2 family proteins.

1.5 Efforts to develop small-molecule Mcl-1 inhibitors

Mcl-1 has been observed to be highly expressed in various of human cancers including melanoma, multiple myeloma, pancreatic, colon, and hematological malignancies.[45] The overexpression of Mcl-1 contributes to the ability of cancer cells to evade cell death. Mcl-1 overexpression is considered a resistance mechanism deployed by cancer against chemotherapeutic agents. Downregulation of Mcl-1 in resistant types of cancer increases their sensitivity to chemotherapeutics.[46-48] Thus, developing Mcl-1 inhibitors has been a hot topic of research in the past few years. There are several approaches designed to target Mcl-1, either directly through blocking its BH3 binding site, or targeting upstream pathways that upregulate its degradation [49], or downregulating its protein level through inhibition of expression [50], or translation. [51]

Developing selective small-molecule BH3 mimetics to inhibit Mcl-1 has been far from trivial. Despite the extensive efforts to develop potent and selective small molecules, to date there

are no Mcl-1 inhibitors that reached clinical trials. Several small-molecule potent and selective inhibitors of Mcl-1 have been developed and well characterized. Using high throughput screening (HTS) of 53,000 compounds and optimization of hit compound **UMI-59**, the selective Mcl-1 inhibitor **UMI-77** ($K_i = 490$ nM) was developed and exhibited Bax/Bak dependent induction of apoptosis and caspase-3 activation in pancreatic cancer cell lines (Figure 1.7). *In vivo* studies using the pancreatic xenograft model showed effective inhibition of tumor growth by **UMI-77**.^[52] The more potent analog **21** ($K_i = 180$ nM) showed similar selectivity profile as **UMI-77**. **21** inhibited leukemia cell growth, and showed dose-dependent induction of apoptosis and activation of caspase-3 in the HL60 cell line. Further, similar to **UMI-77**, compound **21** showed Bak/Bax-dependent induction of cell death. ^[53] Walensky's lab successfully identified a selective Mcl-1 inhibitor **MIM1** ($IC_{50} = 4.78$ μ M) using HTS of 70,000 compounds.^[54]

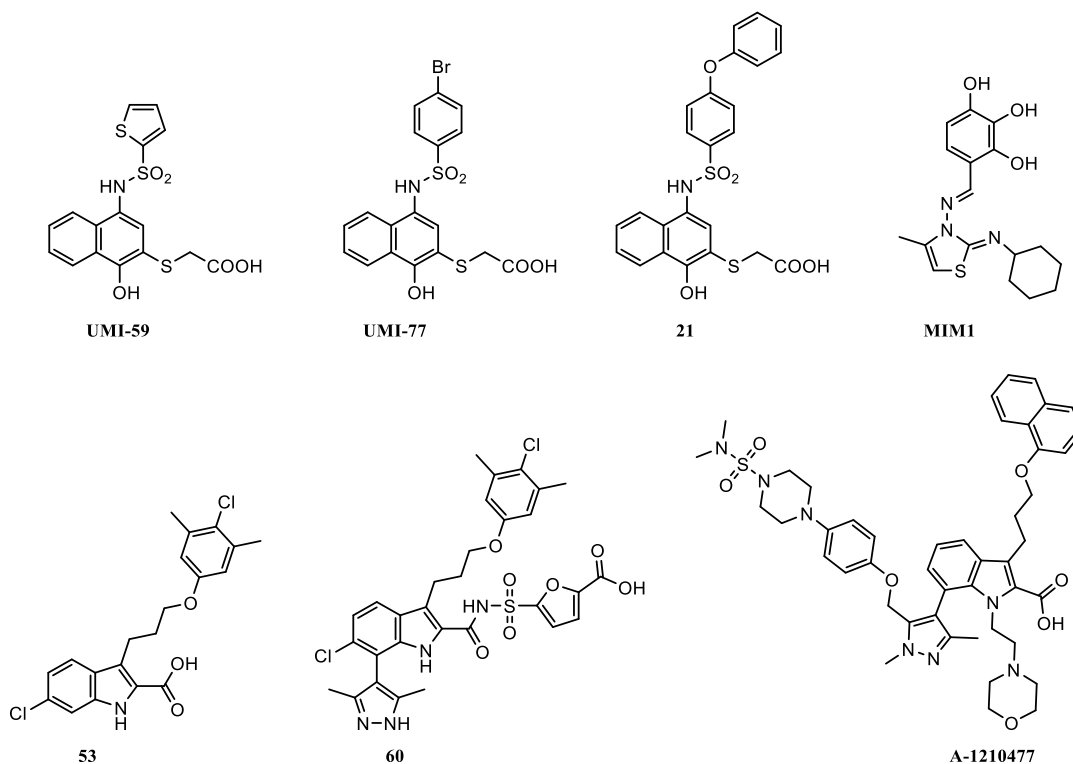


Figure 1.7. Structure of small-molecules selective Mcl-1 inhibitors.

MIM1 was able to show Bax/Bak dependent induction of apoptosis in leukemia. Using fragment based screening, Fesik's lab developed compound **53** ($K_i = 55$ nM) as a selective Mcl-1 inhibitor. **53** was the first small molecule to be co-crystallized with Mcl-1, which was a breakthrough in aiding the structure-based drug design efforts.^[55] This compound led to further

development of the more potent analog **60** ($K_i = 0.36$ nM).[56] Despite the high potency of this compound, it did not show permeability in PAMPA assay, which hindered its biological characterization. Abbvie team developed a potent and selective Mcl-1 inhibitor, **A-1210477** ($K_i = 0.43$ nM). This compound exhibited promising results in several cell lines, including multiple myeloma, breast cancer, and pancreatic cancer, either as a single agent or in combination with Navitoclax.[57, 58] However, no *in vivo* studies have been conducted using this inhibitor. Thus there is still a need for Mcl-1 inhibitors that can exhibit solid biological characterization and *in vivo* efficacy which can be taken further to clinical studies.

1.6 References

- [1] Lozano R, Naghavi M, Foreman K, Lim S, Shibuya K, Aboyans V, et al. Global and regional mortality from 235 causes of death for 20 age groups in 1990 and 2010: a systematic analysis for the Global Burden of Disease Study 2010. *Lancet*. 2012;380:2095-128.
- [2] Hanahan D, Weinberg RA. Hallmarks of cancer: the next generation. *Cell*. 2011;144:646-74.
- [3] Jones PA, Baylin SB. The epigenomics of cancer. *Cell*. 2007;128:683-92.
- [4] Pages F, Galon J, Dieu-Nosjean MC, Tartour E, Sautes-Fridman C, Fridman WH. Immune infiltration in human tumors: a prognostic factor that should not be ignored. *Oncogene*. 2010;29:1093-102.
- [5] Kerr JF, Wyllie AH, Currie AR. Apoptosis: a basic biological phenomenon with wide-ranging implications in tissue kinetics. *Br J Cancer*. 1972;26:239-57.
- [6] Chaabane W, User SD, El-Gazzah M, Jaksik R, Sajjadi E, Rzeszowska-Wolny J, et al. Autophagy, apoptosis, mitoptosis and necrosis: interdependence between those pathways and effects on cancer. *Arch Immunol Ther Exp (Warsz)*. 2013;61:43-58.
- [7] Thompson CB. Apoptosis in the pathogenesis and treatment of disease. *Science*. 1995;267:1456-62.
- [8] Norbury CJ, Hickson ID. Cellular responses to DNA damage. *Annu Rev Pharmacol Toxicol*. 2001;41:367-401.
- [9] Fulda S, Debatin KM. Targeting apoptosis pathways in cancer therapy. *Curr Cancer Drug Targets*. 2004;4:569-76.
- [10] Fulda S, Debatin KM. Extrinsic versus intrinsic apoptosis pathways in anticancer chemotherapy. *Oncogene*. 2006;25:4798-811.
- [11] Tsujimoto Y, Gorham J, Cossman J, Jaffe E, Croce CM. The t(14;18) chromosome translocations involved in B-cell neoplasms result from mistakes in VDJ joining. *Science*. 1985;229:1390-3.
- [12] Oltvai ZN, Millman CL, Korsmeyer SJ. Bcl-2 heterodimerizes in vivo with a conserved homolog, Bax, that accelerates programmed cell death. *Cell*. 1993;74:609-19.
- [13] Kvensakul M, Yang H, Fairlie WD, Czabotar PE, Fischer SF, Perugini MA, et al. Vaccinia virus anti-apoptotic F1L is a novel Bcl-2-like domain-swapped dimer that binds a highly selective subset of BH3-containing death ligands. *Cell death and differentiation*. 2008;15:1564-71.

- [14] Hartley EJ, Seeman P. The effect of varying 3H-spiperone concentration on its binding parameters. *Life Sci.* 1978;23:513-7.
- [15] Sattler M, Liang H, Nettlesheim D, Meadows RP, Harlan JE, Eberstadt M, et al. Structure of Bcl-xL-Bak peptide complex: recognition between regulators of apoptosis. *Science.* 1997;275:983-6.
- [16] Bajwa N, Liao C, Nikolovska-Coleska Z. Inhibitors of the anti-apoptotic Bcl-2 proteins: a patent review. *Expert Opin Ther Pat.* 2012;22:37-55.
- [17] Lee EF, Czabotar PE, Yang H, Sleebs BE, Lessene G, Colman PM, et al. Conformational changes in Bcl-2 pro-survival proteins determine their capacity to bind ligands. *J Biol Chem.* 2009;284:30508-17.
- [18] Danial NN. BCL-2 family proteins: critical checkpoints of apoptotic cell death. *Clin Cancer Res.* 2007;13:7254-63.
- [19] Adams JM, Cory S. The Bcl-2 apoptotic switch in cancer development and therapy. *Oncogene.* 2007;26:1324-37.
- [20] Kuwana T, Bouchier-Hayes L, Chipuk JE, Bonzon C, Sullivan BA, Green DR, et al. BH3 domains of BH3-only proteins differentially regulate Bax-mediated mitochondrial membrane permeabilization both directly and indirectly. *Mol Cell.* 2005;17:525-35.
- [21] Merino D, Giam M, Hughes PD, Siggs OM, Heger K, O'Reilly LA, et al. The role of BH3-only protein Bim extends beyond inhibiting Bcl-2-like prosurvival proteins. *J Cell Biol.* 2009;186:355-62.
- [22] Llambi F, Moldoveanu T, Tait SW, Bouchier-Hayes L, Temirov J, McCormick LL, et al. A unified model of mammalian BCL-2 protein family interactions at the mitochondria. *Mol Cell.* 2011;44:517-31.
- [23] Griffiths GJ, Dubrez L, Morgan CP, Jones NA, Whitehouse J, Corfe BM, et al. Cell damage-induced conformational changes of the pro-apoptotic protein Bak in vivo precede the onset of apoptosis. *J Cell Biol.* 1999;144:903-14.
- [24] Suzuki M, Youle RJ, Tjandra N. Structure of Bax: coregulation of dimer formation and intracellular localization. *Cell.* 2000;103:645-54.
- [25] Beroukhi R, Mermel CH, Porter D, Wei G, Raychaudhuri S, Donovan J, et al. The landscape of somatic copy-number alteration across human cancers. *Nature.* 2010;463:899-905.
- [26] Kolluri SK, Zhu X, Zhou X, Lin B, Chen Y, Sun K, et al. A short Nur77-derived peptide converts Bcl-2 from a protector to a killer. *Cancer Cell.* 2008;14:285-98.
- [27] LaBelle JL, Katz SG, Bird GH, Gavathiotis E, Stewart ML, Lawrence C, et al. A stapled BIM peptide overcomes apoptotic resistance in hematologic cancers. *J Clin Invest.* 2012;122:2018-31.
- [28] Reed JC. Apoptosis-based therapies. *Nat Rev Drug Discov.* 2002;1:111-21.
- [29] Smoot RL, Blechacz BR, Werneburg NW, Bronk SF, Sinicrope FA, Sirica AE, et al. A Bax-mediated mechanism for obatoclax-induced apoptosis of cholangiocarcinoma cells. *Cancer Res.* 2010;70:1960-9.
- [30] Joudeh J, Claxton D. Obatoclax mesylate : pharmacology and potential for therapy of hematological neoplasms. *Expert Opin Investig Drugs.* 2012;21:363-73.
- [31] Hwang JJ, Kuruvilla J, Mendelson D, Pishvaian MJ, Deeken JF, Siu LL, et al. Phase I dose finding studies of obatoclax (GX15-070), a small molecule pan-BCL-2 family antagonist, in patients with advanced solid tumors or lymphoma. *Clin Cancer Res.* 2010;16:4038-45.

- [32] Wei J, Kitada S, Stebbins JL, Placzek W, Zhai D, Wu B, et al. Synthesis and biological evaluation of Apogossypolone derivatives as pan-active inhibitors of antiapoptotic B-cell lymphoma/leukemia-2 (Bcl-2) family proteins. *J Med Chem.* 2010;53:8000-11.
- [33] Baggstrom MQ, Qi Y, Koczywas M, Argiris A, Johnson EA, Millward MJ, et al. A phase II study of AT-101 (Gossypol) in chemotherapy-sensitive recurrent extensive-stage small cell lung cancer. *J Thorac Oncol.* 2011;6:1757-60.
- [34] Wang Z, Song W, Aboukameel A, Mohammad M, Wang G, Banerjee S, et al. TW-37, a small-molecule inhibitor of Bcl-2, inhibits cell growth and invasion in pancreatic cancer. *Int J Cancer.* 2008;123:958-66.
- [35] Zeitlin BD, Joo E, Dong Z, Warner K, Wang G, Nikolovska-Coleska Z, et al. Antiangiogenic effect of TW37, a small-molecule inhibitor of Bcl-2. *Cancer Res.* 2006;66:8698-706.
- [36] Mohammad RM, Goustin AS, Aboukameel A, Chen B, Banerjee S, Wang G, et al. Preclinical studies of TW-37, a new nonpeptidic small-molecule inhibitor of Bcl-2, in diffuse large cell lymphoma xenograft model reveal drug action on both Bcl-2 and Mcl-1. *Clin Cancer Res.* 2007;13:2226-35.
- [37] Oltersdorf T, Elmore SW, Shoemaker AR, Armstrong RC, Augeri DJ, Belli BA, et al. An inhibitor of Bcl-2 family proteins induces regression of solid tumours. *Nature.* 2005;435:677-81.
- [38] Konopleva M, Contractor R, Tsao T, Samudio I, Ruvolo PP, Kitada S, et al. Mechanisms of apoptosis sensitivity and resistance to the BH3 mimetic ABT-737 in acute myeloid leukemia. *Cancer Cell.* 2006;10:375-88.
- [39] Tse C, Shoemaker AR, Adickes J, Anderson MG, Chen J, Jin S, et al. ABT-263: a potent and orally bioavailable Bcl-2 family inhibitor. *Cancer Res.* 2008;68:3421-8.
- [40] Wilson WH, O'Connor OA, Czuczman MS, LaCasce AS, Gerecitano JF, Leonard JP, et al. Navitoclax, a targeted high-affinity inhibitor of BCL-2, in lymphoid malignancies: a phase 1 dose-escalation study of safety, pharmacokinetics, pharmacodynamics, and antitumour activity. *Lancet Oncol.* 2010;11:1149-59.
- [41] Roberts AW, Seymour JF, Brown JR, Wierda WG, Kipps TJ, Khaw SL, et al. Substantial susceptibility of chronic lymphocytic leukemia to BCL2 inhibition: results of a phase I study of navitoclax in patients with relapsed or refractory disease. *J Clin Oncol.* 2012;30:488-96.
- [42] Souers AJ, Levenson JD, Boghaert ER, Ackler SL, Catron ND, Chen J, et al. ABT-199, a potent and selective BCL-2 inhibitor, achieves antitumor activity while sparing platelets. *Nat Med.* 2013;19:202-8.
- [43] Fischer K, Fink A-M, Bishop H, Dixon M, Bahlo J, Choi MY, et al. Results of the Safety Run-in Phase of CLL14 (BO25323): A Prospective, Open-Label, Multicenter Randomized Phase III Trial to Compare the Efficacy and Safety of Obinutuzumab and Venetoclax (GDC-0199/ABT-199) with Obinutuzumab and Chlorambucil in Patients with Previously Untreated CLL and Coexisting Medical Conditions. *Blood.* 2015;126:496-.
- [44] Bojarczuk K, Sasi BK, Gobessi S, Innocenti I, Pozzato G, Laurenti L, et al. BCR signaling inhibitors differ in their ability to overcome Mcl-1-mediated resistance of CLL B cells to ABT-199. *Blood.* 2016;127:3192-201.
- [45] Placzek WJ, Wei J, Kitada S, Zhai D, Reed JC, Pellecchia M. A survey of the anti-apoptotic Bcl-2 subfamily expression in cancer types provides a platform to predict the efficacy of Bcl-2 antagonists in cancer therapy. *Cell death & disease.* 2010;1:e40.

- [46] Thallinger C, Wolschek MF, Wacheck V, Maierhofer H, Gunsberg P, Polterauer P, et al. Mcl-1 antisense therapy chemosensitizes human melanoma in a SCID mouse xenotransplantation model. *J Invest Dermatol.* 2003;120:1081-6.
- [47] Nguyen M, Marcellus RC, Roulston A, Watson M, Serfass L, Murthy Madiraju SR, et al. Small molecule obatoclax (GX15-070) antagonizes MCL-1 and overcomes MCL-1-mediated resistance to apoptosis. *Proc Natl Acad Sci U S A.* 2007;104:19512-7.
- [48] Wertz IE, Kusam S, Lam C, Okamoto T, Sandoval W, Anderson DJ, et al. Sensitivity to antitubulin chemotherapeutics is regulated by MCL1 and FBW7. *Nature.* 2011;471:110-4.
- [49] Sun H, Kapuria V, Peterson LF, Fang D, Bornmann WG, Bartholomeusz G, et al. Bcr-Abl ubiquitination and Usp9x inhibition block kinase signaling and promote CML cell apoptosis. *Blood.* 2011;117:3151-62.
- [50] Tong WG, Chen R, Plunkett W, Siegel D, Sinha R, Harvey RD, et al. Phase I and pharmacologic study of SNS-032, a potent and selective Cdk2, 7, and 9 inhibitor, in patients with advanced chronic lymphocytic leukemia and multiple myeloma. *J Clin Oncol.* 2010;28:3015-22.
- [51] Rahmani M, Davis EM, Bauer C, Dent P, Grant S. Apoptosis induced by the kinase inhibitor BAY 43-9006 in human leukemia cells involves down-regulation of Mcl-1 through inhibition of translation. *J Biol Chem.* 2005;280:35217-27.
- [52] Abulwerdi F, Liao C, Liu M, Azmi AS, Aboukameel A, Mady AS, et al. A novel small-molecule inhibitor of mcl-1 blocks pancreatic cancer growth in vitro and in vivo. *Mol Cancer Ther.* 2014;13:565-75.
- [53] Abulwerdi FA, Liao C, Mady AS, Gavin J, Shen C, Cierpicki T, et al. 3-Substituted-N-(4-hydroxynaphthalen-1-yl)arylsulfonamides as a novel class of selective Mcl-1 inhibitors: structure-based design, synthesis, SAR, and biological evaluation. *J Med Chem.* 2014;57:4111-33.
- [54] Cohen NA, Stewart ML, Gavathiotis E, Tepper JL, Bruekner SR, Koss B, et al. A competitive stapled peptide screen identifies a selective small molecule that overcomes MCL-1-dependent leukemia cell survival. *Chemistry & biology.* 2012;19:1175-86.
- [55] Friberg A, Vigil D, Zhao B, Daniels RN, Burke JP, Garcia-Barrantes PM, et al. Discovery of potent myeloid cell leukemia 1 (Mcl-1) inhibitors using fragment-based methods and structure-based design. *J Med Chem.* 2013;56:15-30.
- [56] Pelz NF, Bian Z, Zhao B, Shaw S, Tarr JC, Belmar J, et al. Discovery of 2-Indole-acylsulfonamide Myeloid Cell Leukemia 1 (Mcl-1) Inhibitors Using Fragment-Based Methods. *J Med Chem.* 2016;59:2054-66.
- [57] Levenson JD, Zhang H, Chen J, Tahir SK, Phillips DC, Xue J, et al. Potent and selective small-molecule MCL-1 inhibitors demonstrate on-target cancer cell killing activity as single agents and in combination with ABT-263 (navitoclax). *Cell death & disease.* 2015;6:e1590.
- [58] Xiao Y, Nimmer P, Sheppard GS, Bruncko M, Hessler P, Lu X, et al. MCL-1 Is a Key Determinant of Breast Cancer Cell Survival: Validation of MCL-1 Dependency Utilizing a Highly Selective Small Molecule Inhibitor. *Mol Cancer Ther.* 2015;14:1837-47.

CHAPTER 2

Utilization of PubChem's BioAssay Database for drug discovery: Integrated HTS and virtual screening for identification of novel small-molecule Mcl-1 inhibitors

2.1 Introduction

Protein-protein interactions (PPIs) play a crucial role in regulating many biological functions. Advances in genomics and proteomics have shaped our understanding of PPIs. Dysregulation of PPIs is the basis of many diseases, including cancer. Our growing understanding of cancer biology raised interest in targeting PPIs for the treatment of cancer.[1] A major challenge in PPIs is developing small molecules that target these relatively flat and large interfaces.[2] Many of these protein interfaces are hydrophobic in nature so the developed drug leads are often hydrophobic with high molecular weight. These physicochemical properties are usually unfavorable for drug candidates due to low solubility, cell permeability, or oral bioavailability.[3] Although developing small molecules that target PPIs is challenging, there are successful examples of compounds that exhibit highly potent and selective inhibition to their designated targets and some have been FDA approved in the last few years.

There are numerous PPIs that have a pivotal role in the development of the hallmarks of cancer and maintaining its uncontrolled proliferation.[4] For example, the activation of Ras via mutated epidermal growth factor receptor (EGFR), or Neurofibromin 1 (NF1) mutation or deletion resulted in continuous proliferation of cancer cells and resistance to cell death.[5, 6] The same hallmark occurs with the XIAP/Caspase 9 interaction and Bcl-2 family pro- and anti-apoptotic proteins.[7, 8] Some PPIs such as Mouse Double Minute 2 homolog (MDM2)/p53 and Cyclin-dependent kinase 4 (CDK4)/retinoblastoma protein (pRB) lack tumor suppressive functions[9, 10] Epigenetic aberrations in PPIs also play a role in cancer development.[11] Since several PPIs are involved in tumorigenesis, inhibiting them can block several pathways that the cancer

depends on for survival and proliferation. Thus, targeting PPIs can be of great importance in the field of anticancer drug discovery.[12]

2.2 Approaches and strategies to identify inhibitors of PPIs

The rational design of PPI inhibitors (PPII) has improved dramatically thanks to the increasing structural and functional knowledge of PPIs. There are numerous approaches that are employed in order to identify and optimize inhibitors of PPIs.

2.2.1 High-throughput screening (HTS)

HTS has been used to identify small molecules that can bind to the PPI interface's hot spots. HTS is usually coupled with structure-based design in order to develop inhibitors with better activity and physicochemical properties.[1] Fluorescent polarization (FP) and time-resolved fluorescence resonance energy transfer (TR-FRET) are the most frequently used techniques in HTS campaigns. [13] Some other techniques are surface plasmon resonance (SPR), flow cytometry, and enzyme-linked immunosorbent assay (ELISA).[14] HTS has also been performed to identify fragments that target the PPI (fragment based screening). Since these fragments usually have a low affinity to the target, highly sensitive biophysical techniques for screening are used, such as X-ray crystallography, nuclear magnetic resonance (NMR), and surface plasmon resonance (SPR) to identify hits.[15-17] Following optimization of initial fragment hits, small molecules can be designed to take advantage of the fragments' scaffolds and identify interactions with the target protein.[18, 19] Some examples of successful fragment based screening campaigns were used to identify inhibitors for Mcl-1, Bcl-2, XIAP and HSP90.[20-23]

2.2.2 Virtual screening

There are two methods of virtual screening. The first one is pharmacophore-based virtual screening where a model is designed to take advantage of key chemical features of a group of compounds that are known to bind to the target proteins. These features aid in identifying compounds that align with the requirements of the model. Some successful examples are the development of MDM2 and Bcl-xL inhibitors.[24, 25] The second method is structure-based

screening where the approach depends on identifying key hot spots in the binding site of the targeted protein. In this method the screened compounds are docked into the binding site and the binding affinity is predicted. Using this approach, several inhibitors has been successfully identified against MDM2 and β -catenin.[26, 27]

2.3 Reported Mcl-1 inhibitors

Myeloid cell leukemia-1 (Mcl-1) is a member of the anti-apoptotic Bcl-2 family proteins. [28] Increased levels of anti-apoptotic Bcl-2 proteins are connected with the maintenance of malignant diseases, resistance to chemotherapy, and poor clinical outcomes. [29] Strategies seeking to inhibit the function of anti-apoptotic Bcl-2 proteins have been extensively studied for developing novel cancer therapies. [30] Previous studies employing different approaches identified a number of promising Mcl-1 inhibitors with unique scaffolds. As discussed in chapter 1, Obatoclax is a pan-inhibitor of Bcl-2 family of anti-apoptotic proteins (Figure 2.1). [31] Several analogs were developed based on Obatoclax scaffold such as pyrrolyl-methylene-pyrrolyl-indole (SC-2001) [32], which shows more potent cellular activity compared to Obatoclax.[33] Another pan-inhibitor is Gossypol with a binaphthalene scaffold.[34] Apogossypol (Sabutoclax), a more potent derivative of Gossypol, is developed based on the same scaffold. Other derivatives of Gossypol, such as BI97C10 and BI112D1, were also developed. [35-37] TW-37 is a second generation benzenesulphonyl derivative of Gossypol which exhibits pan inhibition to anti-apoptotic proteins. [38] Several unique scaffolds were reported as selective Mcl-1 inhibitors. For example, **MIM1** with a methylthiazol scaffold exhibits low micromolar inhibition of Mcl-1 [39]. As mentioned in Chapter 1, we described small-molecule selective Mcl-1 inhibitors (**UMI-77** and compound **21**) with hydroxynaphthalen-arylsulfonamide core scaffolds, and demonstrated their on-target cellular activity [40], activity in pancreatic cancer [41, 42] and acute myeloid leukemia cells [43].

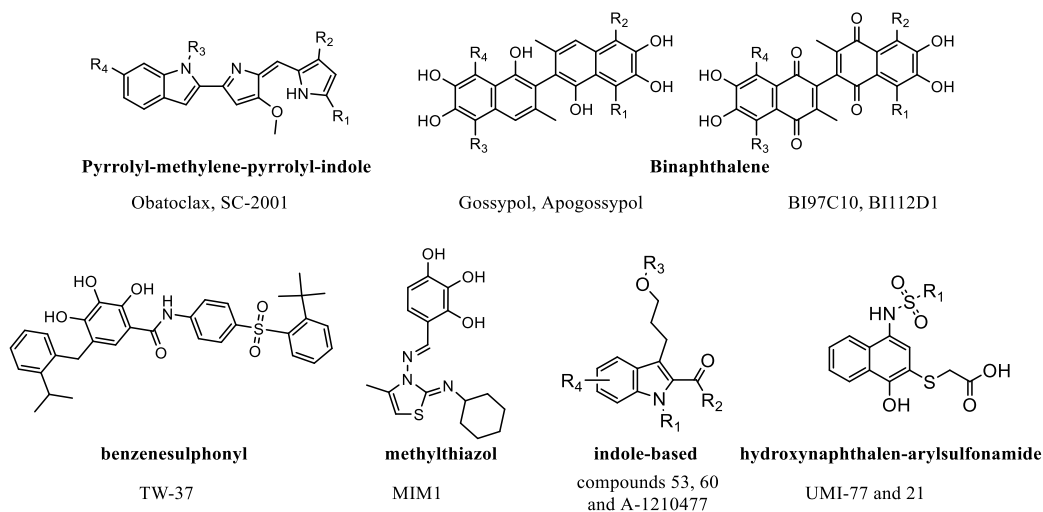


Figure 2.1. Reported scaffolds of small-molecule Mcl-1 inhibitors.

Recently, two groups described the synthesis of Mcl-1 inhibitors containing indole-2-carboxylic acid cores. Fesik's group described the synthesis of Mcl-1 inhibitors (**53** and **60**) with low nanomolar and subnanomolar binding affinities respectively, but the compounds lack sufficient permeability and failed to show cellular activity.[22, 44] Abbvie group developed an Mcl-1 inhibitor (A-1210477) with subnanomolar affinity and on-target cellular activity in cell lines that rely on Mcl-1 for survival, but no *in vivo* efficacy studies were conducted with this compound.[45, 46]

All of the above reported inhibitors with their unique scaffolds are targeting the BH3-binding groove to inhibit the function of anti-apoptotic Bcl-2 family proteins. [29, 30] Each of the six members of the anti-apoptotic Bcl-2 family proteins, Bcl-2, Bcl-xL, Mcl-1, Bcl-2, Bcl-w and A1, has 8 – 9 α -helices and a ~ 20 Å hydrophobic cleft, the “BH3-binding groove”. As described in Chapter 1, the BH3 domain of the pro-apoptotic Bcl-2 family proteins possesses four conserved hydrophobic residues with three to four residues apart (Figure 1.3b), which insert into the four hydrophobic pockets (P1-4 pockets) within the BH3-binding groove of the anti-apoptotic Bcl-2 family proteins (Figure 2.2). Additionally, a conserved aspartic acid forms a salt bridge with a conserved arginine on the anti-apoptotic Bcl-2 family proteins. [30] These Mcl-1 inhibitors, as demonstrated by the X-ray crystallography and Heteronuclear Single Quantum Coherence NMR spectroscopy (^1H , ^{15}N HSQC NMR) studies coupled with docking studies, can mimic at least two

conserved interactions of the four interactions observed for the BH3-only peptides (hydrophobic interactions in the P2, P3 and P4 pockets and hydrogen bonds with the conserved Arg 263).

In order to identify and enrich the diversity of the chemical scaffolds as Mcl-1 inhibitors, and at the same time to take advantage of the structural information and interactions between pro- and anti-apoptotic proteins, we applied an integrated screening approach by combining HTS and structure-based virtual screening approaches.

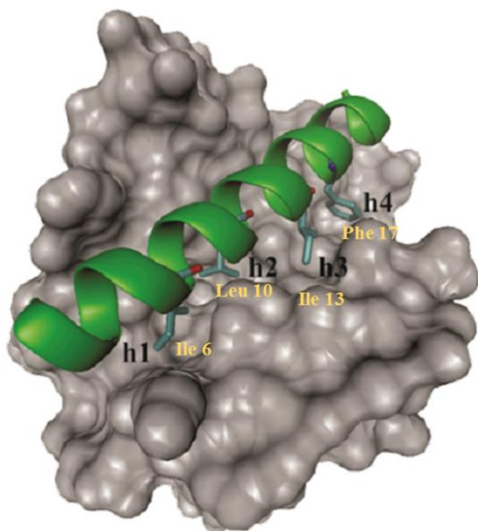


Figure 2.2. Interaction of conserved residues of pro-apoptotic proteins with anti-apoptotic proteins. Mcl-1 and Bim complex structure (PDB ID: 2PQK)

2.4 Results

2.4.1 Integrated screening for identification of novel small-molecule Mcl-1 inhibitors

PubChem, hosted by the NIH, is a free public repository for the chemical structures and their biological results, contributed by more than a hundred organizations. [47, 48] Three interconnected databases comprise PubChem: Substance, BioAssay, and Compound. Bioactivity information generated by high-throughput screenings (HTS) and medicinal chemistry studies is deposited in the BioAssay database. [49, 50] It holds bioactivity results from more than 1600 HTS programs and covers around 10000 unique protein targets and 30,000 gene targets with over 130 million bioactivity outcomes and thus makes it an excellent resource for the chemical biology and the drug discovery community. [49, 50] This is reflected by the fact that the number of research

publications using the PubChem chemical library and bioassay data has increased rapidly since the launch of PubChem. [51]

We have previously reported two optimized ultra-HTS time-resolved fluorescence resonance energy transfer (TR-FRET) based assays to screen 102,255 compounds. The results from this screen were deposited into the PubChem's BioAssay Database as: AID 1417 reporting the dose response confirmation of Mcl-1/Noxa interaction inhibitors[52], and AID 1418 dose response confirmation for Mcl-1/Bid interaction inhibitors[53]. 875 compounds, identified with AID 1417 assay and 509 compounds from AID 1418 assay with 170 common compounds, were confirmed after secondary dose dependent screening.

In order to incorporate the known structural information between pro- and anti-apoptotic proteins, a computational structure-based screening strategy was integrated in the next step. This was followed by biochemical and biophysical binding methods to validate and confirm the identified inhibitors to the Mcl-1 protein (Figure 2.3)

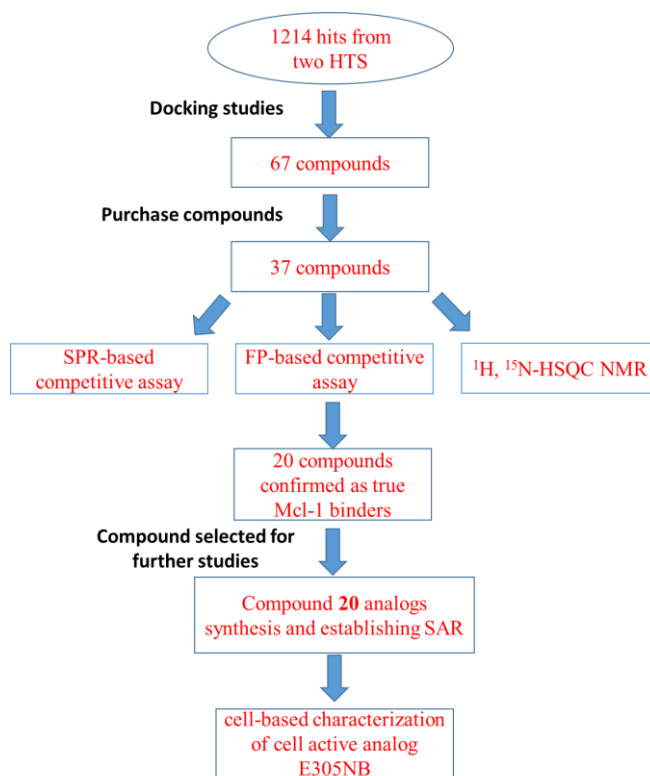


Figure 2.3. Workflow of the validation of the Mcl-1 inhibitors and further optimization of compound 20.

The 1214 identified hits from the two performed HTS assays were docked into the active site of the Mcl-1 protein using the X-ray co-crystal structure between Noxa BH3 peptide and Mcl-1 (PDB ID: 2NLA). The goal of integrating structure-based screening was to determine whether or not these compounds could dock into the BH3 binding groove of the Mcl-1 protein and mimic the conserved interactions of the BH3-only peptides with Mcl-1. [54] Considering the high flexibility and adaptability of the anti-apoptotic Bcl-2 family proteins, the Schrödinger's Induced Fit Docking (IFD) protocol was employed for the docking studies. [55],[56] The center of the grid box of the Mcl-1 that was used in the virtual screening was defined by the Phe 270 (in the p2 pocket), Val 220 (in the p3/p4 pocket), Val 216 (in the p4 pocket), as well as charged Arg 263.

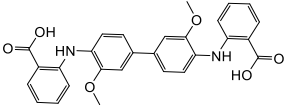
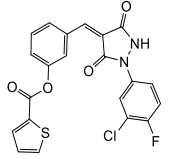
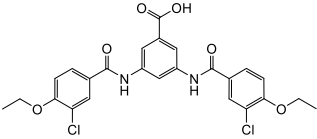
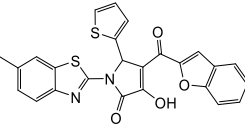
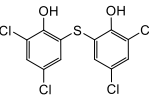
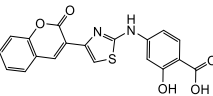
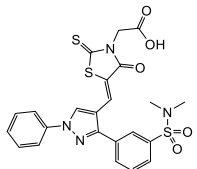
Generated docking poses were visually examined for predicted binding geometries and analyzed the interactions between the compounds and the Mcl-1 protein. 67 compounds with reasonably predicted poses that mimicked at least two conserved interactions of BH3 peptides with the Mcl-1 protein (hydrophobic interactions with p1, p2, p3, or p4, and hydrogen bond interaction with the Arg 263 residue) were selected for further studies. 37 compounds were purchased to be carefully validated as potential Mcl-1 inhibitors. The chemical structures of these compounds cover a diverse chemical space (Table 2.1).

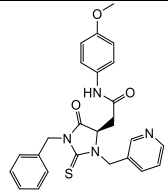
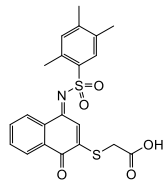
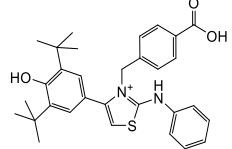
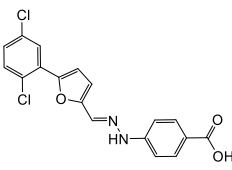
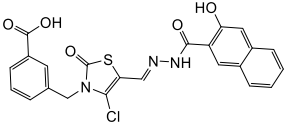
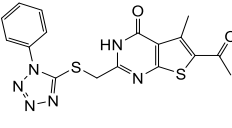
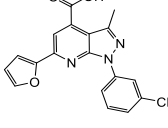
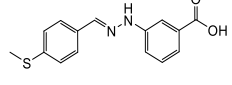
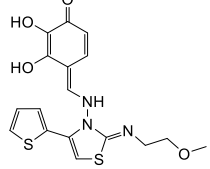
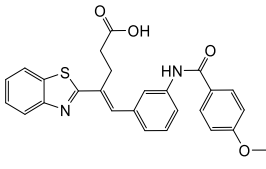
2.4.2 Biochemical assays and ^1H , ^{15}N HSQC NMR validation experiments

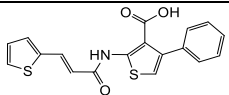
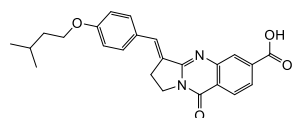
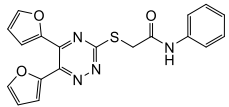
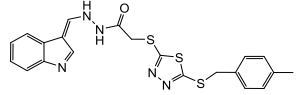
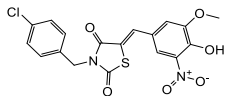
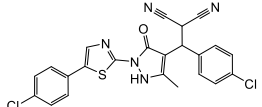
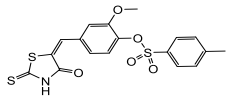
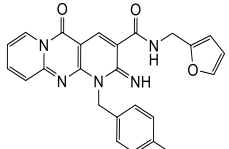
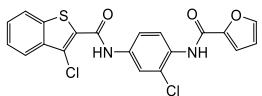
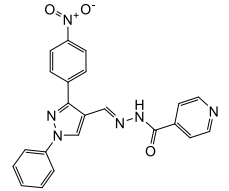
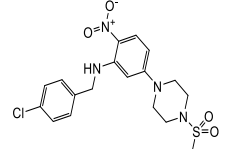
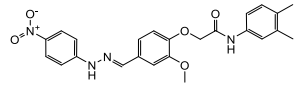
To validate the most promising from the list of 37 potential Mcl-1 inhibitors obtained after integrated screening, we applied biochemical and biophysical methods. Using established and optimized FP-based competitive assay, with Flu-BID-BH3 peptide as the fluorophore probe and the SPR-based competitive binding assays using biotin (BL) labeled Bim BH3 peptide, would allow us to demonstrate that these inhibitors can competitively displace different BH3 proapoptotic proteins. The biophysical method, ^1H , ^{15}N HSQC NMR spectroscopy was conducted to conclusively confirm that identified compounds directly bind to Mcl-1 protein. Assigning residues of ^{15}N labeled Mcl-1 protein allowed us to identify the residues which show chemical shift, map the binding site, support the predicted docking pose, and confirm that the compounds bind to the BH3-binding groove. Twenty compounds (labeled from **1** to **20**) were confirmed with these three binding assays. Their chemical structures and binding results are presented in Table 2.1. Fourteen compounds showed similar binding affinities to the HTS results in one or both SPR and FP assays.

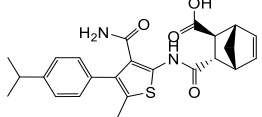
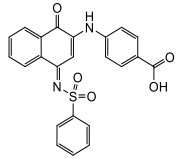
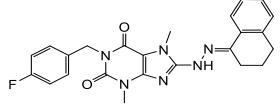
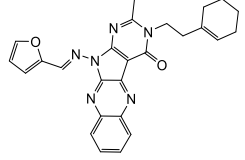
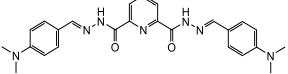
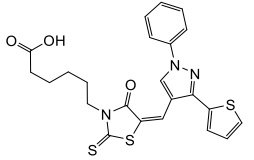
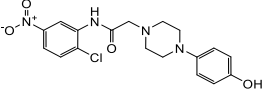
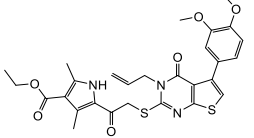
Two compounds, **13** and **29**, showed auto fluorescence, and thus were tested only with SPR competitive binding assay and HSQC NMR. Compound **13** was confirmed in both of these assays. Compound **29** showed significant lower IC₅₀ value in the SPR competitive binding assay, 25 to 50 fold, in comparison with the HTS dose response data, so we did not proceed to test this compound with HSQC NMR assay.

Table 2.1. Binding results of the assayed 38 selected compounds.

Cpd	Structure	IC ₅₀ (μM, FP)	IC ₅₀ (μM, SPR)	IC ₅₀ HTS 1417 (μM) ^a	IC ₅₀ HTS 1418 (μM) ^b	NMR (+ or -)
1		2.58±0.36	3.80±1.80	1.52	0.85	+
2		5.86±1.24	8.84±2.71	7.17	N.D.	+
3		9.59±2.45	21.27±5.41	14.28	N.D.	+
4		2.36±1.13	4.46±0.28	2.37	N.D.	+
5		1.87±0.17	4.14±0.36	1.90	1.67	+
6		39.42±4.30	31.98±7.65	5.58	N.D.	+
7		23.72±3.24	18.68±11.50	4.80	N.D.	+

8		5.15±1.91	11.67±4.07	N.D.	26.82	+
9		16.51±1.38	4.86±2.38	7.55	N.D.	+
10		1.21±0.22	2.69±0.36	2.01	0.66	+
11		5.45±1.68	3.68±0.19	2.17	N.D.	+
12		9.43±3.81	2.79±0.86	3.74	N.D.	+
13		N.D.	10.70±4.20	1.71	N.D.	+
14		17.87±2.10	66.08±7.98	9.55	N.D.	+
15		1.86±0.63	1.70±0.48	2.19	N.D.	+
16		2.65±0.98	6.50±2.20	5.17	N.D.	+
17		39.00±9.37	19.99±1.71	4.32	N.D.	+

18		23.66±1.64	14.91±0.69	N.D.	0.54	+
19		11.14±1.76	50.02±9.27	7.19	N.D.	+
20		13.77±1.39	13.44±0.20	3.11	N.D.	+
21		17.00±3.06	33.80±5.80	3.91	0.53	-
22		N.C.	N.C.	7.21	16.95	N.D. ^d
23		N.C.	N.C.	1.7	N.D.	N.D.
24		N.C.	N.C.	3.44	9.94	N.D.
25		N.C.	N.C.	3.14	N.D.	N.D.
26		N.C.	N.C.	N.D.	0.89	N.D.
27		N.C.	N.C.	N.D.	1.85	N.D.
28		N.C.	N.C.	N.D.	1.76	N.D.
29		N.D.	47.88±24.90	1.84	0.87	N.D.

30		140.70±18.82	>100	N.D.	0.57	N.D.
31		N.C.	N.C.	2.91	0.46	N.D.
32		N.C.	N.C.	2.91	0.58	N.D.
33		N.C.	N.C.	4.90	N.D.	N.D.
34		N.C.	N.C.	1.15	N.D.	N.D.
35		N.C.	N.C.	2.31	9.29	N.D.
36		N.C.	N.C.	5.07	N.D.	N.D.
37		N.C.	N.C.	N.D.	0.84	N.D.

^a This is the IC₅₀ value deposited into PubChem's BioAssay (AID 1417: Dose Response Confirmation for Mcl-1/Noxa Interaction Inhibitors).

^b This is the IC₅₀ value deposited into PubChem's BioAssay (AID 1418: Dose Response Confirmation for Mcl-1/Bid Interaction Inhibitors).

^c N.C. Not confirmed. ^d N.D. Not determined.

Compound **21** was confirmed in both biochemical assays, but we were not able to confirm the direct binding to Mcl-1 using HSQC NMR because of low solubility and precipitation in the sample. The remaining compounds (**22** to **37**) were considered as non-confirmed due to their unfavorable binding behavior either in the FP or SPR assays or both assays. The non-confirmed compounds were not tested further in the ¹H,¹⁵N HSQC NMR experiments. In Figure 2.3 the

binding modes of selected validated hit compounds **9**, **14**, **15**, **16** and **20** along with the corresponding obtained ^1H , ^{15}N HSQC NMR data are presented. Data for the remaining confirmed compounds can be accessed in the Chapter Appendix.

It was confirmed that all compounds bind to the BH3 binding groove. Compound **9** occupies the p2 and p3 hydrophobic pockets in Mcl-1, thus mimicking the two conserved interactions between p2 and p3, conserved hydrophobic residues from the BH-3 mNoxaB, Leu78 and Ile81 present in 2NLA, respectively (Figure 2.3a). The trimethylphenyl group occupied the p2 pocket and Val243, Met250, Val253, Leu267 and Phe270 residues are highly perturbed in the obtained NMR. The naphthalenyl ring of **9** resides in the p3 pocket where Val220 showed significant chemical shift. The carboxylic group of **9** forms hydrogen bond interactions with Arg263 similar to the conserved aspartate in pro-apoptotic BH-3 proteins. This is confirmed by the significant perturbation of this residue. As a result, the binding model derived from the docking model aligns well with the chemical shift perturbations generated from the HSQC NMR experiments. It should be noted that the scaffold of **9** closely resembles the class of selective Mcl-1 inhibitors that was developed by our group based on another HTS performed at the University of Michigan, providing further validation of the integrated screening strategy. [41, 43]

Based on the predicted binding model generated from molecular docking (Figure 2.3b) hit compound **14** interacted with the p2 and p3 pockets. The proposed model is in accordance with the obtained ^1H , ^{15}N HSQC NMR data where the 3-chlorophenyl moiety's occupation of the p2 pocket was proven by chemical shift perturbations of Val243, Val249, Met250, and Val253 residues. In the docking model, the 6-furyl occupied the interface of P2 and P3 pockets, and Phe270 and Met231 were observed as highly perturbed in the NMR. In addition, Arg263 residue was also showing perturbations, confirming the proposed interaction with the 4-carboxylic acid of **14**.

In the docking studies, confirmed hit compound **15** was predicted to occupy the Mcl-1 p2 pocket while its benzoic acid part interacted with the Arg263 residue (Figure 2.3c). Using HSQC NMR, we observed significant perturbations in the Met231, Val243, Met250, Val253, and Phe270, all pointing to the potential interaction of the ligand with the Mcl-1 p2 pocket. Arg263 was also significantly perturbed, which was in accordance with the proposed docking interaction of the carboxylic group present in **15**. Our group developed a series of Mcl-1 inhibitors based on this validated hit, and recently published the patent describing this class of compounds.[57]

Compound **41** binding mode suggested interactions with the p2 and p3 Mcl-1 hydrophobic pockets (Figure 2.3d). Significant NMR shifts were observed for Val243, Val253 and Phe270 residues being in line with the predicted interaction exhibited by the thiophene moiety of **16** with the Mcl-1 p2 pocket. Arg263 residue also showed perturbation in the HSQC NMR experiment which provided more confidence in the predicted interaction of the 2-hydroxy phenyl moiety of **16** with this residue. Interestingly, compound **16** possesses a similar scaffold to a reported Mcl-1 inhibitor, MIM1, by the Walensky group, outlining another compound to validate the applied screening procedure with literature data.[39]

The binding of the hit compound **20 (E238)** to the Mcl-1 protein was also analyzed based on the determined HSQC NMR (Figure 2.3e). As previously confirmed compounds, the analysis of the obtained HSQC chemical shift changes displayed that compound **20** affected several amino acid residues forming the Mcl-1 BH3-binding groove. The significant NMR shifts of several p2 residues Lys234 and Leu235 confirmed the generated docking model of **20**, where the terminal phenyl ring occupies the pocket. Arg263 was also significantly perturbed in the NMR studies, which aligned with the predicted interaction with oxygen of the furan ring.

More precisely, in the produced IFD binding model, hydrogen bonds formed by the oxygen atom of one furan ring, one nitrogen atom of the triazine ring of compound **20**, and two residues (Asp 263 and Asn 260 of the protein of Mcl-1), can be observed mimicking the conserved aspartate in pro-apoptotic BH3 proteins. The phenyl ring of **20** projects into the conserved hydrophobic pocket 2 (p2), mimicking one conserved hydrophobic residue of many different BH3 peptides. Additionally, another furan ring has weak hydrophobic interaction with residues of Phe318 and Phe319, which are proximal to the p4 pocket. These two residues contribute to the additional hydrophobic contacts with a hydrocarbon staple of a reported stabilized α -helix of the Bcl-2 domain.[39, 58] The sulfur-acetamide chain did not have direct interactions with the protein of Mcl-1, playing the role as a linker. With the confirmed binding of **20 (E238)** and the relatively facile synthetic modification that could be applied on that compound, we decided to proceed by synthesizing several analogs based on the 1,2,4-triazine scaffold, outlining the exemplary next step in the drug discovery pipeline after the validation of the hit compound.

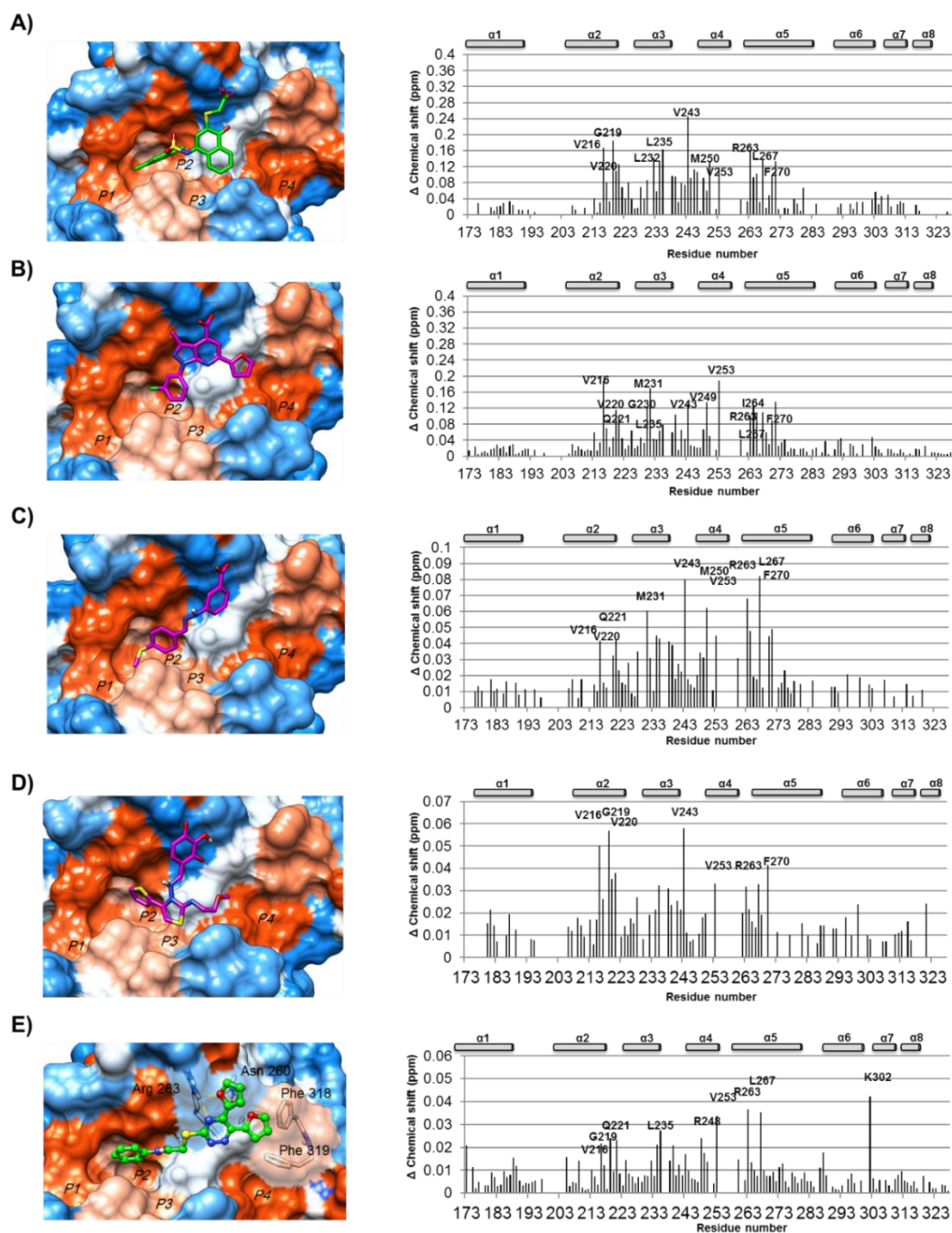


Figure 2.3. Predicted binding poses and the HSQC NMR analysis of the selected hit compounds 9 (A), 14 (B), 15 (C), 16 (D) and 20 (e). Left: Computational predicted binding poses of the hit compounds in Mcl-1 binding site using the mNoxa BH3 peptide-bound Mcl-1 crystal structure (PDB ID: 2NLA). Orange: hydrophobic surface of the protein; blue: hydrophilic surface of the protein. The hydrogen bonds are indicated by magenta lines. Right: Chemical shift

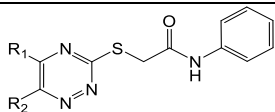
differences for Mcl-1 in the presence of these corresponding compounds (2 equivalents) against residue number.

2.4.3 SAR investigation of the validated hit compound 20

We wanted to gain further insight into the structure-activity relationship (SAR) of the validated hit compound **E238** (**20**), 2-[(5,6-di-2-furanyl-1,2,4-triazin-3-yl)thio]-N-phenylacetamide, with the determined IC_{50} value of $13.77 \pm 1.39 \mu\text{M}$ in the FP assay of Mcl-1 inhibitors. Compound **E238** was selected since it showed good potential for synthetic optimization, and we also tested the binding of **E238** to Bcl-2 and Bcl-xL proteins, and we were pleased to establish that no binding could be detected up to $100 \mu\text{M}$ (Table 2.5). This data motivated us to proceed with the re-synthesis of **E238** and further probe the proposed binding mode and provide additional structure-activity relationship (SAR) of this validated Mcl-1 hit compound. Our goal was to primarily examine the importance of the furan interaction with Arg263 and also produce derivatives that would probe the interactions with the Mcl-1 p2 binding pocket. It should be noted that Resynthesized **E238** compound showed the same behavior as the commercial sources in all binding assays. The inhibition of all synthesized compounds was tested using FP-assay and binding of selected active compounds was further investigated using SPR and TR-FRET experiments.

When replacing the furan with thiophene or phenyl rings, the inhibition of new compounds **E309** and **E323** to Mcl-1 was significantly decreased (Table 2.2). The main reason could be the orientation requirement of the hydrogen bond between Mcl-1 Arg 263 and the ligands. Compound **E325**, where the two furan rings were replaced with two pyridine rings, also did not show inhibition, indicating the importance of the proper hydrogen bond placement for the successful interaction with Mcl-1 Arg 263 residue.

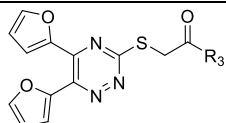
Table 2.2. Exploring the influence of substituting the two five-membered furan moieties R1 and R2 in the initial hit compound E238.



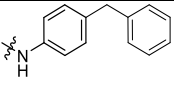
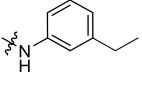
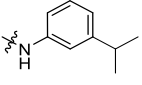
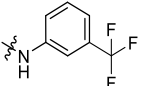
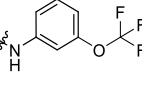
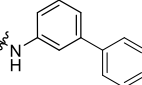
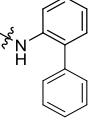
Cpd	R ₁	R ₂	FP IC ₅₀ [μM]	FP Ki [μM]	SPR IC ₅₀ [μM]	TR-FRET IC ₅₀ [μM]
E238			13.77±1.39	3.23±0.33	13.44±0.20	11.90±3.65
E309			>100	>25	>100	>100
E323			>20	>5	>100	N.D.
E325			>50	>12.5	>100	N.D.

When analyzing the available Mcl-1 structural data, it can be established that its p2 binding pocket is relatively larger in volume compared to the other three pockets of the BH3 binding groove, therefore, to enhance the affinity against Mcl-1, we tried to introduce more hydrophobic moieties. Compounds **E63** – **E262** with various substitutions introduced to the phenyl end of the thioacetamide linker were synthesized to probe this change (Table 2.3). Firstly, the para substitution on the benzene ring was explored. The added short alkyl group on the para position of the phenyl ring in compounds **E63** (IC₅₀ = 4.98±0.25 μM) and **E215** (IC₅₀ = 2.27±0.65 μM) showed improved affinity over **E238**. This improvement was shown to be dependent on the nature of the substitutions: when at the para position the methoxy or phenoxy groups were introduced in **E225** and **E357** respectively, the affinity dropped to IC₅₀ = 33.06±7.69 and 6.87±1.90 μM respectively.

Table 2.3. Measured Mcl-1 inhibition properties for the series of compounds that explore the influence of variation of the R3 group interacting with the Mcl-1 p2 pocket.



Cpd	R ₃	FP IC ₅₀ [μM]	FP Ki [μM]	SPR IC ₅₀ [μM]	TR-FRET IC ₅₀ [μM]
E238		13.77±1.39	3.23±0.33	13.44±0.20	11.90±3.65
E63		4.98±0.25	1.17±0.06	14.25±2.01	5.53±1.77
E215		2.27±0.65	0.53±0.15	11.62±1.12	N.D.
E225		33.06±7.69	7.76±1.80	47.38±3.88	N.D.
E357		6.87±1.90	2.83±0.78	N.D.	8.97±3.79
E326		>100	>25	>100	>80
E329		>100	>25	>100	N.D.
E217		8.09±0.79	1.90±0.18	12.47±1.65	11.56±4.00
E232		2.49±0.07	0.58±0.02	5.1±2.27	4.96±2.73

E346		2.52±0.59	0.59±0.14	4.21±0.39	5.12±1.46
E229		5.27±0.45	1.24±0.11	N.D.	N.D.
E221		2.62±0.25	0.61±0.06	N.D.	N.D.
E305		5.09±0.48	1.19±0.11	6.3±0.62	7.13±2.81
E343		2.71±0.44	0.64±0.10	5.3±2	4.02±1.69
E263		4.14±1.50	0.62±0.19	7.3±2.12	7.93±4.66
E262		4.40±0.45	1.03 ±0.11	1.94±0.67	12.73±4.50

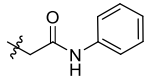
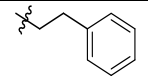
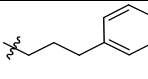
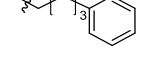
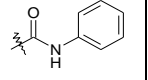
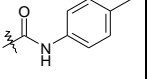
This indicated that introduction of polar oxygen reduces the binding activity. This was also confirmed when attaching amino group at the para position of the phenyl ring of **E238**, resulting in a complete loss of inhibition affinity in compounds **E326**, **E329**. Fluorine atom at the para position in **E217** showed comparable inhibition to **E238**, and introduction of the additional phenyl or benzyl moiety at the para position in **E232** or **E346** respectively resulted in similar binding to **E215**, indicating that introduction of bulkier hydrophobic moieties does not significantly improve the binding for this class. Further investigation with introduced various bulkier substitutions in compounds from **E229** to **E262** were in line with this observation (Table 2.3).

In the final series of compounds, we substituted the amide in **E238** with a two carbon linker, yielding **E245** with improved activity. Shortening of this linker length by one carbon in **E244** slightly reduced activity and increasing the linker length in **E284** preserved the activity. When the triazine ring was changed to the rigid fused quinoxaline ring in compounds **E311** and **E312**, inhibition was abrogated, confirming that flexible smaller parts are crucial for successful

binding (Table 2.4). We performed competitive SPR and TR-FRET experiments and in most cases the results align nicely with the discussed SAR FP binding data.

The selectivity profiles of the hit compound and several potent analogs, **E305**, **E245**, and **E284** were determined against other members of the Bcl-2 family, namely Bcl-2 and Bcl-xL (Table 2.5). All compounds showed selective binding against Mcl-1, as observed for the starting hit compound **20**. Importantly, the new designed and synthesized compound had improved selectivity profile and did not show binding to Bcl-2 or Bcl-xL up to 100 μM .

Table 2.4. Determining the effect of variation of the R3 and R4 groups on binding to Mcl-1.

Cpd	R3	R4	FP IC ₅₀ [μM]	FP Ki [μM]	SPR IC ₅₀ [μM]	TR-FRET IC ₅₀ [μM]
E238		-	13.77 \pm 1.39	3.23 \pm 0.33	13.44 \pm 0.2	11.90 \pm 3.65
E244		-	2.15 \pm 0.22	0.50 \pm 0.05	N.D.	5.20 \pm 0.05
E245		-	1.50 \pm 0.29	0.35 \pm 0.07	N.D.	2.39 \pm 0.07
E284		-	1.36 \pm 0.17	0.32 \pm 0.03	N.D.	2.49 \pm 0.03
E311	-		>50	>12.5	N.D.	N.D.
E312	-		67.10 \pm 9.07	15.75 \pm 2.31	N.D.	N.D.

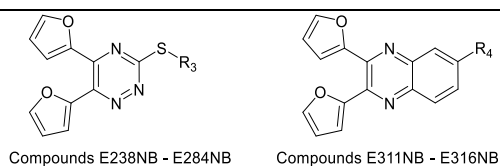


Table 2.5. Selectivity profile of E238 and other analogs.

Compounds	Mcl-1	Mcl-1	Bcl-2	Bcl-2	Bcl-xL	Bcl-xL
	IC ₅₀ ± SD (μM)	K _i ± SD (μM)	IC ₅₀ ± SD (μM)	K _i ± SD (μM)	IC ₅₀ ± SD (μM)	K _i ± SD (μM)
E238	13.77±1.39	3.23±0.33	>100	>23.6	>100	>20
E305	5.09±0.48	1.19±0.11	>100	>23.6	>100	>20
E245	1.50±0.29	0.35±0.07	>100	>23.6	>100	>20
E284	1.36±0.17	0.32±0.03	>100	>23.6	>100	>20

2.4.4 Using model cell lines to better understand the cellular activity of E305

The activity of the apoptosis effectors Bak and Bax can be suppressed by multidomain anti-apoptotic proteins such as Mcl-1. If cell death induction is specifically mediated by Mcl-1 protein, Bax or Bak would be required for release of cytochrome *c* and subsequent cell death. Bax and Bak are considered as major players in triggering apoptosis, and inhibitors of anti-apoptotic proteins (e.g. Mcl-1) are expected to induce cell death in a Bax/Bak-dependent manner.[59] In order to explore the mechanism of **E305** cellular activity, we used murine embryonic fibroblasts (MEFs) wild-type (WT) and either Bax or Bak knockout in addition to Bax/Bak double knockout (DKO). Treating WT MEFs with **E305** for 15 h results in a dose-dependent increase of cell death, detected by propidium iodide (PI) as shown of (Figure 2.4a). The knockout of either or both Bax and Bak rescued the cells from the effect of **E305**, indicating that the presence of both Bax and Bak is necessary to induce cell death using our Mcl-1 inhibitor.

The target specificity of this class of inhibitors was further confirmed using the reported retroviral transduced lymphoma cells isolated from Eμ-myc transgenic mice, which differ only in their expression of anti-apoptotic Bcl-2 family proteins. [60] Lymphoma cells overexpressing Mcl-1, Bcl-2 or Bcl-xL were treated with increasing concentrations of **E305** for 15 h and the cell viability was determined by flow cytometry using the fluorescent reactive dye (LIVE/DEAD fixable violet stain kit). Eμ-myc cells overexpressing Mcl-1 showed sensitivity to **E305** in a concentration-dependent manner. On the contrary, **E305** was significantly less effective against Eμ-myc cells overexpressing Bcl-2 or Bcl-xL (Figure 2.4b). This confirms that **E305** selectively binds to Mcl-1 with no effect on Bcl-2 and Bcl-xL, which is consistent with the selectivity profile based on the FP-based assay (Table 2.5).

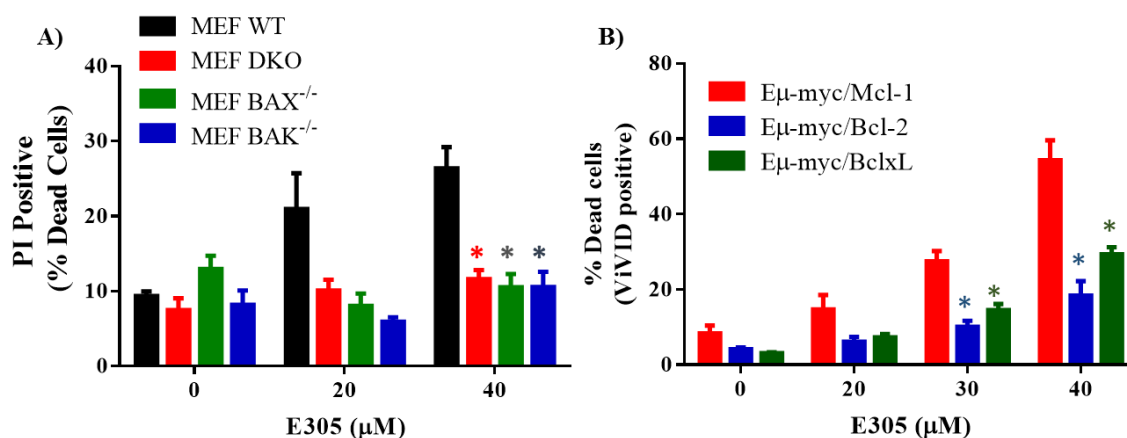


Figure 2.4. Mcl-1 inhibitor E305 induce Bax/Bak-dependent cell death to MEFs and on-target Mcl-1 cell activity. (A) MEFs were treated for 15 h with increasing concentrations of **E305**. Cell viability was assessed using propidium iodide staining detected with flow cytometry. (*) is $p < 0.05$. (B) Cells were treated for 15 h with increasing concentrations of **E305**. The percentage of dead cells was calculated using LIVE/DEAD fixable violet dead cell stain (ViVID) and detected with flow cytometry. (*) is $p < 0.05$

2.5 Conclusions

Mcl-1 is a validated target of importance in the progression of cancer and resistance of cancer cells to chemotherapies and radiation. It has been shown that for the apoptosis to occur, both arms of the anti-apoptotic proteins (Mcl-1 and Bcl-2/Bcl-xL) need to be neutralized.[61, 62] In this article, we have identified Mcl-1 inhibitors with novel scaffolds using results from the two previously reported HTS campaigns (AID: 1417 and 1418) deposited into PubChem's BioAssay Database. These HTS assays were conducted to experimentally screen a large database of 102,255 compounds in an attempt to discover small molecular inhibitors that disrupt the interaction between Mcl-1 protein and its binding partners: Noxa (HTS AID: 1417), a specific Mcl-1 binding BH3-only protein that exhibits selectivity to Bcl-2 family proteins; and Bid (HTS AID: 1418), a

broad acting BH-3 only protein that binds Mcl-1 as well as other anti-apoptotic proteins, including Bcl-2 and Bcl-xL.

After analyzing the docking poses of 1214 hits and identifying 67 compounds that mimic at least two conserved interactions that BH3 peptides have with the Mcl-1 protein, we purchased 37 compounds. These compounds were then fully characterized with different biochemical and biophysical methods to validate their binding to the Mcl-1 protein. Among the most potent identified compounds, 20 new chemical scaffolds were confirmed as true binders to Mcl-1. To further develop the medicinal chemistry of these validated hits, SAR of the experimentally confirmed hit **20 (E238)** was synthetically elaborated followed by selectivity and cell-based studies to gain more insight into this class of Mcl-1 inhibitors.

Overall, this approach aims to highlight the advantages of integrating the structure-based searching strategy with experimental methods for analyzing available results deposited in the PubChem's BioAssay Database and as such represents a useful tool for identifying the most promising leads for the purpose of drug discovery. In addition, synthetic and cell-based elaboration of the selected validated hit will also be highlighted showing the exemplary next step in the drug discovery pipeline. This study and presented approach will guide the drug discovery community, especially those who do not have immediate access to the HTS facilities, on how to obtain valuable hits for further medicinal chemistry or chemical biology purposes by using the public resource of PubChem's BioAssay database.

In addition, we have successfully explored SAR of one discovered Mcl-1 hit compound **E238** with the 5,6-difuran-2-yl-1,2,4-triazine core by synthesizing several novel derivatives. In this phase we exemplified the succeeding step in the drug discovery pipeline after validation of the hit compounds. The hit compound **E238** was chosen since it also showed selectivity to Mcl-1 versus Bcl-2 and Bcl-xL. The SAR studies led to the development of Mcl-1 inhibitors that were ten times more potent, e.g. **E284**. Selected cell-based experiments conducted using MEFs and Eμ-myc lymphoma model cell lines showed that the optimized compound **E305** can selectively target the Mcl-1 protein and induce selective Bax- and Bak-dependent cell death. These synthesized compounds outline that hit compound **20** uncovered a promising class of compounds, paving the way to efficient Mcl-1 inhibitors for the treatment of complex tumors.

In this study, we tried to depict the added value of the utilization of PubChem's BioAssay Database in the hit identification process for the drug discovery community. These datasets

provide a vast amount of bioactivity results from hundreds of preformed HTS programs. HTS is a valuable tool to identify active compounds against a particular target and is a starting point for the medicinal chemistry community. However, HTS is mostly out of reach for standard utilization in smaller academic groups. This workflow shows, for academics as well as researchers in industry, an example of taking advantage of PubChem's BioAssay Database, with the integration of computational and experimental pipelines to screen these libraries of potential hits, identify and validate real binders for a particular target, and further develop them using medicinal chemistry.

2.6 Materials and methods

High throughput screening compounds

37 compounds were purchased from Sigma-Aldrich (1), SPECS (2-4,22,23), Princeton biomolecular research (5-9, 21,24-31), Interbioscreen (10-12,32-34), and Enamine (13-19,35-37).

Molecular Modeling

The chemical structures of the 1384 compounds from the two performed HTS campaigns, AIDs 1417 and 1418, were downloaded from PubChem's Bioassay database as two sdf files. After removing 170 duplicated compounds, LigPrep 2.5 of the Schrödinger suite was employed to convert them into 3D structures.[63] Glide 5.6 SP of the Schrödinger suite was used to dock the remaining 1214 compounds into the Mcl-1 active site.[64, 65] The PDB ID of the employed Mcl-1 structure is 2NLA, which also contains bound BH3-only peptide Noxa. At the same time, Schrödinger's IFD was also employed for the docking studies, to consider the flexibility of the Mcl-1 protein. Schrödinger's IFD predicts ligand binding modes and concomitant structural changes in the protein by combining Glide (the docking program of Schrödinger) and the refinement module in Prime (the protein structure prediction program of Schrödinger). Its main application is to generate an accurate complex structure for a ligand known to be active but that cannot be docked in a rigid structure of the receptor. IFD was used in our study because it incorporates protein flexibility as well as ligand flexibility, which is important for accurate docking, especially when the protein is showing increased levels of flexibility experimentally. The docking protocol that was used for the IFD studies consisted of the following steps: (1) Constrained

minimization of the protein with an RMSD cutoff of 0.18 Å. (2) Initial Glide docking of the ligand using a softened potential (Van der Waals radii scaling). (3) One round of Prime side-chain prediction for each protein/ligand complex, on residues within defined distance of any ligand pose. (4) Prime minimization of the same set of residues and the ligand for each protein/ligand complex pose. (5) Glide re-docking of each protein/ligand complex structure within a specified energy of the lowest energy structure. (6) Estimation of the binding energy (IFDScore) for each output pose. In our study, all docking calculations were run in the extra precision (XP) mode of Glide. During both docking studies, the center of the grid box of Mcl-1 was defined by Val 249 (in h1), Phe 270 (in h2), Val 220 (in h3/h4) and Val 216 (in h4). The size of the grid box was set to 15 Å. Default values were used for all other parameters.

Protein purification

His-tagged proteins containing Human Mcl-1 (residues 171–323), Bcl-2 (The isoform 2 construct of the human Bcl-2), and Bcl-xL (Human Bcl-xL protein, which has an internal deletion for the 45-85 amino acid residues and a C-terminal truncation for the amino acid residues 212-233) were expressed from the pHis-TEV vector (a modified pET vector) in *E. coli* BL21 (DE3) cells. Cells were grown at 37 °C in 2×YT containing antibiotics to an OD600 density of 1.5, 1, and 0.8 for Mcl-1, Bcl-xL, and Bcl-2 respectively. Protein expression was induced by 0.4 mM IPTG at 20 °C overnight. Cells were lysed in 20 mM HEPES pH 7.5, 200 mM NaCl, 0.1% βME, and 40 μL of Leupeptin/Aprotinin (Mcl-1), 25mM Tris pH 8.5, 200mM NaCl (Bcl-2), and 50mM Tris pH 7.5, 200 mM NaCl (Bcl-xL). All proteins were purified from the soluble fraction using Ni-NTA resin (QIAGEN), following the manufacturer's instructions. For purification of TEV-cleaved protein, the amino terminal His tag was cleaved by incubation with TEV protease and the protein was further purified by anion exchange (Source Q) and gel filtration chromatography (Superdex 75, Amersham Biosciences) in 20mM HEPES pH 7.0, 50 mM NaCl (Mcl-1), 25 mM Tris pH 8.5, 150 mM NaCl, 0.1% βME (Bcl-2), and 20 mM Tris pH 7.5, 150 mM NaCl, 0.1% βME (Bcl-xL). His-tagged Mcl-1 protein was used for TR-FRET assay and HSQC-NMR. His-TEV cleaved Mcl-1, Bcl-2 and Bcl-xL were used in fluorescent polarization and surface plasmon resonance binding assays.

Fluorescence polarization based binding assay

FP-based binding assays were developed and optimized to determine the binding affinities of Bcl-2 family protein inhibitors to the recombinant Mcl-1, Bcl-2, and Bcl-xL proteins. Fluorescein tagged Bid peptide (Flu-Bid) was used as a fluorescent probe in the FP-based binding assays. One fluorescein tagged Bid peptide named Flu-Bid (generously provided by Dr. Shaomeng Wang) was labeled with fluorescein on the N-terminus of the BH3 peptide (79-99), while the second tracer was purchased from Abgent (Catalog # SP2121a), named FAM-Bid, where the BH3 peptide (80-99) is labeled with 5-FAM. Their K_d values were determined for Mcl-1, Bcl-2, and Bcl-xL with a fixed concentration of the tracer (2 nM of Flu-Bid and FAM-Bid) and different concentrations of the tested proteins, in a final volume of 125 μ L in the assay buffer (20 mM phosphate pH 7.4, 50 mM NaCl, 1 mM EDTA and 0.05% Pluronic F68). Plates were mixed and incubated at room temperature for 3 hours and the polarization values in millipolarization units (mP) were measured at an excitation wavelength of 485 nm and an emission wavelength of 530 nm. Equilibrium dissociation constants (K_d) were calculated by fitting the sigmoidal dose-dependent FP increases as a function of protein concentrations using Graphpad Prism 6.0 software (Graphpad Software). Based upon analysis of the dynamic ranges for the signals and their K_d values, Flu-Bid was selected as the tracer in the Mcl-1 competitive binding assays, while FAM-Bid was selected as the tracer for Bcl-2 and Bcl-xL. In our saturation experiments, the K_d value of Flu-Bid with Mcl-1 was 3.04 ± 0.06 nM, and the K_d values of FAM-Bid with Bcl-2 was 18.44 ± 1.40 nM, and to Bcl-xL was 20.04 ± 2.34 nM respectively. For testing of purchased compounds based on the K_d values, the concentrations of the proteins used in the competitive binding experiments were 20 nM of Mcl-1 with Flu-Bid in assay buffer (50 mM Tris pH 7.4, 50 mM NaCl and 0.005% Tween 20). For testing the synthesized library of compounds based on compound **47**, we used 10 nM of Mcl-1 with Flu-Bid for Mcl-1, and 60 nM and 80 nM of FAM-Bid with Bcl-2 and Bcl-xL respectively, in assay buffer (20 mM potassium phosphate, pH 7.5; 50 mM NaCl, 1 mM EDTA and 0.05% Pluronic F68). The fluorescent probes, Flu-Bid and FAM-Bid were fixed at 2 nM for all assays. 5 μ L of the tested compound in DMSO and 120 μ L of protein/probe complex in the assay buffer were added to assay plates (Corning #3792), incubated at room temperature for 3 h, and the polarization values (mP) were measured at an excitation wavelength at 485 nm and an emission wavelength at 530 nm using the plate reader Synergy H1 Hybrid, BioTek. IC_{50} values were determined by nonlinear

regression fitting of the competition curves (GraphPad Prism 6.0 Software). The K_i values were calculated as described previously.

Surface plasmon resonance (SPR) based binding assay

The solution competitive SPR-based assay was performed on Biacore 2000. N terminal biotin-labeled Bim BH3 peptide (141–166 amino acids) was immobilized on streptavidin (SA) chip giving a density of 800 RU (Response Units). The preincubated Mcl-1 protein (20 nM), with tested small-molecule inhibitors for at least 30 min, was injected over the surfaces of the chip with two minutes of association and one minute of dissociation using assay buffer HBS-P (GE, #BR100368). Response units were measured at 15 s in the dissociation phase, and binding was calculated by subtracting the control surface (Fc1) signal from the surfaces with immobilized biotin-labeled Bim BH3. IC_{50} values were determined by nonlinear least-squares analysis using GraphPad Prism 6.0 software.

Time-resolved fluorescence energy transfer (TR-FRET) binding assay

TR-FRET was performed using black 384-well plates in an Envision Multilabel plate reader (PerkinElmer Life Sciences). To each well, a mixture of 10 nM Bid-Dy647 peptide (79-99), 10 nM Mcl-1 protein, and Eu-W1024 anti-6xHis antibody (1 nM, PerkinElmer) were added to a final volume of 25 μ L in the assay buffer (20 mM potassium phosphate, pH 7.5; 50 mM NaCl, 1.3 mM EDTA and 0.05% Pluronic F68). The TR-FRET signals were measured with an Envision Multilabel plate reader after 2 h of incubation, (Ex 337 nm, Em1 655 nm and Em2 615 nm) and expressed as FRET signal ratio ($F_{665nm} / F_{615nm} * 104$)

1H , ^{15}N HSQC NMR

NMR studies were performed as previously described.[43] In brief, for 1H , ^{15}N -HSQC NMR studies, ^{15}N -labeled Mcl-1 proteins were prepared and purified using the same protocol as for unlabeled protein, with the exception that the bacteria were grown on M9 minimal media supported with 1 g/L of $(^{15}NH_4)_2SO_4$. Protein samples were prepared in a 20 mM sodium phosphate, 150 mM NaCl and 1 mM DTT solution at pH 7 in 7% D_2O . The binding mode of compounds was

characterized with a solution of uniformly ^{15}N -labeled Mcl-1 ($75\mu\text{M}$) in the absence and presence of added compounds (in 1 or 6% final DMSO), with the indicated molar ratio concentrations. Total volume of each sample was $150\ \mu\text{L}$, and samples were prepared in Bruker tubes (Bruker, # Z117724). All Spectra were acquired at $30\ ^\circ\text{C}$ on a Bruker 600 MHz NMR spectrometer equipped with a cryogenic probe, processed using Bruker TopSpin and rNMR[66], and were analyzed with Sparky.[67] Plots of chemical shift changes were calculated as $((\Delta^1\text{H ppm})^2 + (0.2(\Delta^{15}\text{N ppm}))^2)^{0.5}$ of Mcl-1 amide upon addition of compound. The absence of a bar in a chemical shift plot indicates no chemical shift difference, or the presence of a proline or residue that is overlapped or not assigned.

Cell viability assays

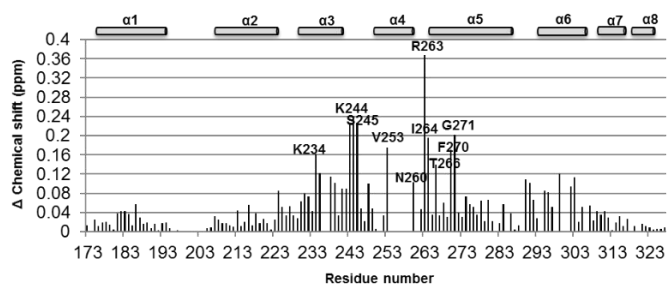
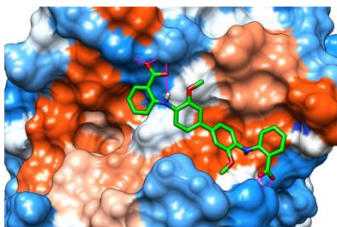
MEFs cells, wild type, Bax knock out, Bak knock out, Bax/Bak double knock out, and Mcl-1 knock out were gifts from Dr. Shaomeng Wang at the University of Michigan and were cultured in DMEM (Life Technologies), supplemented with 10% fetal bovine serum (FBS) (Thermo Scientific HyClone) and 1% Penicillin/streptomycin solution (Life Technologies). The retroviral transduced lymphoma cells isolated from $\text{E}\mu$ -myc transgenic mice were gifts from Ricky W. Johnstone at the University of Melbourne, Melbourne, Australia and cultured as previously described. 80 PANC-1 was obtained from the American Type Culture Collection (ATCC). The cells were cultured in DMEM (Life Technologies), supplemented with 10% FBS and 1% Penicillin/streptomycin solution. MEFs cells were seeded in 24-well plates at 0.5×10^5 cells/well, left to adhere for 5 hours and then treated for 15 hours with increasing concentrations of the compounds. The cells were harvested, washed with phosphate-buffered saline (PBS), and stained with 0.025 mg/ml propidium iodide (MP Biomedicals). The percentage of propidium iodide positive population was determined by flow cytometry and calculated using WinList 3.0. The Mcl-1, Bcl-2, and Bcl-xL retroviral transduced lymphoma $\text{E}\mu$ -myc cells were seeded in 12-well plates at 0.5×10^6 cells/well. They were treated with different concentrations of tested compounds for 16 hours. The cells were harvested and stained with violet LIVE/DEAD Fixable Dead Cell Stain Kit (Invitrogen) according to manufacturer's protocol. The percentage of fluorescent positive cells was determined by flow cytometry and calculated using WinList 3.0.

2.7 Contributions

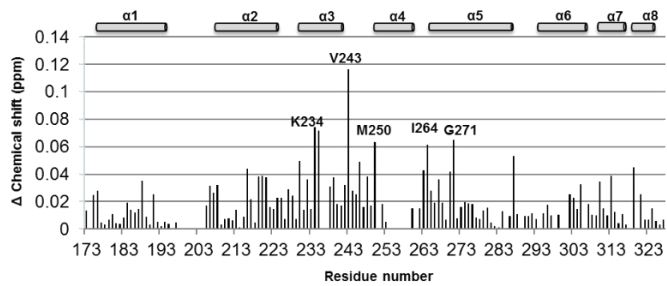
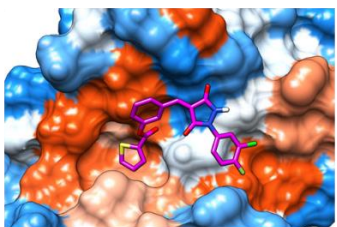
Ahmed Mady performed FP and SPR binding assays as well as the cell-based assays. Dr. Naval Bajwa synthesized all E-compounds except **E357**, which was synthesized by Dr. Lei Miao. Dr. Chenzhong Liao performed all the molecular docking studies and contributed to the design of analogs. Dr. Fardokht Abulwerdi expressed and purified labeled Mcl-1, prepared NMR samples, and analyzed HSQC NMR data. Expression and purification of all proteins was performed in Dr. Jeanne Stuckey lab at LSI. TR-FRET binding assays were performed by Dr. Yuhong Du in Dr. Haiyan Fu's lab at Emory University.

2.8 Appendix

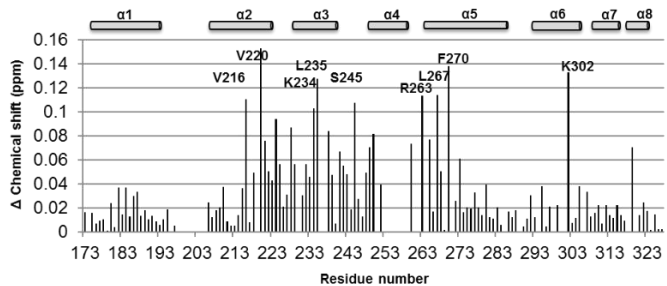
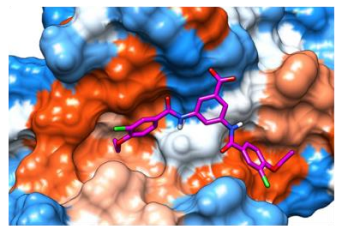
1)



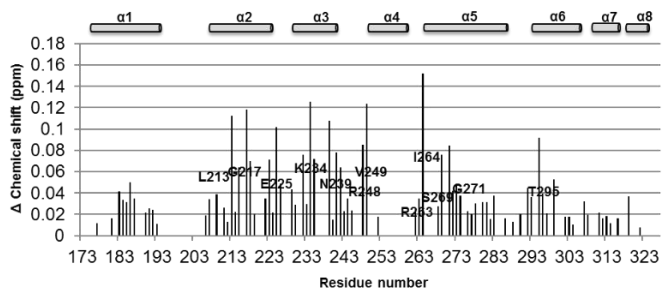
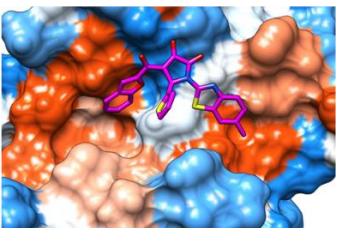
2)



3)



4)



5)

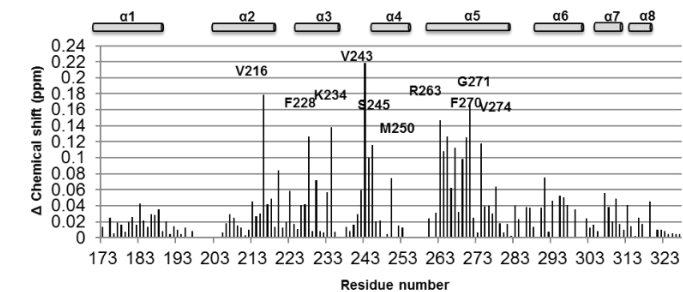
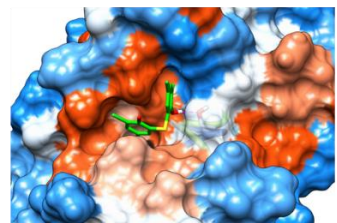


Figure 2.5. Predicted binding poses and the HSQC NMR analysis of the confirmed compounds 1,2,3,4 and 5.

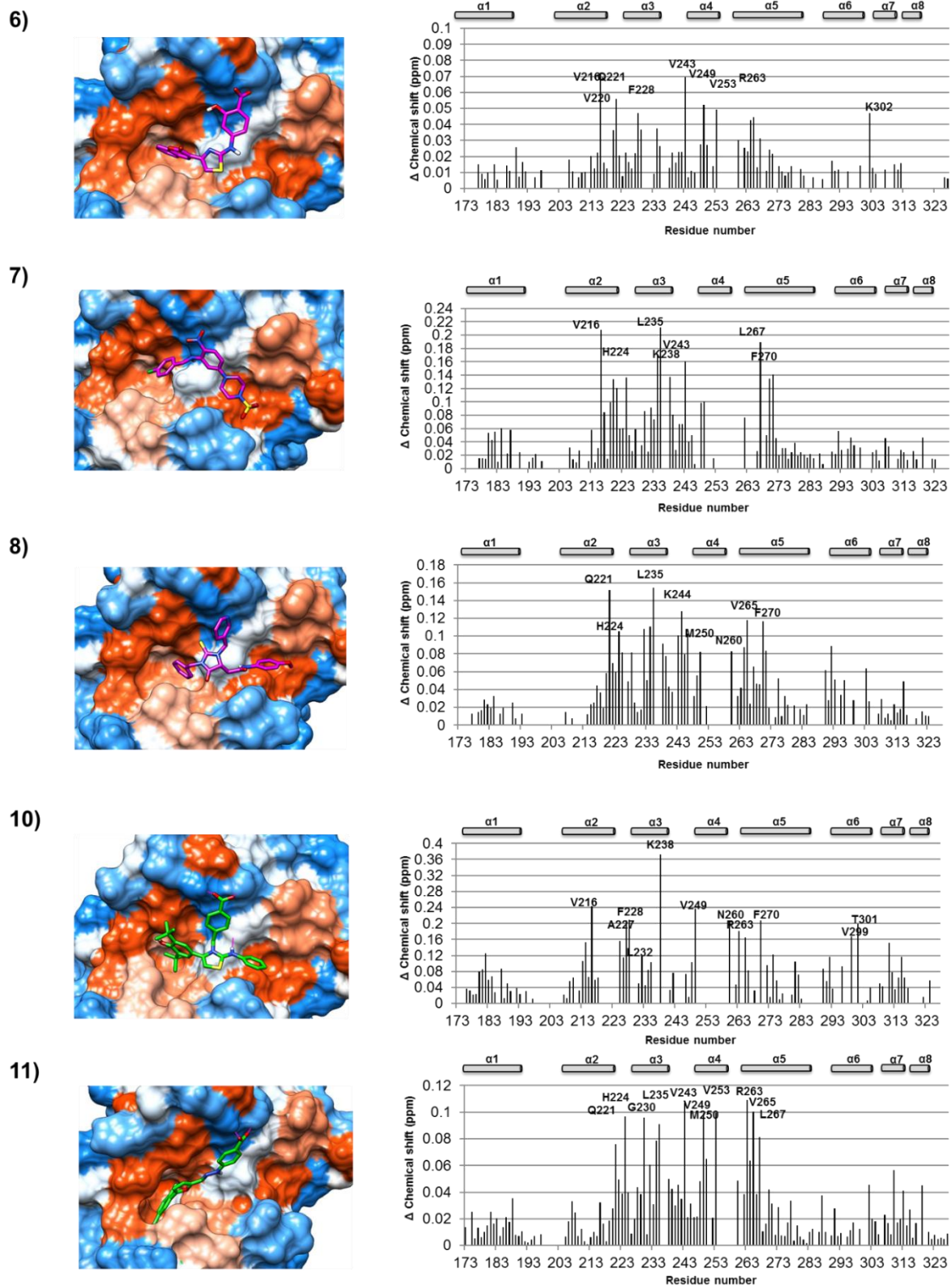
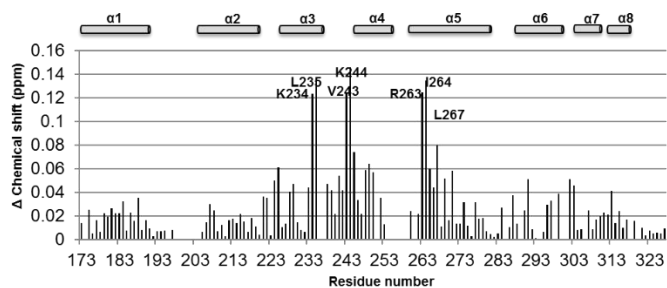
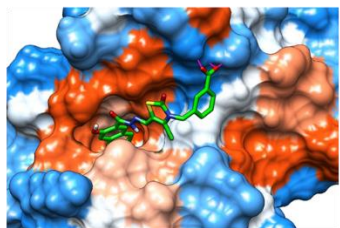
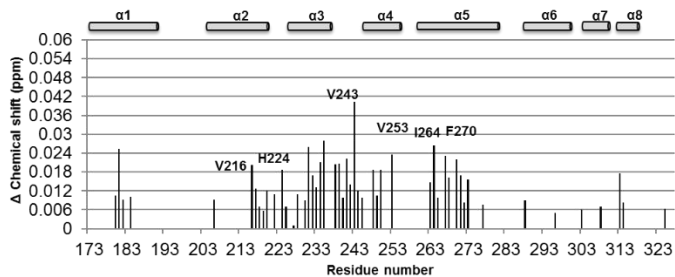
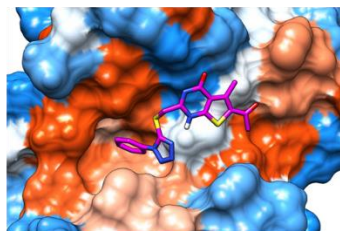


Figure 2.6. Predicted binding poses and the HSQC NMR analysis of the confirmed compounds 5, 6, 7, 8, and 10.

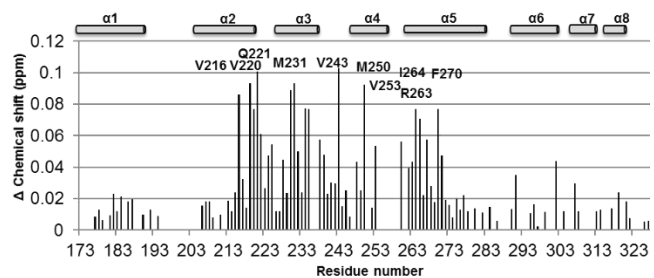
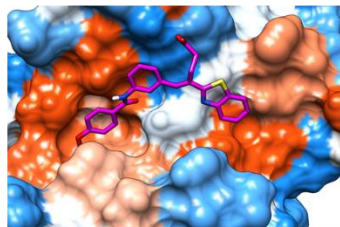
12)



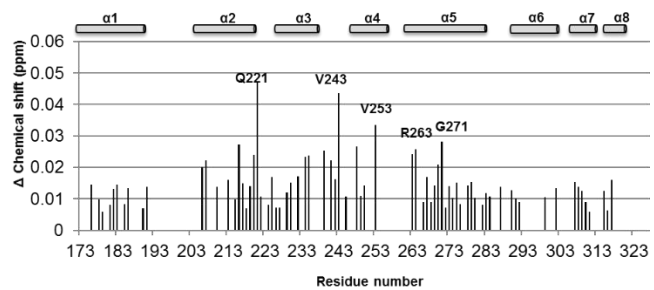
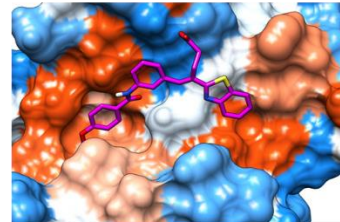
13)



17)



18)



19)

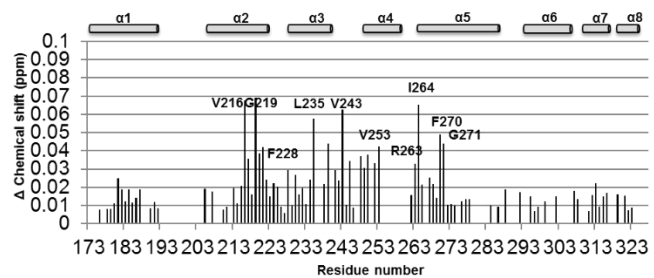
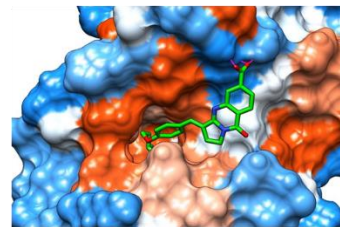


Figure 2.7. Predicted binding poses and the HSQC NMR analysis of the confirmed compounds 12, 13, 17, 18, and 19.

2.9 References

- [1] Wells JA, McClendon CL. Reaching for high-hanging fruit in drug discovery at protein-protein interfaces. *Nature*. 2007;450:1001-9.
- [2] Blundell TL, Burke DF, Chirgadze D, Dhanaraj V, Hyvonen M, Innis CA, et al. Protein-protein interactions in receptor activation and intracellular signalling. *Biol Chem*. 2000;381:955-9.
- [3] Lipinski CA, Lombardo F, Dominy BW, Feeney PJ. Experimental and computational approaches to estimate solubility and permeability in drug discovery and development settings. *Adv Drug Deliv Rev*. 2001;46:3-26.
- [4] Hennessy BT, Smith DL, Ram PT, Lu Y, Mills GB. Exploiting the PI3K/AKT pathway for cancer drug discovery. *Nat Rev Drug Discov*. 2005;4:988-1004.
- [5] Lau N, Feldkamp MM, Roncari L, Loehr AH, Shannon P, Gutmann DH, et al. Loss of neurofibromin is associated with activation of RAS/MAPK and PI3-K/AKT signaling in a neurofibromatosis 1 astrocytoma. *J Neuropathol Exp Neurol*. 2000;59:759-67.
- [6] Hannan F, Ho I, Tong JJ, Zhu Y, Nurnberg P, Zhong Y. Effect of neurofibromatosis type I mutations on a novel pathway for adenylyl cyclase activation requiring neurofibromin and Ras. *Hum Mol Genet*. 2006;15:1087-98.
- [7] Shiozaki EN, Chai J, Rigotti DJ, Riedl SJ, Li P, Srinivasula SM, et al. Mechanism of XIAP-mediated inhibition of caspase-9. *Mol Cell*. 2003;11:519-27.
- [8] Yip KW, Reed JC. Bcl-2 family proteins and cancer. *Oncogene*. 2008;27:6398-406.
- [9] Nag S, Qin J, Srivenugopal KS, Wang M, Zhang R. The MDM2-p53 pathway revisited. *J Biomed Res*. 2013;27:254-71.
- [10] Maelandsmo GM, Florenes VA, Hovig E, Oyjord T, Engebraaten O, Holm R, et al. Involvement of the pRb/p16/cdk4/cyclin D1 pathway in the tumorigenesis of sporadic malignant melanomas. *Br J Cancer*. 1996;73:909-16.
- [11] Kelly TK, De Carvalho DD, Jones PA. Epigenetic modifications as therapeutic targets. *Nature biotechnology*. 2010;28:1069-78.
- [12] Ivanov AA, Khuri FR, Fu H. Targeting protein-protein interactions as an anticancer strategy. *Trends Pharmacol Sci*. 2013;34:393-400.
- [13] Du Y, Nikolovska-Coleska Z, Qui M, Li L, Lewis I, Dingleline R, et al. A dual-readout F2 assay that combines fluorescence resonance energy transfer and fluorescence polarization for monitoring bimolecular interactions. *Assay Drug Dev Technol*. 2011;9:382-93.
- [14] Arkin MR, Glicksman MA, Fu H, Havel JJ, Du Y. Inhibition of Protein-Protein Interactions: Non-Cellular Assay Formats. In: Sittampalam GS, Coussens NP, Nelson H, Arkin M, Auld D, Austin C, et al., editors. *Assay Guidance Manual*. Bethesda (MD)2004.
- [15] Meireles LM, Mustata G. Discovery of modulators of protein-protein interactions: current approaches and limitations. *Curr Top Med Chem*. 2011;11:248-57.
- [16] Winter A, Higuieruelo AP, Marsh M, Sigurdardottir A, Pitt WR, Blundell TL. Biophysical and computational fragment-based approaches to targeting protein-protein interactions: applications in structure-guided drug discovery. *Q Rev Biophys*. 2012;45:383-426.
- [17] Maurer T. Advancing fragment binders to lead-like compounds using ligand and protein-based NMR spectroscopy. *Methods Enzymol*. 2011;493:469-85.
- [18] Valkov E, Sharpe T, Marsh M, Greive S, Hyvonen M. Targeting protein-protein interactions and fragment-based drug discovery. *Top Curr Chem*. 2012;317:145-79.
- [19] Scott DE, Coyne AG, Hudson SA, Abell C. Fragment-based approaches in drug discovery and chemical biology. *Biochemistry*. 2012;51:4990-5003.

- [20] Wu B, Zhang Z, Noberini R, Barile E, Giulianotti M, Pinilla C, et al. HTS by NMR of combinatorial libraries: a fragment-based approach to ligand discovery. *Chemistry & biology*. 2013;20:19-33.
- [21] Lugovskoy AA, Degterev AI, Fahmy AF, Zhou P, Gross JD, Yuan J, et al. A novel approach for characterizing protein ligand complexes: molecular basis for specificity of small-molecule Bcl-2 inhibitors. *J Am Chem Soc*. 2002;124:1234-40.
- [22] Friberg A, Vigil D, Zhao B, Daniels RN, Burke JP, Garcia-Barrantes PM, et al. Discovery of potent myeloid cell leukemia 1 (Mcl-1) inhibitors using fragment-based methods and structure-based design. *J Med Chem*. 2013;56:15-30.
- [23] Miura T, Fukami TA, Hasegawa K, Ono N, Suda A, Shindo H, et al. Lead generation of heat shock protein 90 inhibitors by a combination of fragment-based approach, virtual screening, and structure-based drug design. *Bioorg Med Chem Lett*. 2011;21:5778-83.
- [24] Lu Y, Nikolovska-Coleska Z, Fang X, Gao W, Shangary S, Qiu S, et al. Discovery of a nanomolar inhibitor of the human murine double minute 2 (MDM2)-p53 interaction through an integrated, virtual database screening strategy. *J Med Chem*. 2006;49:3759-62.
- [25] Mukherjee P, Desai P, Zhou YD, Avery M. Targeting the BH3 domain mediated protein-protein interaction of Bcl-xL through virtual screening. *J Chem Inf Model*. 2010;50:906-23.
- [26] Lawrence HR, Li Z, Yip ML, Sung SS, Lawrence NJ, McLaughlin ML, et al. Identification of a disruptor of the MDM2-p53 protein-protein interaction facilitated by high-throughput in silico docking. *Bioorg Med Chem Lett*. 2009;19:3756-9.
- [27] Tian W, Han X, Yan M, Xu Y, Duggineni S, Lin N, et al. Structure-based discovery of a novel inhibitor targeting the beta-catenin/Tcf4 interaction. *Biochemistry*. 2012;51:724-31.
- [28] Thomas LW, Lam C, Edwards SW. Mcl-1; the molecular regulation of protein function. *FEBS Lett*. 2010;584:2981-9.
- [29] Thomas S, Quinn BA, Das SK, Dash R, Emdad L, Dasgupta S, et al. Targeting the Bcl-2 family for cancer therapy. *Expert Opin Ther Targets*. 2013;17:61-75.
- [30] Bajwa N, Liao C, Nikolovska-Coleska Z. Inhibitors of the anti-apoptotic Bcl-2 proteins: a patent review. *Expert Opin Ther Pat*. 2012;22:37-55.
- [31] Nguyen M, Marcellus RC, Roulston A, Watson M, Serfass L, Murthy Madiraju SR, et al. Small molecule obatoclax (GX15-070) antagonizes MCL-1 and overcomes MCL-1-mediated resistance to apoptosis. *Proc Natl Acad Sci U S A*. 2007;104:19512-7.
- [32] Diaz de Grenu B, Iglesias Hernandez P, Espona M, Quinonero D, Light ME, Torroba T, et al. Synthetic prodiginine obatoclax (GX15-070) and related analogues: anion binding, transmembrane transport, and cytotoxicity properties. *Chemistry*. 2011;17:14074-83.
- [33] Chen KF, Su JC, Liu CY, Huang JW, Chen KC, Chen WL, et al. A novel obatoclax derivative, SC-2001, induces apoptosis in hepatocellular carcinoma cells through SHP-1-dependent STAT3 inactivation. *Cancer Lett*. 2012;321:27-35.
- [34] Kitada S, Leone M, Sareth S, Zhai D, Reed JC, Pellecchia M. Discovery, characterization, and structure-activity relationships studies of proapoptotic polyphenols targeting B-cell lymphocyte/leukemia-2 proteins. *J Med Chem*. 2003;46:4259-64.
- [35] Wei J, Kitada S, Rega MF, Stebbins JL, Zhai D, Cellitti J, et al. Apogossypol derivatives as pan-active inhibitors of antiapoptotic B-cell lymphoma/leukemia-2 (Bcl-2) family proteins. *Journal of medicinal chemistry*. 2009;52:4511-23.
- [36] Wei J, Stebbins JL, Kitada S, Dash R, Placzek W, Rega MF, et al. BI-97C1, an optically pure Apogossypol derivative as pan-active inhibitor of antiapoptotic B-cell lymphoma/leukemia-2 (Bcl-2) family proteins. *Journal of medicinal chemistry*. 2010;53:4166-76.

- [37] Wei J, Stebbins JL, Kitada S, Dash R, Zhai D, Placzek WJ, et al. An optically pure apogossypolone derivative as potent pan-active inhibitor of anti-apoptotic bcl-2 family proteins. *Frontiers in oncology*. 2011;1:28.
- [38] Wang Z, Song W, Aboukameel A, Mohammad M, Wang G, Banerjee S, et al. TW-37, a small-molecule inhibitor of Bcl-2, inhibits cell growth and invasion in pancreatic cancer. *Int J Cancer*. 2008;123:958-66.
- [39] Cohen NA, Stewart ML, Gavathiotis E, Tepper JL, Bruekner SR, Koss B, et al. A competitive stapled peptide screen identifies a selective small molecule that overcomes MCL-1-dependent leukemia cell survival. *Chemistry & biology*. 2012;19:1175-86.
- [40] Koss B, Ryan J, Budhreja A, Szarama K, Yang X, Bathina M, et al. Defining specificity and on-target activity of BH3-mimetics using engineered B-ALL cell lines. *Oncotarget*. 2016;7:11500-11.
- [41] Abulwerdi F, Liao C, Liu M, Azmi AS, Aboukameel A, Mady AS, et al. A novel small-molecule inhibitor of mcl-1 blocks pancreatic cancer growth in vitro and in vivo. *Mol Cancer Ther*. 2014;13:565-75.
- [42] Wei D, Zhang Q, Schreiber JS, Parsels LA, Abulwerdi FA, Kausar T, et al. Targeting mcl-1 for radiosensitization of pancreatic cancers. *Transl Oncol*. 2015;8:47-54.
- [43] JAbulwerdi FA, Liao C, Mady AS, Gavin J, Shen C, Cierpicki T, et al. 3-Substituted-N-(4-hydroxynaphthalen-1-yl)arylsulfonamides as a novel class of selective Mcl-1 inhibitors: structure-based design, synthesis, SAR, and biological evaluation. *J Med Chem*. 2014;57:4111-33.
- [44] Pelz NF, Bian Z, Zhao B, Shaw S, Tarr JC, Belmar J, et al. Discovery of 2-Indole-acylsulfonamide Myeloid Cell Leukemia 1 (Mcl-1) Inhibitors Using Fragment-Based Methods. *J Med Chem*. 2016;59:2054-66.
- [45] Bruncko M, Wang L, Sheppard GS, Phillips DC, Tahir SK, Xue J, et al. Structure-guided design of a series of MCL-1 inhibitors with high affinity and selectivity. *J Med Chem*. 2015;58:2180-94.
- [46] Levenson JD, Zhang H, Chen J, Tahir SK, Phillips DC, Xue J, et al. Potent and selective small-molecule MCL-1 inhibitors demonstrate on-target cancer cell killing activity as single agents and in combination with ABT-263 (navitoclax). *Cell death & disease*. 2015;6:e1590.
- [47] Wang Y, Xiao J, Suzek TO, Zhang J, Wang J, Bryant SH. PubChem: a public information system for analyzing bioactivities of small molecules. *Nucleic Acids Res*. 2009;37:W623-33.
- [48] Li Q, Cheng T, Wang Y, Bryant SH. PubChem as a public resource for drug discovery. *Drug Discov Today*. 2010;15:1052-7.
- [49] Wang Y, Xiao J, Suzek TO, Zhang J, Wang J, Zhou Z, et al. PubChem's BioAssay Database. *Nucleic Acids Res*. 2012;40:D400-12.
- [50] Kim S, Thiessen PA, Bolton EE, Chen J, Fu G, Gindulyte A, et al. PubChem Substance and Compound databases. *Nucleic Acids Res*. 2016;44:D1202-13.
- [51] Xie XQ. Exploiting PubChem for Virtual Screening. *Expert Opin Drug Discov*. 2010;5:1205-20.
- [52] National Center for Biotechnology Information. PubChem BioAssay Database; AID=1417, <https://pubchem.ncbi.nlm.nih.gov/bioassay/1417> (accessed Sept. 1, 2013).
- [53] National Center for Biotechnology Information. PubChem BioAssay Database; AID=1418, <https://pubchem.ncbi.nlm.nih.gov/bioassay/1418> (accessed Sept. 1, 2013).
- [54] Czabotar PE, Lee EF, van Delft MF, Day CL, Smith BJ, Huang DC, et al. Structural insights into the degradation of Mcl-1 induced by BH3 domains. *Proc Natl Acad Sci U S A*. 2007;104:6217-22.

- [55] Yang C-Y, Wang S. Analysis of Flexibility and Hotspots in Bcl-xL and Mcl-1 Proteins for the Design of Selective Small-Molecule Inhibitors. *ACS Medicinal Chemistry Letters*. 2012;3:308-12.
- [56] Schrödinger Suite 2010 Induced Fit Docking protocol; Glide version 5.6, Schrödinger, LLC, New York, NY, 2009; Prime version 2.2, Schrödinger, LLC, New York, NY. 2010.
- [57] Nikolovska-Coleska Z, Abulwerdi F, Showalter H, Miao L, Stuckey J, Mady A. Small molecule inhibitors of MCL-1 and uses thereof. US patent 20150284387; 2016.
- [58] Stewart ML, Fire E, Keating AE, Walensky LD. The MCL-1 BH3 helix is an exclusive MCL-1 inhibitor and apoptosis sensitizer. *Nat Chem Biol*. 2010;6:595-601.
- [59] Wei MC, Zong WX, Cheng EH, Lindsten T, Panoutsakopoulou V, Ross AJ, et al. Proapoptotic BAX and BAK: a requisite gateway to mitochondrial dysfunction and death. *Science*. 2001;292:727-30.
- [60] Whitecross KF, Alsop AE, Cluse LA, Wiegman A, Banks KM, Coomans C, et al. Defining the target specificity of ABT-737 and synergistic antitumor activities in combination with histone deacetylase inhibitors. *Blood*. 2009;113:1982-91.
- [61] Choudhary GS, Al-Harbi S, Mazumder S, Hill BT, Smith MR, Bodo J, et al. MCL-1 and BCL-xL-dependent resistance to the BCL-2 inhibitor ABT-199 can be overcome by preventing PI3K/AKT/mTOR activation in lymphoid malignancies. *Cell death & disease*. 2015;6:e1593.
- [62] Punnoose EA, Levenson JD, Peale F, Boghaert ER, Belmont LD, Tan N, et al. Expression Profile of BCL-2, BCL-XL, and MCL-1 Predicts Pharmacological Response to the BCL-2 Selective Antagonist Venetoclax in Multiple Myeloma Models. *Mol Cancer Ther*. 2016;15:1132-44.
- [63] Schrödinger Release 2016-3: LigPrep v, Schrödinger, LLC, New York, NY, 2016.
- [64] Halgren TA, Murphy RB, Friesner RA, Beard HS, Frye LL, Pollard WT, et al. Glide: a new approach for rapid, accurate docking and scoring. 2. Enrichment factors in database screening. *J Med Chem*. 2004;47:1750-9.
- [65] Friesner RA, Banks JL, Murphy RB, Halgren TA, Klicic JJ, Mainz DT, et al. Glide: a new approach for rapid, accurate docking and scoring. 1. Method and assessment of docking accuracy. *J Med Chem*. 2004;47:1739-49.
- [66] Lewis IA, Schommer SC, Markley JL. rNMR: open source software for identifying and quantifying metabolites in NMR spectra. *Magn Reson Chem*. 2009;47 Suppl 1:S123-6.
- [67] Goddard TDK, D. G. SPARKY 3.

CHAPTER 3

Structure-based design of novel potent and selective small-molecule Mcl-1 inhibitors

3.1 Introduction

A drug discovery program usually initiates because of the need to develop interventions against a certain disease or clinical condition. The first step is often performed in academia where a hypothesis is formulated stating that the inhibition or activation of a certain target protein, gene, RNA, or pathway will generate a therapeutic effect. Target identification and validation is a crucial step in the road to drug discovery. [1] The target has to meet an unmet medical need, and to be safe enough that there is an established relationship with the disease without a mechanism-based side effect. The most important characteristic of a target is druggability; the capability to develop small molecules or biologicals that can bind to the target and trigger the desired biological and therapeutic response. The second step is identification of hits through various methods of screening assays. The hits are compounds that show activity towards the target and are confirmed to bind to the target in a dose dependent manner. High throughput screening (HTS) is one of the approaches used in hit identification. Several approaches of HTS have been described in chapter 2, from libraries of small molecules to fragments or using pharmacophores or structure-based virtual screening of compound libraries. HTS can be cell-based, where a certain outcome that correlates with modulating the target is detected when cells are treated with an active compound. The third step of the drug discovery process is identifying a lead compound based on the hit generated from HTS step. The objective is to refine the hits to generate lead compounds with more potent and selective affinity to the target, as well as good physicochemical properties, to test their *in vivo* efficacy. Once a compound reaches that stage, it undergoes PK/PD, toxicity, metabolic stability, and chemical stability studies.

With the collected information about the compound, a drug candidate profile is submitted to regulator authorities for initiating clinical studies on human subjects.

3.2 Structure-based design approach to develop protein-protein interactions modulators

Protein-protein interactions (PPIs) are involved in various cellular processes from signaling pathways of cells to host-pathogen recognition. We now have a vast knowledge of structural data for thousands of these PPIs through X-ray crystallography or nuclear magnetic resonance (NMR). The atomic structures of thousands of protein complexes have been solved by X-ray crystallography and nuclear magnetic resonance spectroscopy.[2] This knowledge enhances our understanding of PPI interfaces and opens the door for computationally designing novel modulators for these PPIs. With the availability of structure of the targeted protein– protein complex or isolated protein partners, inhibitors can be identified using high-throughput docking [3, 4] or pharmacophore models.[5, 6] The protein structure can be further examined to identify druggable pockets for rigorous medicinal chemistry efforts.[7] Consequently, success in developing PPI inhibitors (PPIIs) will rely mainly on the use of computer-aided drug design to guide the high-throughput screening (HTS) campaigns as well as the optimization of hits emerging from these studies. With the improvements in docking algorithms and scoring functions, developing of PPII is still a challenging task.[8] One of the major obstacle is not accounting for protein flexibility in docking. However, this can be solved using induced fit docking or using a collection of conformations of the targeted protein. Several small-molecule PPIIs were developed using structure-based drug design such as inhibitors of Bcl-2, XIAP and MDM2. [9-11]. These success stories are good encouragement to apply structure-based drug design in targeting the anti-apoptotic protein Mcl-1

3.3 Results

3.3.1 Structure based design of novel Mcl-1 inhibitors based on validated HTS hit

Employing a high throughput screening approach, several novel chemical classes were identified as Mcl-1 inhibitors.[12] Cluster analysis revealed different clusters of compounds including a chemical class with 5,6-difuran-2-yl-1,2,4-triazine core structure. The hit compound **E238** (Figure 3.1a), was resynthesized and its binding to Mcl-1 was confirmed with the IC₅₀ value

of $13.8 \pm 1.4 \mu\text{M}$ ($K_i = 3.2 \pm 0.3 \mu\text{M}$) in the fluorescence polarization (FP) assay and TR-FRET based assay (IC_{50} value of $11.9 \pm 3.7 \mu\text{M}$) using a Bid BH3 peptide as a fluorescent probe. The direct and specific binding of **E238** to the Mcl-1 protein was confirmed with the HSQC NMR spectroscopy and the obtained HSQC spectra showed concentration-dependent perturbations of the backbone amide residues (Figure 3.1b). Overall, the analysis of the HSQC chemical shift changes of the compound **E238** in complex with Mcl-1 showed that the **E238** compound affects the residues forming the Mcl-1 BH3-binding groove, and provided conclusive evidence that it binds to the Mcl-1 protein at the same site where the conserved BH3 peptides interact with the Mcl-1 protein. These results also corroborated the predicted binding model of **E238** in complex with Mcl-1, which revealed that the compound forms hydrogen bonds between the oxygen atom of one furan ring and a nitrogen from the triazine core structure of **E238** and the Arg263 residue of Mcl-1, mimicking the conserved aspartate in pro-apoptotic proteins (Figure 3.1c). The phenyl ring of the **E238** projects into the Mcl-1 hydrophobic pocket 2 (p2), mimicking the conserved hydrophobic residue Leu in the BH3 binding motif of BH3-only pro-apoptotic proteins.[13] The second furan ring sits over the p3 pocket and displays weak hydrophobic interaction with the Thr266. The sulfur-amide chain of **E238** did not show direct interactions with Mcl-1, playing the role of a linker.

As stated in Chapter 2, structure activity relationship (SAR) studies of a synthetic library, with more than 50 analogs based on the **E238** validated hit, showed the essential role of one furan ring which forms the conserved hydrogen bond with Arg263 of Mcl-1 based on the predicted binding model (Figure 3.1c). Decorating the phenyl ring with hydrophobic substituents led to improvement of the binding affinity consistent with the binding model, showing that the phenyl ring is embedded in the p2 hydrophobic pocket. Although the binding affinity of novel analogs was improved by 10-folds, the difuran-triazine core limits the synthetic possibilities for further modification. Thus, based on the SAR findings, compound **368LM** was *de-novo* designed (Figure 3.1d), where one furan ring was replaced with carboxylate moiety to preserve the hydrogen bond. Flexible methylene linker was introduced instead of the amide and the other furan ring was replaced with phenylsulfonamide to further explore and improve hydrophobic interactions with the p2 and p4 pockets, respectively. Interestingly, this compound binds to Mcl-1 with a slightly improved binding affinity ($K_i = 1.2 \pm 0.2 \mu\text{M}$) compared to **E238**, and shows significant chemical shift perturbations in ^{15}N -HSQC NMR spectrum indicative of binding to the Mcl-1 BH3-binding

groove (Figure 3.1e). The predicted binding model of **368LM** in the complex with Mcl-1 revealed that the phenethylthio moiety occupies the p2 pocket and has hydrophobic interactions with Leu267, Val253, Val243 and Leu235 residues (Figure 3.1f). The proposed interactions were confirmed with the HSQC NMR experiments, in which these residues showed significant chemical shift perturbations (Figure 3.1e). The carboxylic group formed a hydrogen bond with the Arg263, mimicking the conserved aspartate in pro-apoptotic proteins, similar to the interactions observed with the furan moiety present in the **E238** structure. Indeed, the HCQS NMR spectrum of **368LM**/Mcl-1 complex showed that Arg263 has a significant chemical shift. The benzenesulfonamide was placed above the p3 pocket and showed weak interactions with Thr266, Ala277 and Phe228 (Figure 3.1f). Taken together, in silico docking and HSQC NMR studies provided conclusive evidence that **368LM** binds to the BH3-binding groove of Mcl-1 protein.

3.3.2 SAR investigation of new class of Mcl-1 inhibitors

The first series of compounds was synthesized to explore the position and importance of the R1, benzene sulfonamide, and R2, phenethylthio, substituents on the Mcl-1 binding affinity (Table 3.1). Deletion of the benzene sulfonamide substituent in **416LM** didn't affect the binding affinity and gave very similar K_i value of $1.13 \pm 0.19 \mu\text{M}$ to the lead compound **368LM**. However, deletion of the R2 substitution in **455LM** resulted in a 50-fold decrease of binding affinity, demonstrating that phenethylthio significantly contributes to the binding potency to Mcl-1. These findings are consistent with the predicted binding model showing that phenethylthio is placed in p2 pocket and has network of hydrophobic interactions (Figure 3.1f).

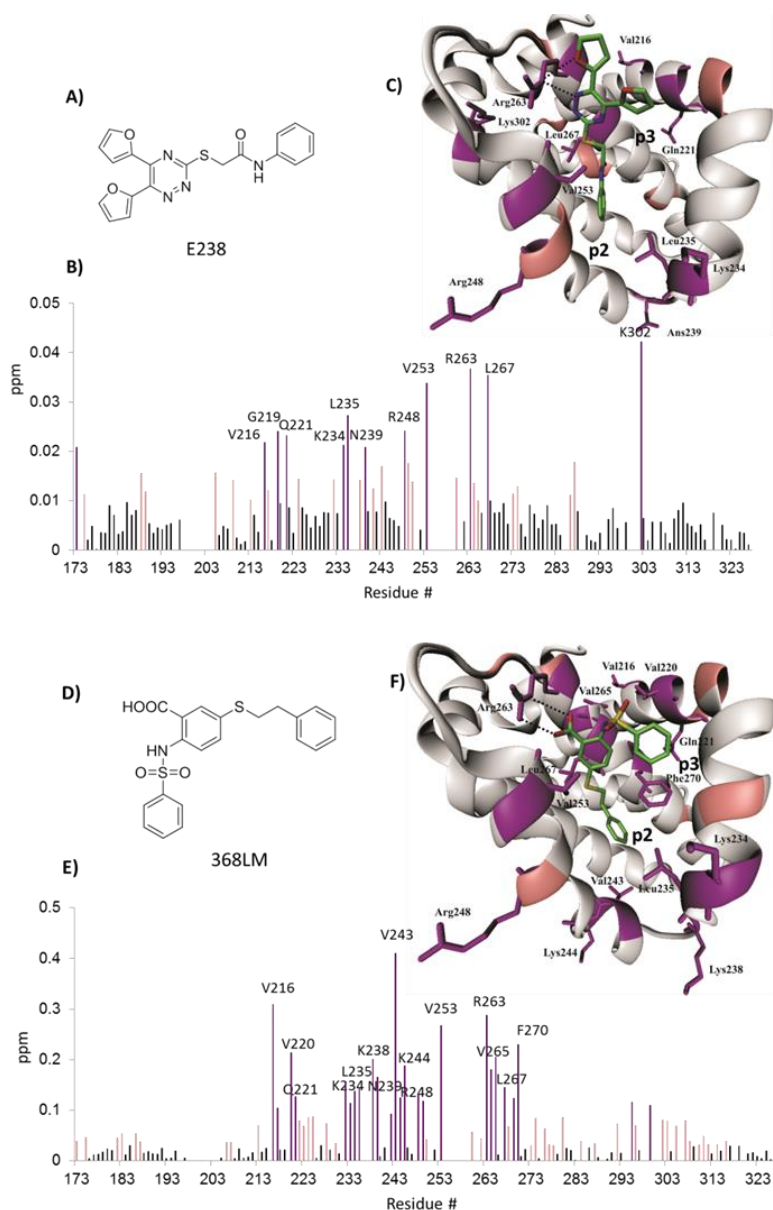
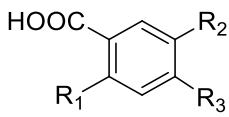
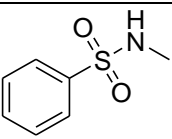
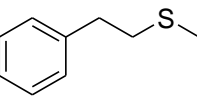
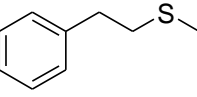
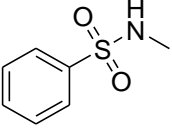
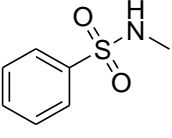
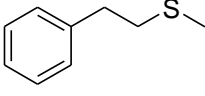
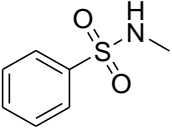
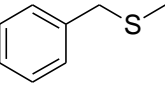
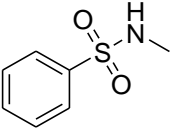
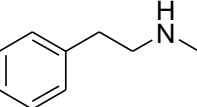
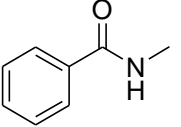
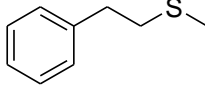


Figure 3.1. Binding models of E238 and 368LM in the BH3 binding pocket of Mcl-1 based on HSQC NMR data. (A) and (D) Chemical structures; (B) and (E) Obtained HSQC NMR chemical shift perturbations; (C) and (F) Predicted binding poses of E238 and designed 368LM compounds in the Mcl-1 binding site (PDB used for binding mode prediction: 4HW2)

The position of the phenethylthio group also plays an important role in binding to Mcl-1, as its introduction at the para position relative to the carboxylic group in **702LL** displayed 9-fold decrease in potency ($K_i = 9.3 \pm 1.0 \mu\text{M}$) compared to **368LM**. One carbon reduction of the aliphatic chain at the R2 position in **392LM** gave 2-fold decrease with K_i of $2.3 \pm 0.2 \mu\text{M}$. Replacing the sulfur atom with the amino group also led to 9-fold reduction in the binding potency ($K_i = 8.7 \pm 2.0 \mu\text{M}$).

Table 3.1.Exploring the SAR of substituted benzoic acid scaffold

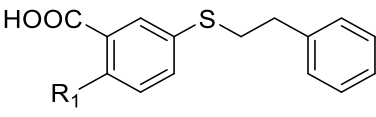
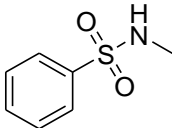
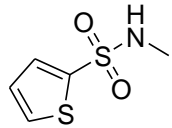
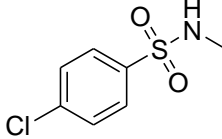
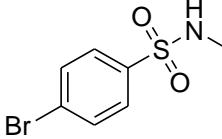
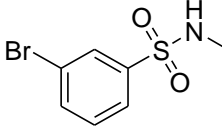
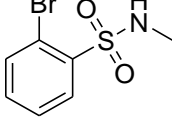
				
N	R₁	R₂	R₃	IC₅₀ (Ki) [μM]
368LM			H	5.0±0.7 (1.2±0.2)
416LM	H ₂ N—		H	4.8±0.8 (1.1±0.2)
455LM		H	H	204.0±16.1 (47.9±3.8)
702LL		H		39.8±4.3 (9.3±1.0)
392LM			H	9.8±0.7 (2.3±0.2)
404LM			H	37.0±8.3 (8.7±2.0)

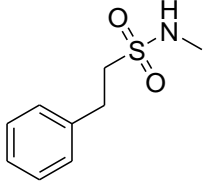
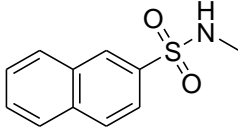
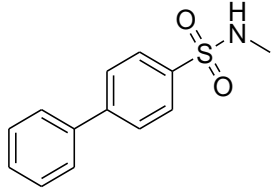
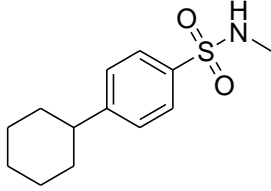
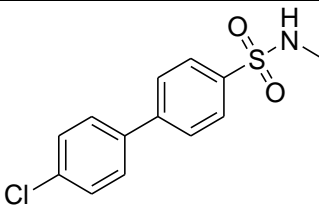
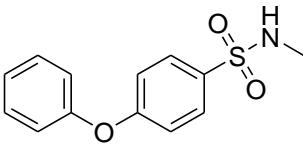
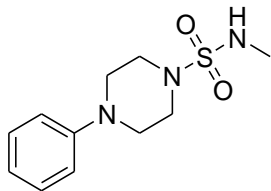
364LM			H	10.4±0.2 (2.4±0.1)
--------------	---	---	---	-----------------------

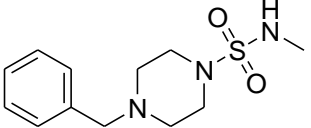
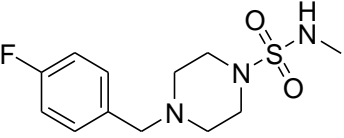
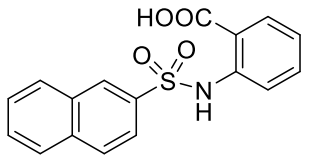
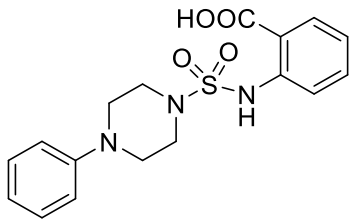
Changing the sulfonamide linker at the R1 position to the amide linker in compound **364LM** gave similar binding affinity in comparison with **368LM** ($K_i = 2.4 \pm 0.1 \mu\text{M}$). Based on these results, we synthesized a series of Mcl-1 inhibitors, **387LM-460LM**, where the R2 phenethylthio group was fixed at the meta position relative to the carboxylic group, and studied the SAR of the substituents at the R₁ position (Table 3.2). Bioisosteric replacement of the R₁ benzene with the thiophene moiety (**387LM**) gave a similar binding affinity. Introducing small hydrophobic substituents at the benzene ring, including a chlorine or bromine atom in ortho, meta and para positions, led to 5-fold improvement over the **368LM** (**384LM** with $K_i = 0.3 \pm 0.1 \mu\text{M}$ and **389LM** ($K_i = 0.4 \pm 0.1 \mu\text{M}$). Introducing a larger lipophilic moiety resulted in further improvement of the binding affinity (**382LM** to **376LM**).

The replacement of benzene at R₁ with bulkier naphthalene resulted in compound **382LM** with the $K_i = 0.2 \pm 0.01 \mu\text{M}$. Based on our previously reported series of Mcl-1 inhibitors [14] biphenyl and phenoxy-phenyl moieties proved again to be favourable substituents for targeting these PPIs and led to 13-fold (**378LM** $K_i = 0.09 \pm 0.02 \mu\text{M}$) and 12-fold (**376LM** $K_i = 0.10 \pm 0.02 \mu\text{M}$) improvements in binding affinity. Replacing the distal phenyl ring with saturated cyclohexyl group (**418LM** $K_i = 0.04 \pm 0.01 \mu\text{M}$) or introducing a chlorine in para position (**380LM** $K_i = 0.03 \pm 0.003 \mu\text{M}$), the binding affinity was significantly (34-fold) improved, in comparison with the hit compound **368LM**. To investigate the importance of the adjacent phenyl ring and at the same time to improve the physicochemical properties of the inhibitor series, especially in terms of solubility, this phenyl ring in **378LM** was replaced with the heterocyclic piperazine moiety. Resulting compound **396LM** showed 6-fold decreased binding with K_i of $0.6 \pm 0.1 \mu\text{M}$. Introducing the methylene spacer between the piperazine moiety and the phenyl substituent in compound **414LM** and para-flouro-phenyl derivative, **462LM**, showed similar binding affinity as the parent **396LM** compound. To determine the contribution of the phenethylthio group for the Mcl-1 binding, compounds **453LM** and **460LM** were synthesized. Both compounds showed significantly (about 80-fold) reduced binding affinity in comparison with corresponding compounds, clearly demonstrating the contribution of the R₂ substituent to the overall binding affinity.

Table 3.2. SAR of the phenethylthio benzoic acid derivatives for binding to Mcl-1 determined by FP and for selected compounds with TR-FRET binding assays.

			
N	R₁	IC₅₀ (K_i) [μM]	IC₅₀ (TR-FRET) [μM]
368LM		5.0±0.7 (1.2±0.2)	/
387LM		5.1±0.4 (1.2±0.1)	/
381LM		1.7±0.1 (0.4±0.02)	/
389LM		1.8±0.5 (0.4±0.1)	/
384LM		1.1±0.4 (0.3±0.1)	/
386LM		4.2±0.7 (1.0±0.2)	/

443LM		4.7±0.4 (1.1±0.1)	/
382LM		1.0±0.1 (0.2±0.01)	2.2±0.1
378LM		0.4±0.1 (0.09±0.02)	/
418LM		0.2±0.03 (0.04±0.01)	/
380LM		0.2±0.01 (0.03±0.003)	/
376LM		0.4±0.1 (0.1±0.02)	1.6±0.1
396LM		2.5±0.3 (0.6±0.1)	5.2±0.3

414LM		2.5±0.2 (0.6±0.04)	/
462LM		2.4±0.2 (0.6±0.05)	5.9±0.7
453LM		86.1±15.2 (20.2±3.6)	/
460LM		183.3±23.6 (43.0±5.5)	/

3.3.3 Structural studies of novel Mcl-1 inhibitors

To better understand the key binding elements for novel Mcl-1 inhibitors, co-crystal structures of **382LM**, **396LM**, and **462LM** bound to Mcl-1 were obtained at 2.74, 2.55, and 2.10 Å respectively. Overall, all Mcl-1 structures with bound inhibitors aligned nicely with the previously reported Mcl-1 structures. The alignment of new co-crystal structures with the available apo-MBP-Mcl-1 (PDB: 4WMS [15]) is shown in Figure 3.2a. The structures were aligned to **462LM** using the SSM algorithm in Coot [16] and the resulting root mean square deviations for each structural pair is 1.1725 Å for apo, 0.758 Å for **382LM**, and 0.899 Å for **396LM**. Mcl-1 loop 254-256 is disordered in the apo structure, leading to its larger deviation in this area and the aberrant termini in the BH3 binding site. The most prominent change vs. the apo Mcl-1 structure was the minor repositioning of the α4-helix relative to the apo-Mcl-1 structure. This structural movement was observed before for the Mcl-1 ligands, and helps to accommodate the ligand in the hydrophobic (p2) pocket the top of Mcl-1 α4 helix closer to the ligand.[17] As expected, the acid moiety of investigated ligands interacted with the positively charged Arg263 side chain of Mcl-1

and mimicked the hydrogen bond interaction observed with this residue and the pro-apoptotic proteins of Bim and Noxa.

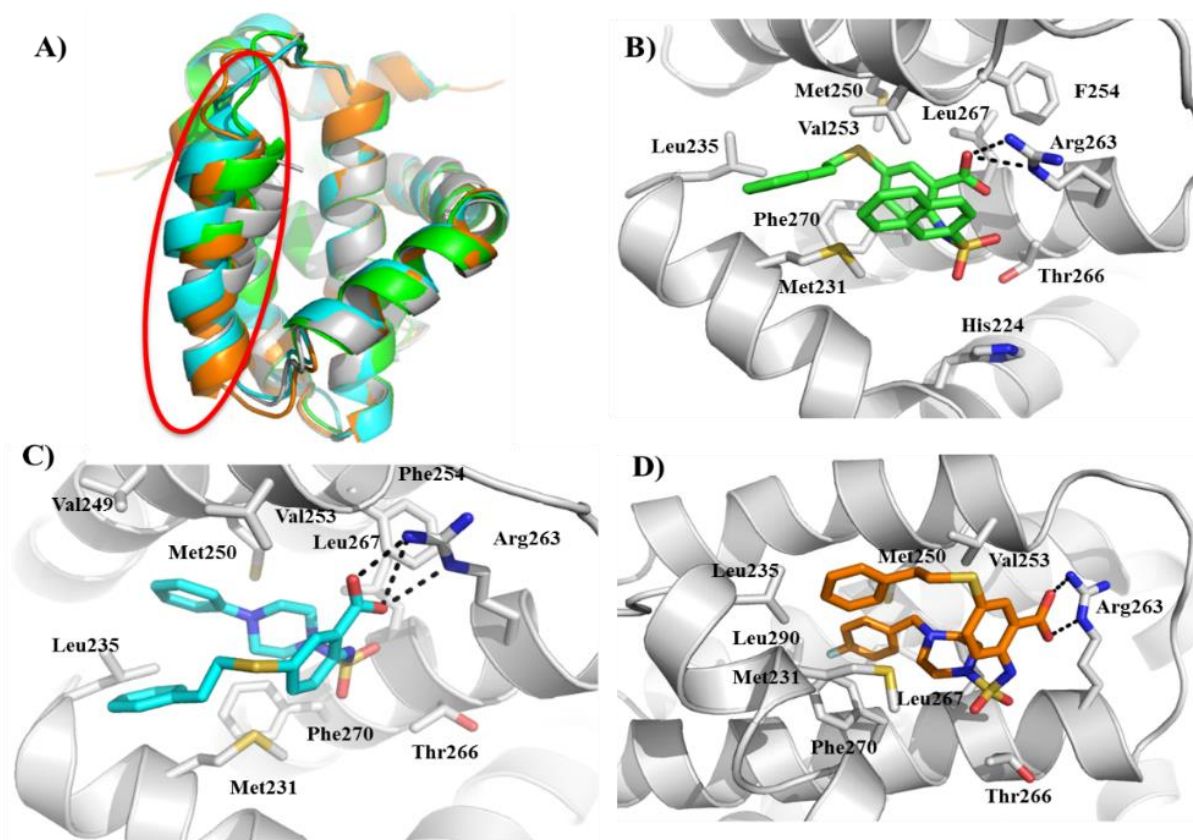


Figure 3.2. Co-crystal structures of 382LM, 496LM and 462LM with Mcl-1. (A) Overlay of the C α traces of 382LM (green), 396 (blue) and 462LM (orange) and apo-MBP-Mcl-1, PDB ID 4WMS, (gray) depicting movement in the α 4-helix (circled in red) upon ligand binding. Loop 254-256 is disordered in the apo structure leading to its larger deviation in this area and the aberrant termini in the BH3 binding site. X-ray crystallography complex of several inhibitors with Mcl-1 protein: (B) 382LM; (C) 396LM and (D) 462LM. The side chains of selected interacting Mcl-1 residues are labeled.

In the **382LM** co-crystal structure, four Mcl-1 protein molecules occupy a single unit cell. The **382LM** molecule binds the Mcl-1 molecule in a U-shaped binding mode with the Arg263 carboxylic group as the main anchoring interaction (Figure 3.2b). When fitting the **382LM** ligand into the obtained electron density for the Omit electron density maps for all bound ligands (Appendix Figure 3.5), it was observed that the R2 phenethylthio moiety is pointing towards the p2 pocket interacting with the hydrophobic side chains of the Mcl-1 α 3 helix (e.g. Met231), and

sulfur-containing side chain of Met250 (Figure 3.2b) on the Mcl-1 α 4 helix, similarly as in the proposed binding model for the initially designed 368LM (Figure 3.1f). Some of the Mcl-1 residues that were observed to form hydrophobic interactions with the ligand were Leu235, Met250, Val253, and Phe270.

The Mcl-1 Met231 side chain residue was located in the conformation that closely resembles the reported three-dimensional structures of the complexes formed between Mcl-1 BH3 peptides (e.g. Bim and Noxa), with less opened p3 pocket compared to some of the previously reported Mcl-1 inhibitor co-crystal structures.[15, 17-19] The compound's **382LM** R1 naphthalene moiety is located on top of the P3 hydrophobic pocket, partially stabilized by the π - π stacking with the **382LM** phenyl group as well as through hydrophobic interaction with Val254.

In the Mcl-1 structure containing **396LM**, one Mcl-1 molecule is occupying a single unit cell. Interestingly, the **396LM** compound is bound to the Mcl-1 BH3 binding site in a U-shaped flipped binding conformation in comparison to the bound **382LM** compound (Figure 3.2c). In addition, the benzene core structure is less buried into the Mcl-1 binding site, occupying a different position compared to the Mcl-1 **382LM** structure. The compound's R1 phenylpiperazine-sulfonamido substituent is placed into the Mcl-1 p2 hydrophobic binding pocket and the attached phenyl moiety interacts with the side chains of Leu267, Val253 and Leu235, and Val231 through hydrophobic interactions. The R2 S-substituted ethylbenzene moiety is located on top of the Mcl-1 α 3 helix and interacts to some extent with the sulfur-containing side chain of Met231 as well as the side chain of Leu235. The folded conformation of **396LM** is also partially stabilized by the π - π stacking of its two distal phenyl groups.

In the co-crystal structure with bound **462LM**, similar to the complex structure with **382LM**, four Mcl-1 protein molecules occupied a single unit cell. In terms of molecule orientation, two pairs of Mcl-1 structures faced one another with the **462LM** ligands occupying all available BH3 binding sites. Staking pairs of Mcl-1 molecules were observed in some previous x-ray experiments.[20] The **462LM** ligand is also bound in the Mcl-1 BH3 binding site in a flipped folded conformation compared to the **382LM** bound conformation. The R1 piperazine-containing substituent of **462LM** interacts with the Mcl-1 p2 hydrophobic binding pocket and the attached terminal 4-fluoro phenyl moiety is placed deeper in the p2 binding site compared to bound **382LM**, forming hydrophobic interactions with the side chains of Phe270, Met250, and Leu290.

The R2 phenethylthio moiety is located on top of the Mcl-1 α 3 helix and has hydrophobic interactions with the sulfur-containing side chain of Met231 as well as the side chain of Leu235 and Val253 (Figure 3.2d). Due to close stacking of two interacting Mcl-1 molecules, the charged side chain of Arg233 from the adjacent Mcl-1 protein is able to interact with the **462LM** compound bound to its neighboring Mcl-1 molecule and *vice versa*. These important structural findings indicate that the binding mode of these compounds depends on the nature of substitution introduced into the molecule. The different binding modes and orientation of investigated ligands demonstrate the complex nature of molecular recognition governing the binding of small molecules to Mcl-1 and the challenges that face structure-based design efforts.

3.3.4 Structure-based optimization of Mcl-1 inhibitors

Encouraged by the binding potency and SAR studies of our compounds, we continued to further optimize their potency, guided by our x-ray co-crystal structures and the structural data available in the literature. Recent studies have reported indole carboxylic acid [17] and salicylate based [20] Mcl-1 inhibitors through fragment-based drug design (FBDD). To facilitate structure-based design of our inhibitors and gain an understanding of the similarities and differences in the interactions of our series of compounds and reported inhibitors, we compared the co-crystal structure of **382LM** with available Mcl-1/inhibitors complex crystal structures (PDB ID: 4OQ6, [20] and PDB ID: 4HW2).[17]

Superposition of **382LM** complex structure and the structure of the salicylate based compound bound to Mcl-1 [20] showed that these inhibitors have similar binding poses (Figure 3.3a). In both structures the core scaffolds, the benzene carboxylic functionalities of the **382LM** and the salicylate moiety in reported compound **36** (PDB ID: 4OQ6), sit in almost the same position and in both cases the carboxylate forms hydrogen bonds with Arg263 of the Mcl-1 protein. The phenethylthio substituent from **382LM** and the 4-propylphenyl moiety of **36** are also closely superimposed and both are directed into the p2 pocket, although the n-propyl moiety extends deeper into the pocket, making Van der Waals contact with the sidechains of Leu235 and Val249 as was reported.[20] We observed the favorable overlap of analyzed co-crystal structures and, to take advantage of additional interactions found in compound **36**, we investigated the replacement

of the phenethylthio substituent in **382LM** by utilizing available SAR data. [20] The resulting compounds, **466LM**, **468LM** and **473LM**, showed 2 to 4-fold improved binding over the **382LM**. Further studies to test the optimum position of the distal trifluoromethyl-benzene and naphthalene substituent showed that the para positions of this functionality in **471LM** ($K_i = 59.3 \pm 10.2$ nM) and **475LM** ($K_i = 25.0 \pm 5.9$ nM) are favored over the ortho substitution present in the compounds **468LM** ($K_i = 85.9 \pm 6.8$ nM) and **473LM** ($K_i = 68.1 \pm 9.1$ nM). Furthermore, **471LM** and **475LM** have 4- and 5-fold, respectively, improved binding affinity in comparison with **382LM**, demonstrating that these substituents at R2 position are more favorable in comparison with the phenethylthio moiety. At the same time, the contribution of the naphthalene-2-sulfonamide to the Mcl-1 binding seems to be essential, as compound **469LM** showed significant 96-fold decrease in binding affinity in comparison with **471LM**. While analyzing the superimposed co-crystal structures of **382LM** with an indole-based ligand (PDB ID: 4HW2), a conformational change of the Met231 side chain was observed (**Fig. 3B**).[17] In the complex structure of the indole-based ligand, the “open confirmation” of the Met231 side chain induced by the compound improved its interaction with the hydrophobic p3 pocket through interactions with Phe228, Phe270, and Met231 residues. Fesik and co-workers, in their previously described series of inhibitors, have demonstrated that a substitution at the 6-position of the indole enhances the binding potency.[17-19] Interestingly, in both Mcl-1 complexes with **382LM** and the salicylate-based ligand, the Met231 side chain is in the “closed confirmation” (Figure 3.3a). Based on these observations, in the next optimization step we hypothesized that the binding affinity to Mcl-1 could be improved by introducing a substitution at the 4-position of the benzene carboxylic core. To test this hypothesis, we synthesized compounds **474LM** and **476LM**, where the iso-propyl group was introduced at the 4-position of the benzene core scaffold. Both compounds showed 2-fold improvement in their binding affinity confirmed with FP- and TR-FRET based assays in comparison with corresponding compounds, **471LM** and **376LM** respectively (Tables 3.2 and 3.3). Subsequent combination of the described structure-based modifications, and introducing favorable substituents based on our SAR results of the phenylsulfonamido substituent, yielded the compounds **477LM** ($K_i = 24.8 \pm 18.9$ nM) and **480LM** ($K_i = 18.5 \pm 1.8$ μ M) with improved binding. Based on our initial exploratory SAR of the designed compound **368LM** (Table 3.1), the sulfonamide linker was replaced with a smaller and more flexible amide linker in molecules **483LM** and **487LM**, providing most potent compounds in this series with the K_i values of 10 nM

(Table 3.3). Using surface plasmon resonance (SPR)-based competitive assay, the binding affinities of **483LM** ($IC_{50} = 29 \pm 4$ nM) and **487LM** ($IC_{50} = 47 \pm 6$ nM) were comparable to Noxa ($IC_{50} = 28 \pm 1$ nM) in competing with Bim peptide. (Appendix Figure 3.6)

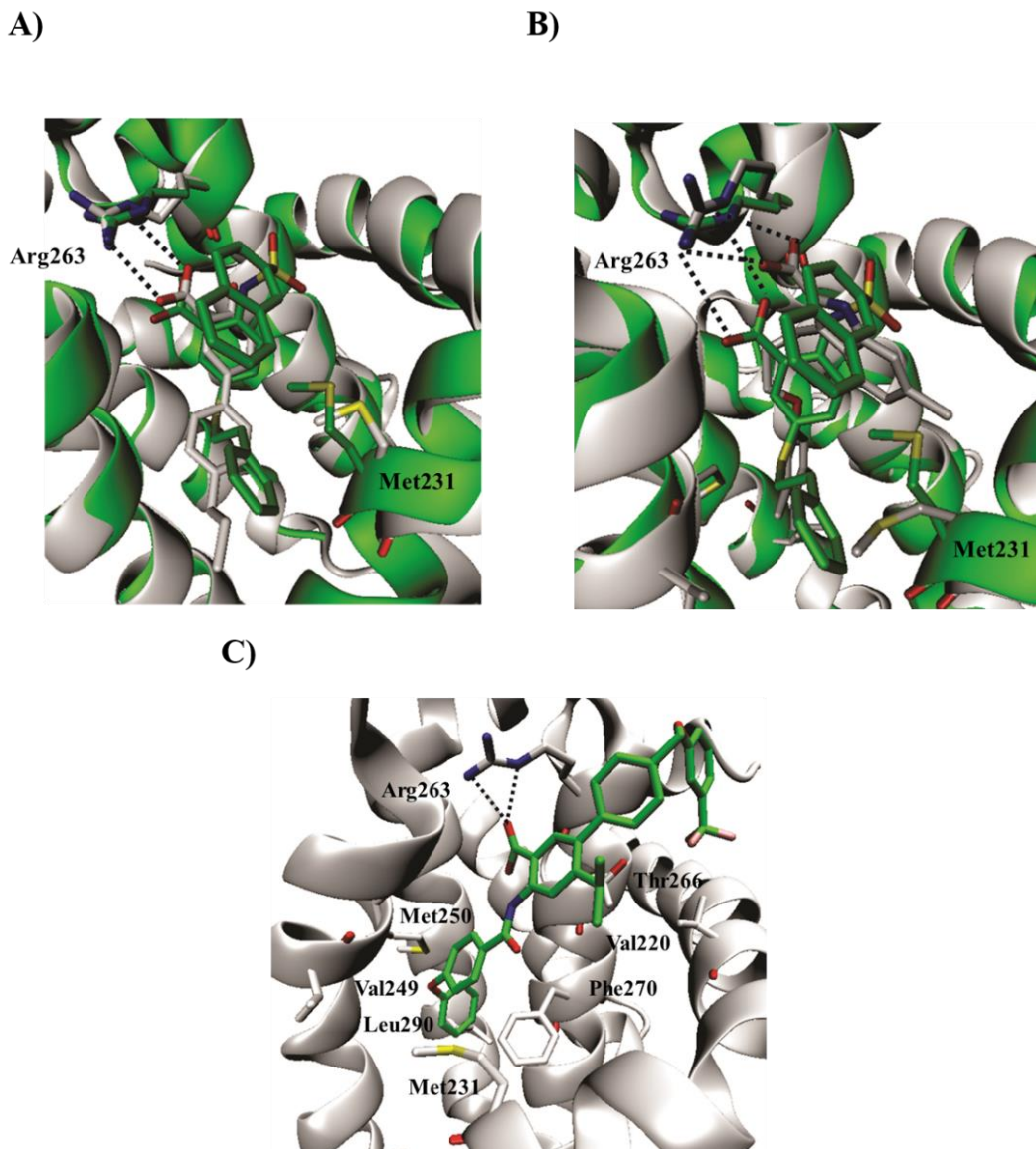
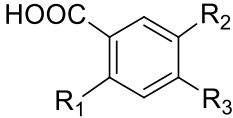
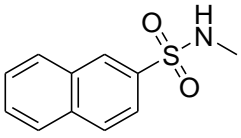
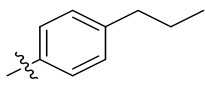
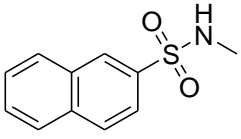
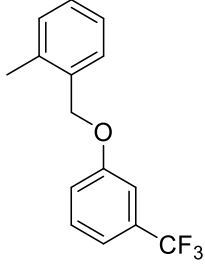
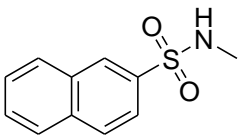
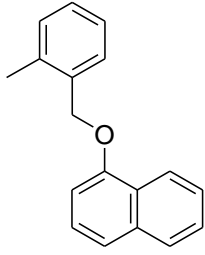
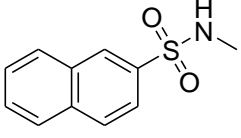
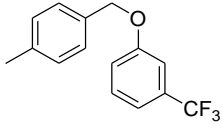
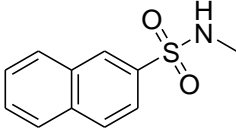
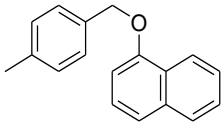
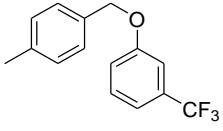
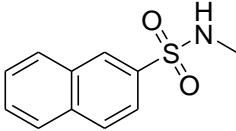
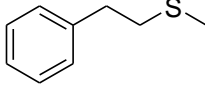
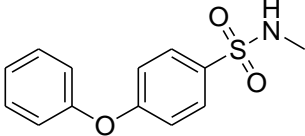
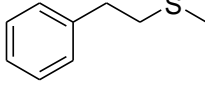
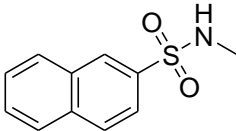
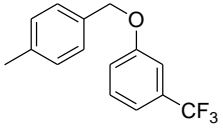
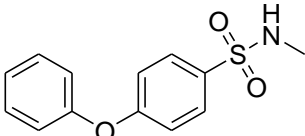
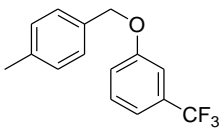
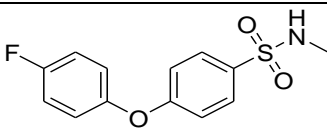
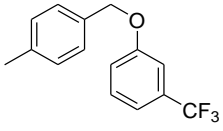
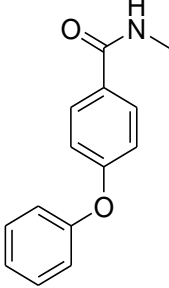
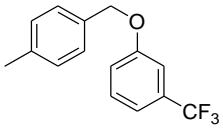


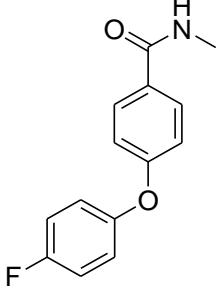
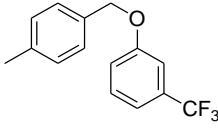
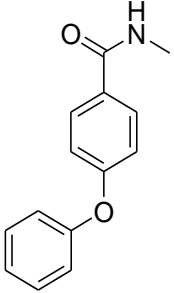
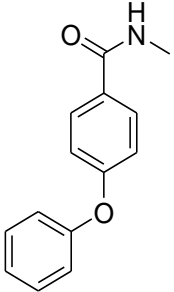
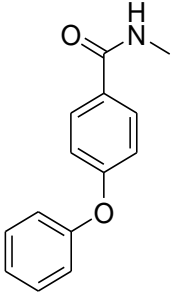
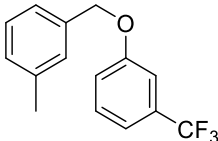
Figure 3.3. Alignment of 382LM co-crystal structure with reported co-crystal structures and predicted binding mode of 483LM. (A) (left) Alignment of the 382LM Mcl-1 complex and 4OQ6 Mcl-1 structure and (right) alignment of the 382LM Mcl-1 complex and 4HW2 Mcl-1 structure (B) Proposed binding mode of the 483LM structure in the Mcl-1 binding site (PDB: 4HW2). Arrow indicates that, several positions of the R2 substituent in the p4 binding site or its immediate vicinity were observed in docking calculations.

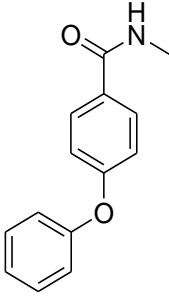
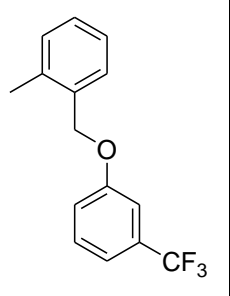
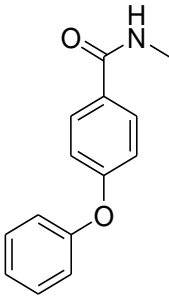
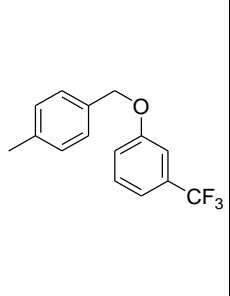
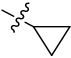
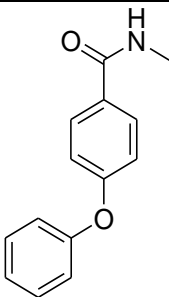
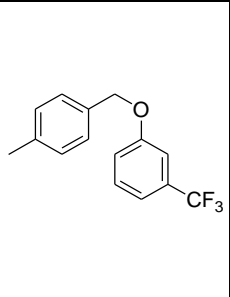
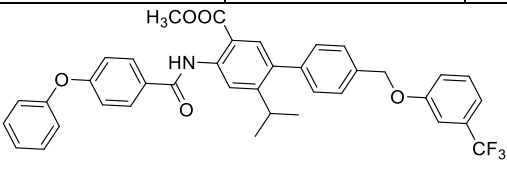
To get more insights about the binding pose and interactions of **483LM**, this compound was docked into the Mcl-1 binding site using the reported Mcl-1 structure, PDB ID: 4HW2 (Figure 3.3c).[17] In the predicted binding model the R₁ phenoxyphenyl substituent is directed deep into the p2 pocket forming hydrophobic interactions with neighboring residues Leu290, Met250, Val249, Phe270, and Leu267. As expected the carboxylic group interacts firmly with the side chain of Arg263. The R₃ *iso*-propyl group of **483LM** sits above the P3 binding pocket with weak hydrophobic interactions. Importantly, all top-ranked poses showed that the R₂ benzyloxy-trifluoromethyl benzene substituent is directed towards the p4 pocket, mimicking the interaction of the conserved hydrophobic Phe residue of the BIM BH3 peptide. To support the predicted binding pose of 483LM and quantify the contribution of its substituents, we synthesized several compounds. Synthesizing compound **511LM**, which has only phenoxyphenyl-sulfonamido substituent in R₁ position led to detrimental decrease of the binding to Mcl-1 protein with K_i of 21 μM, clearly providing evidence of the importance of R₂ and R₃ substituents. To further gain information about the R₂ substituent, since it is hard to exactly define its placement by the molecular docking studies, compounds **495LM** and **496LM** were synthesized where the position of ethoxy-trifluoromethyl benzene moiety was changed. Both compounds showed a 3-fold decrease in binding affinity, confirming that the para position in **483LM** is most optimal for binding to Mcl-1, consistent with **471LM** and **475LM** (Table 3.3). **491LM**, derivative of **483LM**, where the cyclopropyl substituent was introduced at the R₃ position, displayed comparable inhibition. The necessity of the conserved electrostatic and hydrogen bond of carboxylic interaction with Arg263 was assayed by synthesizing **486LM**, methyl ester of the potent compound **483LM**, which did not show binding to Mcl-1 up to 100 μM. Importantly, for several synthesized compounds presented in Tables 2 and 3, the Mcl-1 binding was studied with the (TR-FRET) technique also, yielding consistent binding values.

Table 3.3.SAR of the second-generation benzoic acid derivatives for binding to Mcl-1 determined by FP and for selected compounds with TR-FRET binding assays.

					
N	R₁	R₂	R₃	IC₅₀ (K_i) [nM]	IC₅₀ (TR-FRET) [nM]
466LM			H	58.0±10.0 (13.4±2.3)	/
468LM			H	373.3±28.9 (85.9±6.8)	1895.0±72.0
473LM			H	297.5±38.6 (68.1±9.1)	/
471LM			H	260.0±43.6 (59.3±10.2)	819.0±200.0

475LM			H	207.5±46.9 (25.0±5.9)	/
469LM	H ₂ N—		H	24156.7±27 05.8 (5668.3±63 5.1)	/
478LM			iPr	1046.7±90. (243.9±21.2)	/
476LM			iPr	242.5±90.0 (55.2±21.1)	874.0±63.0
474LM			iPr	267.5±64.0 (67.9±7.5)	434.0±101.0
477LM			iPr	113.0±80.6 (24.8±18.9)	183.0±37.0
480LM			iPr	86.3±7.5 (18.5±1.8)	/
483LM			iPr	51.2±3.3 (10.3±0.8)	73.0±16.0

487LM			iPr	46.2 ± 10.2 (9.1 ± 2.4)	69.0 ± 9.0
509LM		I	iPr	$967.5 \pm 137.$ (225.3 ± 32.3)	
511LM		H	H	90833.3 ± 20 (21318.6 ± 4)	
496LM			iPr	117.0 ± 48.8 (25.7 ± 11.4)	107.0 ± 10.0

495LM			iPr	135.0±35.4 (29.9±8.3)	187.0±16.0
491LM				46.8±5.4 (9.2±1.3)	75.0±17.0
494LM			H	60.0±34.5 (12.3 ±8.1)	112.0±22.0
486LM				>100,00 (>23,50)	>169

3.3.5 Selectivity Profile

The selectivity was determined against two other Bcl-2 anti-apoptotic proteins (Bcl-2 and Bcl-xL) using competitive FP-based assays optimized for each protein. Selected analogs were tested and K_i values were calculated using previously developed equations (Table 3.4).[21] The most potent inhibitor **483LM** shows high selectivity in binding to Mcl-1, at least 100 - and 800-folds compared to Bcl-2 and Bcl-xL, respectively. Interestingly, compounds **477LM** and **480LM**, which have sulfonamide versus amide linkers in corresponding **483LM** and **487LM**, show decreased

selectivity profile, 8 – and 20-fold less binding to Bcl-2. These results indicate that the amide linkers in **483LM** and **487LM** might be important for selective binding profile (Appendix Figure 3.7).

Table 3.4. Selectivity of selected inhibitors against Bcl-2 anti-apoptotic proteins.

Compounds	Mcl-1 <i>K_i</i> ± SD (μM)	Bcl-2 <i>K_i</i> ± SD (μM)	Bcl-xL <i>K_i</i> ± SD (μM)
E238	3.230±0.327	>25	>20
368LM	1.166±0.158	>25	>20
382LM	0.243±0.014	5.585±0.007	5.208±1.141
396LM	0.582±0.062	15.660±0.014	6.170±0.928
462LM	0.561±0.049	>25	>20
477LM	0.025±0.018	0.210±0.050	>3
480LM	0.019±0.002	0.435±0.134	>3
483LM	0.010±0.001	>1	>3
487LM	0.009 ±0.002	>1	>3
491LM	0.009±0.001	>1	>3
486LM	>25	>25	>20

3.3.6 Pulldown Experiment

To confirm the binding of novel inhibitors to endogenous Mcl-1, we employed a pull-down assay using biotin-labeled Noxa (BL-Noxa) and whole cell lysate from the human breast cancer cell line 2LMP. As shown in **Figure 3.4a**, Mcl-1 was pulled down by BL-Noxa and, as was expected, the Bim BH3 peptide disrupted the interaction between BL-Noxa and Mcl-1. Pre-incubation with **483LM** and **491LM** resulted in dose-dependently blocking the binding of BL-Noxa to Mcl-1, with **483LM** disrupting 50% of the Mcl-1/Noxa interactions at 1 μM. Compound **486**, which has the same chemical scaffold but does not bind to Mcl-1 and serves as a negative control, did not disrupt the interactions up to 40 μM. **382LM** completely blocked the interaction at higher concentration, 100 μM, consistent with its lower binding affinity. These results further

demonstrate that these inhibitors can recognize and specifically bind to the BH3 binding groove of endogenous Mcl-1 protein.

3.3.7 483LM and 487LM antagonize Mcl-1 function

To provide direct evidence that these novel inhibitors can selectively bind and antagonize Mcl-1 function, we have employed a cell-free functional assay using purified mitochondria, recombinant Mcl-1 and Bcl-xL proteins, and the BIM BH3 activator peptide which binds to both proteins with high affinity. At 10 nM, the BIM BH3 activator peptide induces substantial release of Smac protein from mitochondria, and 30 nM of Mcl-1 and Bcl-xL completely inhibit this release (**Figure 3.4b**). **483LM** and **487LM** antagonize Mcl-1 and restore BIM-induced release of Smac protein from mitochondria starting at 1 μ M. Consistent with their selective binding profile, in the Bcl-xL functional assay both Mcl-1 inhibitors fail to release Smac at the highest tested concentration of 9 μ M (Appendix Figure 3.8). In contrast, as was expected, Bad BH3 sensitizer peptide binds and antagonizes Bcl-xL mitochondrial function. These data demonstrate that the **483LM** and **487LM** function as potent and selective antagonists of Mcl-1 protein.

3.3.8 483LM has on-target cellular activity

Wild-type (WT), Bax knockout ($Bax^{-/-}$), Bak knockout ($Bak^{-/-}$), Bax/Bak double knockout (DKO), and Mcl-1 knockout ($Mcl-1^{-/-}$) MEFs have been employed as models to establish the mechanism-based apoptosis and on-target activity.[22] At 10 μ M, **483LM** primarily causes cell death in WT and did not show cytotoxicity against DKO and $Mcl-1^{-/-}$ MEFs. There was also no effect on $Bax^{-/-}$ and $Bak^{-/-}$ knockout cell lines, indicating that both Bax and Bak contribute in mediating apoptosis induction by the compound.[23] As was expected, ABT-263, pan inhibitor of Bcl-2, Bcl-xL and Bcl-2 proteins, induced cell death in MEFs wild-type but not in DKO, $Bax^{-/-}$ or $Bak^{-/-}$ MEFs. However, $Mcl-1^{-/-}$ MEFs were even more sensitive to ABT-263 compared to WT cells, confirming the findings that Mcl-1 is a resistant factor to ABT-263 cell activity (**Figure 3.4c**).[24] These results demonstrate that **483LM** has on-target activity and does not kill MEFs indiscriminately through non-apoptotic mechanisms. The specificity of this class of Mcl-1 inhibitors was further confirmed by using mouse E μ -myc lymphoma cells overexpressing an

individual pro-survival protein required for cell survival.[25] **483LM** induced substantial cell death to E μ -myc lymphoma cells overexpressing Mcl-1 with minimal effect on cells overexpressing Bcl-2 or Bcl-xL (**Figure 3.4d**), which are sensitive to ABT-263 (Appendix Figure 3.9a). As expected, the inactive analog 486LM did not affect the cells overexpressing Mcl-1 (Appendix Figure 3.9b). These data demonstrate that **483LM** specifically kills cells that are dependent on Mcl-1 for survival, including tumor cells “addicted” to Mcl-1.

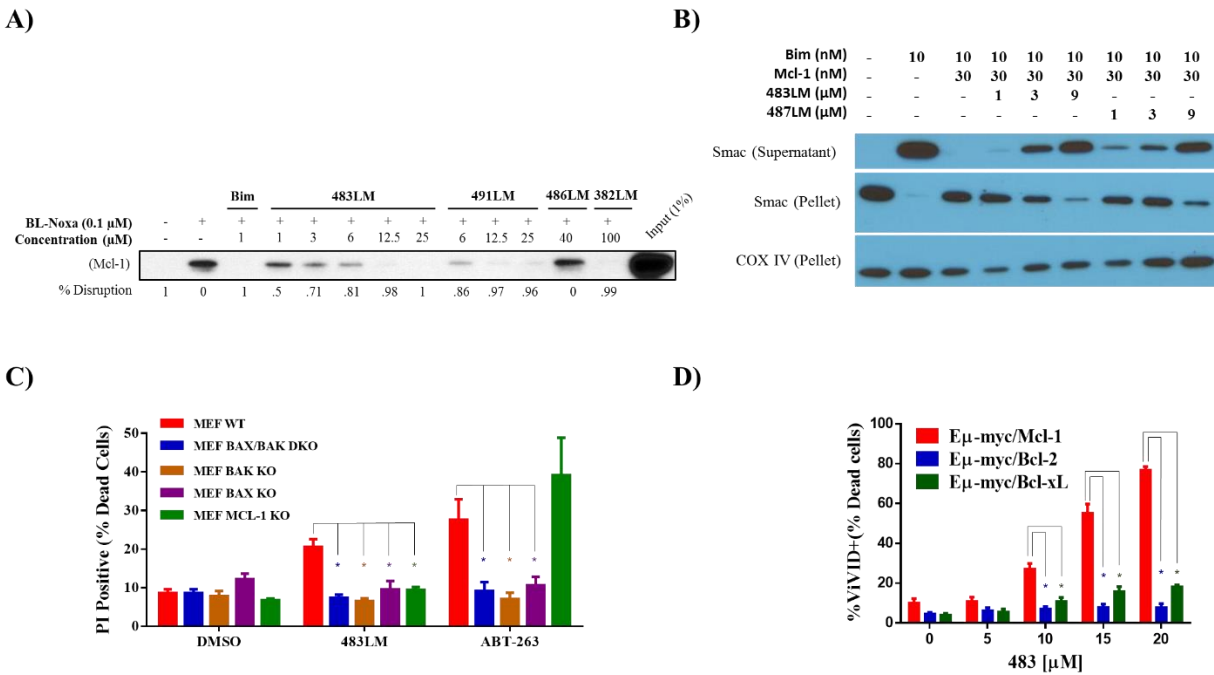


Figure 3.4. Developed inhibitors exhibits on-target activity towards Mcl-1 in *in vitro* and cell-based assays. (A) Pulldown assay showing the ability of 382LM, 483LM, and 491LM to disrupt Mcl-1/Noxa interaction but not the inactive compound 486LM. **(B)** 483LM and 487LM can inhibit the function of Mcl-1 in the mitochondria functional assay. **(C)** 483LM induces Bax/Bak dependent cell death in model MEFs. **(D)** E μ -myc lymphoma model cells overexpressing and dependent on Mcl-1 for survival show the highest sensitivity to 483LM compared to E μ -myc lymphoma cells overexpressing Bcl-2 or Bcl-xL

3.4 Materials and methods

Molecular docking calculations

Molecular docking calculations were performed using the GOLD molecular docking tool.¹ To begin with, the docking software tool GOLD was validated.² For this purpose, the initially reported

bound conformation of ligand in the Mcl-1 active site (PDB: 4HW2) was extracted from its active site and subsequently docked using the GOLD molecular docking package. The binding site was defined as a 10 Å cavity around the corresponding ligand in the Mcl-1 binding site. Hydrogen atoms were added to the Mcl-1 protein using GOLD, with default settings of the amino acid protonation pattern. Side chains of amino acids were treated as rigid entities. Compounds were docked 10 times into the defined binding site by applying the following parameters of the GOLD genetic algorithm (GA) (population size = 100, selection pressure = 1.1, no. of operations = 100000, no. of islands = 5, niche size = 2, migrate = 10, mutate = 95, crossover = 95) and different scoring functions available in GOLD. The best agreement between the crystallized and docked pose was obtained using ChemPLP scoring function. These settings were also used in the molecular docking calculations of the selected compounds from our synthesized series.[26, 27]

Protein purification

His-tagged proteins containing Human Mcl-1 (residues 171–323), the isoform 2 construct of the human Bcl-2 [Bcl2-2 construct for protein production starts with the Bcl2 sequence of 1-34 aa, followed by the Bcl-xL sequence of 35-50 aa, and ends with the Bcl2 sequence of 92-202aa.], and Bcl-xL (Human Bcl-xL protein, which has an internal deletion for the 45-85 amino acid residues and a C-terminal truncation for the amino acid residues 212-233) were expressed from the pHis-TEV vector (a modified pET vector) in *E. coli* BL21 (DE3) cells. Cells were grown at 37 °C in 2×YT, containing antibiotics to an OD600 density of 1.5, 1, and 0.8 for Mcl-1, Bcl-xL, and Bcl-2, respectively. Protein expression was induced by 0.4 mM IPTG at 20 °C overnight. Cells were lysed in 20 mM HEPES pH 7.5, 200 mM NaCl, 0.1% βME and 40 μL of Leupeptin/Aprotinin (Mcl-1), 25mM Tris pH 8.5, 200mM NaCl (Bcl-2), and 50mM Tris pH 7.5, 200 mM NaCl (Bcl-xL). All proteins were purified from the soluble fraction using Ni-NTA resin (QIAGEN), following the manufacturer's instructions. For purification of TEV-cleaved protein, the amino terminal His tag was cleaved by incubation with TEV protease and the protein was further purified by anion exchange (Source Q) and gel filtration chromatography (Superdex 75, Amersham Biosciences) in 20mM HEPES pH 7.0, 50 mM NaCl (Mcl-1), 25 mM Tris pH 8.5, 150 mM NaCl, 0.1% βME (Bcl-2) and 20 mM Tris pH 7.5, 150 mM NaCl, 0.1% βME (Bcl-xL). His-tagged Mcl-1 protein was used for TR-FRET assay and HSQC-NMR. His-TEV cleaved Mcl-1, Bcl-2 and Bcl-xL were used in fluorescent polarization and surface plasmon resonance binding assays.

Crystallization and structure determination of Mcl-1 bound to inhibitors

Prior to crystallization, for the Mcl-1:**396** complex, Mcl-1 protein (residues 171-320) was concentrated to 10.66 mg/mL in 20 mM HEPES pH 7.0, 50 mM NaCl and incubated in a 1:1.5 molar ratio with compound **396** at 4 °C for 48 hours. The final DMSO concentration in the protein-ligand sample was 6%. The complex crystallized in a sitting drop vapor diffusion experiment against well solution of 30% PEG 3350, 0.2 mM MgCl₂ and 0.1 M ADA pH 6.5. The drops consisted of 1.5 µL protein-complex, 0.3 µL of 30% 6-aminohexanoic acid, and 1.2 µL of well solution. Crystals grew within 1 day at 20 °C and were cryoprotected in 30% PEG 3350 prior to data collection.

To crystallize Mcl-1:**382LM** and Mcl-1:**462LM** complexes, protein was concentrated to 10 mg/mL and incubated with compound 1:1.5 ratio for 24 hours at 4 °C. Mcl-1:**382LM** and Mcl-1:**462LM** grew crystals from drops containing equal volumes of protein and well solution setup against 23 % PEG 3350, 0.1 M Tris pH 8.0 and 18% PEG 3350, 200 mM NH₄ Acetate, 100 mM Bis-Tris pH 6.5, respectively. The crystals were cryoprotected in a well solution containing 25% ethylene glycol.

Diffraction data were collected on LS-CAT 21-ID-D (**396LM**) and 21-ID-G (**382 LM** and **462LM**) beamlines at the Advanced Photon Source at Argonne National Laboratory and processed with HKL2000.[28] The structures were solved via molecular replacement in Molrep [29] using an in-house Mcl-1:Bim structure missing helix 237-257 as the search model. Iterative rounds of electron density fitting and refinement were completed using Coot [16] and Buster [30], respectively. The coordinates and geometric restraints for each inhibitor were created from smiles using Grade with the qm+mogul option.[30] The coordinates were validated with Molprobity.[31] Data collection and refinement statistics are listed in (Appendix Table 3.5). Difference electron density maps showed one inhibitor bound in the BH3 binding pocket of each protein chain. In the case of **396LM** and **382LM**, several additional inhibitor compounds act as additives enabling crystal packing. Residues 172-320 are present in protein chains A, B, and D of Mcl-1:**462LM**. Chain C contains residues 171-321 plus one N-terminal residue of the cleaved tag. In the Mcl-1:**382LM** crystal, residues 171, 197-200, and 322-323 are missing from chain A; residues 171, 193-201, and 322-323 are missing in chain B; residues 194–202, 238-240, and 321-323 are missing in chain C; and residues 171, 198-201, and 321-323 are missing from chain D. In the Mcl-

1:396LM structure, residues 171 and 197-202 are missing from the single protein chain in the asymmetric unit.

Fluorescence polarization-based binding assays

Fluorescein tagged BID BH3 peptide was used as a tracer in the FP-based binding assays. Two fluorescent labeled BID BH3 peptides were used: i) fluorescein tagged Bid peptide (Flu-Bid), labeled with fluorescein on the N-terminus of the BH3 peptide (79-99); ii) Bid BH3 peptide (80-99) labeled with 5-FAM, named as FAM-Bid (Abgent). The K_d values were determined using 2 nM of Flu-BID with different concentrations of Mcl-1 protein, or FAM-Bid with different concentrations of Bcl-2 and Bcl-xL proteins in a final volume of 125 μ L in the assay buffer (20 mM potassium phosphate, pH 7.5; 50 mM NaCl, 1 mM EDTA, 0.05% Pluronic F68 and, 4% DMSO). Plates were mixed and incubated on a shaker at room temperature for 3 hours and the polarization values in millipolarization units (mP) were measured at an excitation wavelength of 485 nm and an emission wavelength of 530 nm. Dissociation constants (K_d) were calculated by fitting the sigmoidal dose-dependent FP increases as a function of protein concentrations using Graphpad Prism 6.0 software. Based upon analysis of the dynamic ranges for the signals and their K_d values, Flu-BID was selected as the tracer in the Mcl-1 while FAM-Bid was selected as the tracer for the rest of the proteins, Bcl-2, A1/Bfl-1, Bcl-w, and Bcl-xL. In our saturation experiments, the K_d value of Flu-Bid to Mcl-1 was 3.04 ± 0.06 nM, and the K_d values of FAM-Bid to Bcl-2 was 18.44 ± 1.40 nM, and to Bcl-xL was 20.04 ± 2.34 nM, respectively. Based on the K_d values, the concentrations of the proteins used in the competitive binding experiments were 10 nM for Mcl-1, 60 nM Bcl-2, 80 nM Bcl-xL and 40 nM for Bcl-w. The fluorescent probes, Flu-Bid and FAM-Bid were fixed at 2 nM for all assays. 5 μ L of the tested compound in DMSO and 120 μ L of protein/probe complex in the assay buffer (20 mM potassium phosphate, pH 7.5; 50 mM NaCl, 1 mM EDTA and 0.05% Pluronic F68) were added to assay plates (Corning #3792), incubated at room temperature for 3 h and the polarization values (mP) were measured at an excitation wavelength at 485 nm and an emission wavelength at 530 nm using the plate reader Synergy H1 Hybrid, BioTek. IC_{50} values were determined by nonlinear regression fitting of the competition curves (GraphPad Prism 6.0 Software). The K_i values were calculated as described previously.[21]

Competitive surface plasmon resonance based assay using immobilized Bim BH3 peptide

The solution competitive SPR-based assay was performed on Biacore 2000. Bim BH3 peptide (141–166 amino acids) was immobilized on a streptavidin (CM5) chip with density of 770 RU (Response Units). The preincubated Mcl-1 protein (10 nM) with tested small-molecule inhibitors for at least 30 min (in 20 mM potassium phosphate, pH 7.5; 50 mM NaCl, 1 mM EDTA, 0.05% Pluronic F68 and, 4% DMSO) was injected over the surfaces of the chip in 1x PBS-P buffer (GE healthcare, #28-9950-84). Response units were measured after 15 s from the end of a two-minute association phase, and the specific binding was calculated by subtracting the control surface (Fc1) signal from the surfaces with immobilized biotin-labeled Bim BH3. IC₅₀ values were determined by nonlinear least-squares analysis using GraphPad Prism 6.0 software.

Cell culture and cell viability assays

MEFs, wild type, Bax knock out, Bak knock out and Bax/Bak double knock out, were gifts from Dr. Shaomeng Wang at the University of Michigan and were cultured in DMEM (Life Technologies), supplemented with 10% fetal bovine serum (FBS) (Thermo Scientific HyClone), and 1% Penicillin/streptomycin solution (Life Technologies). The retroviral transduced lymphoma cells isolated from E μ -myc transgenic mice were gifts from Ricky W. Johnstone at University of Melbourne, Melbourne, Australia and cultured as previously described.[25] PANC-1 was obtained from the American Type Culture Collection (ATCC). The cells were cultured in DMEM (Life Technologies), supplemented with 10% FBS and 1% Penicillin/streptomycin solution. MEFs were seeded in 24-well plates at 0.5×10^5 cells/well, left to adhere for 5 h and then treated for 15 h with increasing concentrations of the compounds. The cells were harvested, washed with phosphate-buffered saline (PBS), and stained with 0.025 mg/ml propidium iodide (MP Biomedicals). The percentage of propidium iodide positive population was determined by flow cytometry and calculated using WinList 3.0. The Mcl-1, Bcl-2 and Bcl-xL retroviral transduced lymphoma E μ -myc cells were seeded in 12-well plates at 0.5×10^6 cells/well. They were treated with different concentrations of tested compounds for 16 h. The cells were harvested and stained with violet LIVE/DEAD Fixable Dead Cell Stain Kit (Invitrogen), according to manufacturer's protocol. The percentage of fluorescent positive cells was determined by flow cytometry and calculated using WinList 3.0. In 96-well plates, the effect of the compounds on tested PANC-1 cells viability was evaluated after 48 h by MTT Cell Proliferation Assay (Amresco) where MTT solution (12 mM)

was added to the cultures (10 μ L MTT solution per 100 μ L medium) and incubated for 4 h. Sodium dodecyl sulfate (Fisher) solution (1 g/10 ml) was added to the cultures (100 μ L per well), which was incubated overnight. The absorbance was detected at 570 nM using the plate reader Synergy H1 Hybrid, BioTek. IC₅₀ values were calculated by non-linear regression analysis using GraphPad Prism 6.0 Software.

Pulldown assay

2LMP, a subclone of MDA-MB-231, was kindly provided by Dr. Shaomeng Wang at the University of Michigan. The cells were harvested ($\sim 15 \times 10^6$) and lysed via sonication with CHAPS buffer (10 mM HEPES (pH 7.4), 2.5 mM EDTA, 150 mM NaCl, 1% (w/v) CHAPS). Pre-cleared cell lysates (1 mg/mL) were treated with varying concentrations of compounds and then subject to overnight incubation at 4° C with biotinylated Noxa peptide (18–43). Protein-peptide complexes were pulled down with streptavidin-agarose beads for 2 h. Beads were washed with CHAPS buffer and Mcl-1 protein was eluted by boiling in SDS-PAGE buffer. Samples were analyzed by western blotting with the Mcl-1 antibody (Thermo Scientific #MS-681-P1).

Mitochondria-based functional assay

2LMP cells were cultured in DMEM (Life Technologies), supplemented with 10% FBS and 1% Penicillin/streptomycin solution. Cells were cultured in 150 cm² cell culture dishes up to 80% confluent in a healthy state. The cells were harvested and washed two times with cold PBS.

Cell pellets were suspended in the mitochondrial isolation buffer (MIB, 10 mM Tris Hcl, 0.1 mM EDTA, 250 mM sucrose with protease inhibitors and 1 mM PMSF added immediately prior to the assay, pH 7.4). The cells were incubated at 4°C for 20 min. The cells are homogenized on ice using 40 strokes using 2 ml Dounce glass homogenizer and pestle B. Mitochondria were then isolated by differential centrifugation steps followed by two washes with MIB. Mitochondria is then suspended in mitochondrial reaction buffer (MRB, 20 mM HEPES, 100 mM KCl, 2.5 mM MgCl₂, 100 mM sucrose with 1mM DTT and protease inhibitors and 1 mM PMSF added immediately prior to the assay, pH 7.5).

The concentration of mitochondria suspension was adjusted to 50 μg per aliquot. The aliquots were incubated with 30 nM of Mcl-1, Bcl-2, or Bcl-xL protein, together with BIM (141-166) peptide, and Noxa (20-45), Bad (102-128) or different concentrations of 483LM, at 37°C for 1 h. Mitochondria treated with DMSO were included as the negative control. Cytochrome c and Smac released to the supernatant and remaining in the mitochondria pellets were analyzed by western blotting using primary anti-cytochrome c and anti-Smac antibodies from Cell Signaling and Genlantis, respectively. Anti-COX IV from Cell Signaling is used as loading control.

3.5 Contributions

Ahmed Mady performed FP and SPR binding assays, analyzed the SAR results and participated in the discussion of designing novel analogs. He also established and optimized the functional assay and performed all cell-based assays. Dr. Lei Miao synthesized all compounds. The computational docking studies of novel designed analogs based on the SAR studies were done by Dr. Andrej Perdih, visiting scholar in Dr. Nikolovska-Coleska's laboratory from the National Institute of Chemistry in Ljubljana, Slovenia. Karson Kump performed the pulldown assay. Expression and purification of all proteins as well as crystallographic studies were performed in Dr. Jeanne Stuckey's lab at LSI. TR-FRET binding assay was performed by Dr. Yuhong Du in Dr. Haiyan Fu's laboratory at Emory University.

3.6 Appendix

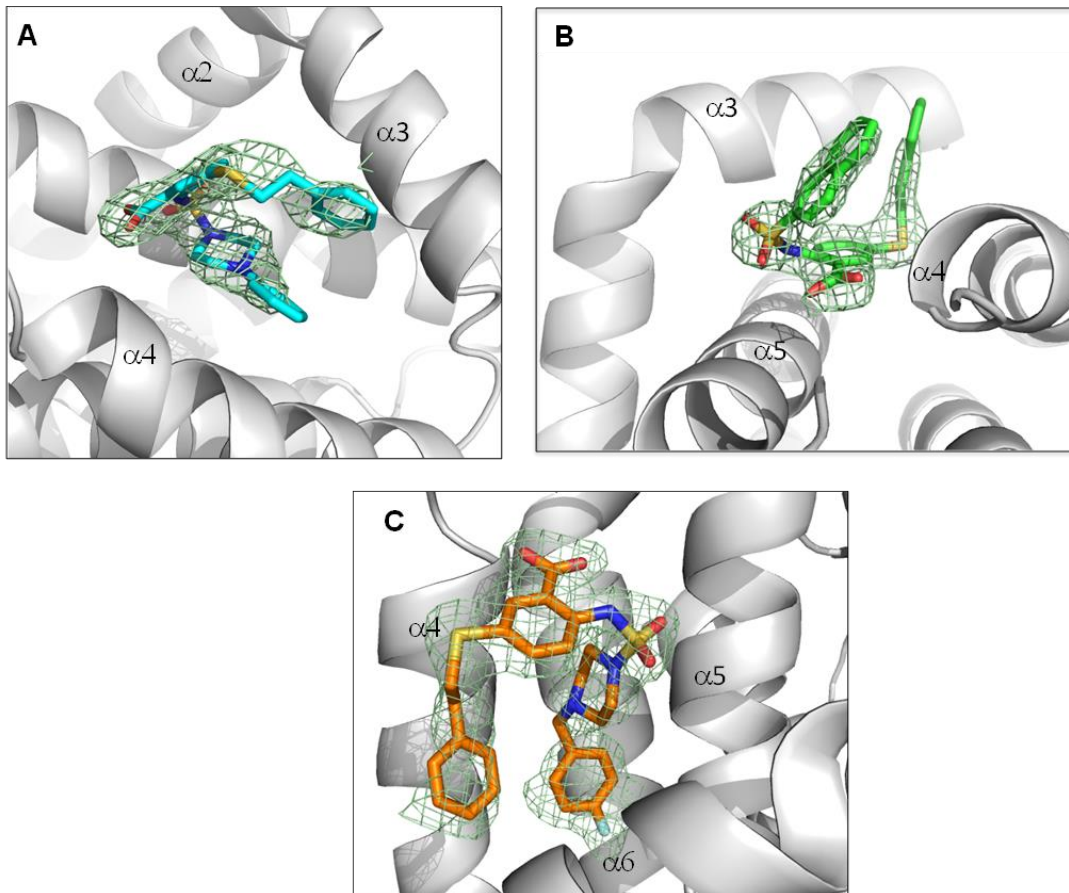


Figure 3.5. Omit electron density maps for the bound ligands of Mcl-1. The structures of Mcl-1 absent the ligands were refined in Buster [30] and their subsequent difference ($F_o - F_c$) electron density maps are shown as green grids contoured at 3 sigma. The positions of the refined ligands are shown as sticks with nitrogens (blue), sulfurs (yellow), oxygens (red) and carbon atoms for (A) 396 (cyan), (B) 382 (green) and (C) 462 (orange).

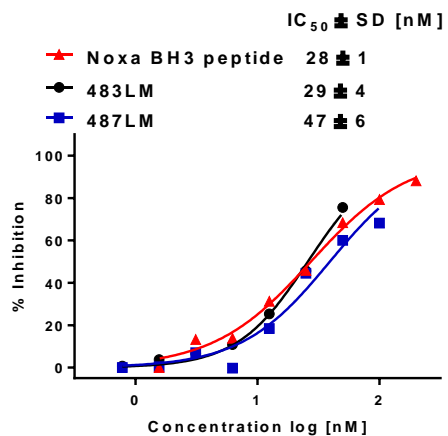


Figure 3.6. Binding affinity of 483LM, 487LM and Noxa using competitive SPR-based assay.

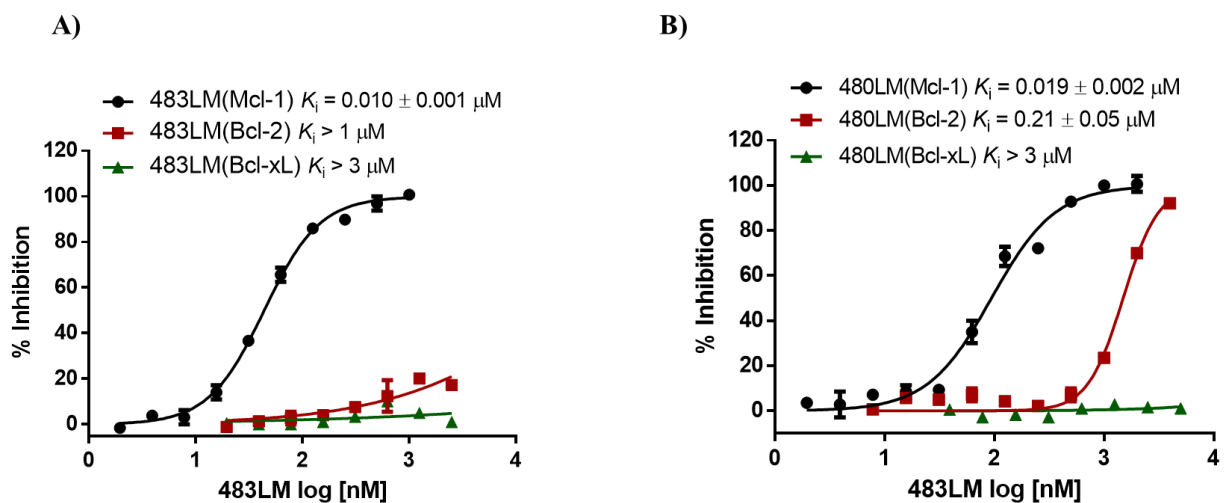


Figure 3.7. Selectivity profile of 483LM and 480LM using Competitive FP-based assay. 483LM shows a notable decrease in binding to Bcl-2 compared 480LM indicating the importance of amide linkers in improving selectivity.

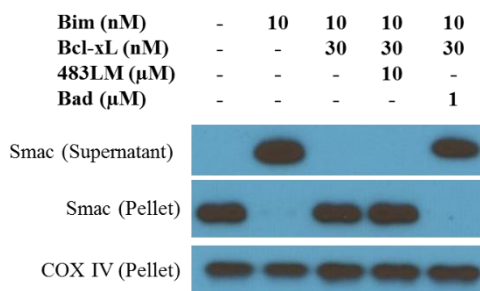


Figure 3.8. Mitochondrial functional assay showing the inability of 483LM to inhibit the function of Bcl-xL like Bad peptide. This confirms the selectivity data generated in biochemical assays.

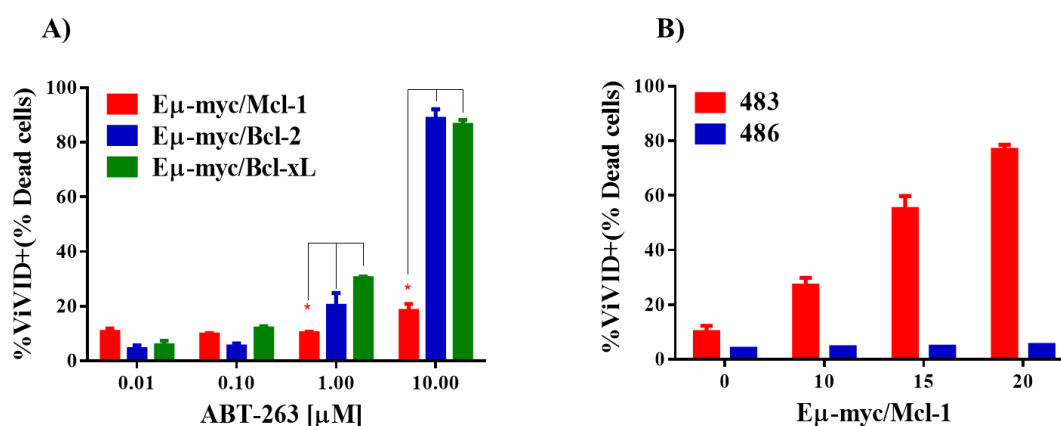


Figure 3.9. Using E μ -myc lymphoma cell lines to confirm the selectivity of ABT-263 and inactivity of 486LM. (A) ABT263 induces cell death in E μ -myc lymphoma cells overexpressing Bcl-2 or Bcl-xL but not Mcl-1. (B) The inactive compound 486LM does not affect E μ -myc/Mcl-1 cells.

Table 3.5. Crystallography data collection and refinement statistics.

Data Collection	Mcl-1:396LM	Mcl-1:382LM	Mcl-1:462LM
PDB ID	XXXX	XXXX	XXXX
Space Group	R32	P2 ₁ 2 ₁ 2 ₁	P2 ₁ 2 ₁ 2 ₁
Unit Cell a, b, c (Å)	111.68, 111.67, 72.34	68.980, 69.600, 110.340	69.712, 85.223, 109.753
Wavelength (Å)	0.96295	0.97856	0.97856
Resolution (Å) ¹	2.55 (2.55-2.59)	2.74 (2.74-2.79)	2.10 (2.10-2.14)

Rmerge ²	0.069 (0.649)	0.095 (0.355)	0.064 (0.464)
$\langle I/\sigma I \rangle^3$	20 (5)	10 (3)	10 (3)
Completeness (%) ⁴	99.6 (100)	99.3 (97.6)	100 (100)
Redundancy	20.5 (21.5)	5.3 (4.9)	7.4 (7.5)
Refinement			
Resolution (Å)	2.55	2.75	2.1
R-Factor ⁵	0.212	0.2297	0.1874
Rfree ⁶	0.251	0.2616	0.2215
Protein atoms	1081	4256	4725
Water Molecules	10	24	188
Unique Reflections	5816	14204	39167
R.m.s.d. ⁷			
Bonds (Å)	0.010	0.008	0.01
Angles (°)	1.04	0.90	0.90
Molecules/ASU	1	4	4
MolProbity Score	2.38	1.54	0.94
Clash Score	4.52	2.39	1.76
Z-Score ⁸			
RSCC (%) ⁸			
RSRV (%) ⁸			

¹Statistics for highest resolution bin of reflections in parentheses.

² $R_{\text{merge}} = \sum_h \sum_j |I_{hj} - \langle I_h \rangle| / \sum_h \sum_j I_{hj}$, where I_{hj} is the intensity of observation j of reflection h and $\langle I_h \rangle$ is the mean intensity for multiply recorded reflections.

³Intensity signal-to-noise ratio.

⁴Completeness of the unique diffraction data.

⁵R-factor = $\sum_h ||F_o| - |F_c|| / \sum_h |F_o|$, where F_o and F_c are the observed and calculated structure factor amplitudes for reflection h .

⁶ R_{free} is calculated against a 5% random sampling of the reflections that were removed before structure refinement.

⁷Root mean square deviation of bond lengths and bond angles.

⁸Values calculated using the Predisposition Electron-Density Server (EDS). [32]

3.7 References

- [1] Manning AM. Target Identification and Validation. Drug Discovery: John Wiley & Sons, Inc.; 2013. p. 43-65.
- [2] Rose PW, Bi C, Bluhm WF, Christie CH, Dimitropoulos D, Dutta S, et al. The RCSB Protein Data Bank: new resources for research and education. *Nucleic Acids Res.* 2013;41:D475-82.
- [3] Diller DJ, Merz KM, Jr. High throughput docking for library design and library prioritization. *Proteins.* 2001;43:113-24.
- [4] Alvarez JC. High-throughput docking as a source of novel drug leads. *Curr Opin Chem Biol.* 2004;8:365-70.
- [5] Leach AR, Gillet VJ, Lewis RA, Taylor R. Three-dimensional pharmacophore methods in drug discovery. *J Med Chem.* 2010;53:539-58.
- [6] Horvath D. Pharmacophore-based virtual screening. *Methods in molecular biology.* 2011;672:261-98.
- [7] Meireles LM, Domling AS, Camacho CJ. ANCHOR: a web server and database for analysis of protein-protein interaction binding pockets for drug discovery. *Nucleic Acids Res.* 2010;38:W407-11.
- [8] Kruger DM, Jessen G, Gohlke H. How good are state-of-the-art docking tools in predicting ligand binding modes in protein-protein interfaces? *J Chem Inf Model.* 2012;52:2807-11.
- [9] Billard C. Design of novel BH3 mimetics for the treatment of chronic lymphocytic leukemia. *Leukemia.* 2012;26:2032-8.
- [10] Flygare JA, Beresini M, Budha N, Chan H, Chan IT, Cheeti S, et al. Discovery of a potent small-molecule antagonist of inhibitor of apoptosis (IAP) proteins and clinical candidate for the treatment of cancer (GDC-0152). *J Med Chem.* 2012;55:4101-13.
- [11] Rew Y, Sun D, Gonzalez-Lopez De Turiso F, Bartberger MD, Beck HP, Canon J, et al. Structure-based design of novel inhibitors of the MDM2-p53 interaction. *J Med Chem.* 2012;55:4936-54.
- [12] Du Y, Nikolovska-Coleska Z, Qui M, Li L, Lewis I, Dingleline R, et al. A dual-readout F2 assay that combines fluorescence resonance energy transfer and fluorescence polarization for monitoring bimolecular interactions. *Assay Drug Dev Technol.* 2011;9:382-93.
- [13] Bajwa N, Liao C, Nikolovska-Coleska Z. Inhibitors of the anti-apoptotic Bcl-2 proteins: a patent review. *Expert Opin Ther Pat.* 2012;22:37-55.
- [14] JAbulwerdi FA, Liao C, Mady AS, Gavin J, Shen C, Cierpicki T, et al. 3-Substituted-N-(4-hydroxynaphthalen-1-yl)arylsulfonamides as a novel class of selective Mcl-1 inhibitors: structure-based design, synthesis, SAR, and biological evaluation. *J Med Chem.* 2014;57:4111-33.
- [15] Liu G, Poppe L, Aoki K, Yamane H, Lewis J, Szyperski T. High-quality NMR structure of human anti-apoptotic protein domain Mcl-1(171-327) for cancer drug design. *PLoS One.* 2014;9:e96521.
- [16] Emsley P, Cowtan K. Coot: model-building tools for molecular graphics. *Acta Crystallogr D Biol Crystallogr.* 2004;60:2126-32.
- [17] Friberg A, Vigil D, Zhao B, Daniels RN, Burke JP, Garcia-Barrantes PM, et al. Discovery of potent myeloid cell leukemia 1 (Mcl-1) inhibitors using fragment-based methods and structure-based design. *J Med Chem.* 2013;56:15-30.
- [18] Burke JP, Bian Z, Shaw S, Zhao B, Goodwin CM, Belmar J, et al. Discovery of tricyclic indoles that potently inhibit Mcl-1 using fragment-based methods and structure-based design. *J Med Chem.* 2015;58:3794-805.

- [19] Pelz NF, Bian Z, Zhao B, Shaw S, Tarr JC, Belmar J, et al. Discovery of 2-Indole-acylsulfonamide Myeloid Cell Leukemia 1 (Mcl-1) Inhibitors Using Fragment-Based Methods. *J Med Chem*. 2016;59:2054-66.
- [20] Petros AM, Swann SL, Song D, Swinger K, Park C, Zhang H, et al. Fragment-based discovery of potent inhibitors of the anti-apoptotic MCL-1 protein. *Bioorg Med Chem Lett*. 2014;24:1484-8.
- [21] Nikolovska-Coleska Z, Wang R, Fang X, Pan H, Tomita Y, Li P, et al. Development and optimization of a binding assay for the XIAP BIR3 domain using fluorescence polarization. *Anal Biochem*. 2004;332:261-73.
- [22] Willis SN, Fletcher JI, Kaufmann T, van Delft MF, Chen L, Czabotar PE, et al. Apoptosis initiated when BH3 ligands engage multiple Bcl-2 homologs, not Bax or Bak. *Science*. 2007;315:856-9.
- [23] Germain M, Milburn J, Duronio V. MCL-1 inhibits BAX in the absence of MCL-1/BAX Interaction. *J Biol Chem*. 2008;283:6384-92.
- [24] Gandhi L, Camidge DR, Ribeiro de Oliveira M, Bonomi P, Gandara D, Khaira D, et al. Phase I study of Navitoclax (ABT-263), a novel Bcl-2 family inhibitor, in patients with small-cell lung cancer and other solid tumors. *J Clin Oncol*. 2011;29:909-16.
- [25] Whitecross KF, Alsop AE, Cluse LA, Wiegman A, Banks KM, Coomans C, et al. Defining the target specificity of ABT-737 and synergistic antitumor activities in combination with histone deacetylase inhibitors. *Blood*. 2009;113:1982-91.
- [26] Jones G, Willett P, Glen RC, Leach AR, Taylor R. Development and validation of a genetic algorithm for flexible docking. *J Mol Biol*. 1997;267:727-48.
- [27] Kirchmair J, Markt P, Distinto S, Wolber G, Langer T. Evaluation of the performance of 3D virtual screening protocols: RMSD comparisons, enrichment assessments, and decoy selection--what can we learn from earlier mistakes? *J Comput Aided Mol Des*. 2008;22:213-28.
- [28] Otwinowski Z, Minor W. [20] Processing of X-ray diffraction data collected in oscillation mode. *Methods in Enzymology: Academic Press*; 1997. p. 307-26.
- [29] Vagin A, Teplyakov A. Molecular replacement with MOLREP. *Acta Crystallogr D Biol Crystallogr*. 2010;66:22-5.
- [30] Bricogne G. BE, Brandl M., Flensburg C., Keller P., Paciorek W., Roversi P, Sharff A., Smart O.S., Vonrhein C., Womack T.O. BUSTER version 2.11.2 Cambridge, United Kingdom: Global Phasing Ltd. 2016.
- [31] Chen VB, Arendall WB, 3rd, Headd JJ, Keedy DA, Immormino RM, Kapral GJ, et al. MolProbity: all-atom structure validation for macromolecular crystallography. *Acta Crystallogr D Biol Crystallogr*. 2010;66:12-21.
- [32] Kleywegt GJ, Harris MR, Zou JY, Taylor TC, Wahlby A, Jones TA. The Uppsala Electron-Density Server. *Acta Crystallogr D Biol Crystallogr*. 2004;60:2240-9.

CHAPTER 4

Functional genomics to predict response to cancer therapies

4.1 Introduction

Taking individual differences into account while exploring prevention and treatment strategies for diseases is not a new idea. This concept of precision medicine has been used for a long time in tackling individual patient variabilities. An example is determining the blood type of patients before blood transfusion. This concept is under continuous improvement due to advances in understanding diseases and characterizing of patients through various assays and tests in addition to genomics, proteomics, and metabolomics. [1]

4.1.1 Promise and limitations of genetic markers for patient stratification

Although there are assays that can predict the sensitivity or resistance of some types of cancer, there are still unanswered questions and a lot to explore in the realm of precision oncology. There are numerous challenges that need to be addressed such as understanding drug resistance, the use of optimized drug combinations, the heterogeneity of tumor genomics, as well as the ability to closely monitor tumor response and recurrence. One of the methods to determine the sensitivity of tumors to certain therapeutics is the use of functional assays. The idea is to monitor the states of a live tumor and help in guiding individualized therapy, for example determining tumor death when treated with certain drugs *ex vivo*. [2] There is recent progress in the area of functional assays that guide clinicians in gaining predictive information about tumors under investigation. These assays can be combined with next-generation gene sequencing and immune-profiling for a more precise treatment.

An example of novel functional assays is 3D organoid drug toxicity where cancer cells from patients are grown into a semi-solid extracellular matrix using media enriched with growth factor.[3] Another example is 3D culture cytotoxicity where tumor cells are grown in a multi-cell-type 3D model to preserve the gene expression patterns similar to the tumor microenvironment. This type of culture shows significant differences in drug sensitivity when compared with cancer cells grown in a monolayer or in 3D organoid culture.[4] There are also patient-derived xenograft (PDX) mouse models that are used in order to closely mimic the tumor microenvironment where patient-derived tumors are implanted subcutaneously or orthotopically. These models are not only used for drug discovery to test efficacy, but they could be used as a method for determining the most accurate patient therapies.[5] Another functional assay that has been used in the last years is Bcl-2 homology domain 3 (BH3) profiling which is the focus of this chapter.

4.1.2 BH3 profiling assay

BH3 profiling is a method to determine how a certain tumor evades apoptosis.[6] The advantage of this method is the ability to quickly detect expected drug responses within a few hours without the need for tedious cell culture. BH3 profiling is used in identifying the dependence on anti-apoptotic proteins, which is more accurate than determining the expression of these proteins on the transcriptional or translational level.[7, 8]

Mitochondria regulate apoptosis

As stated previously, the Bcl-2 family of proteins is a key regulator of the intrinsic apoptotic pathway. This is controlled by the interaction between anti-apoptotic and pro-apoptotic proteins.[9] The pro-apoptotic proteins are divided into activators, sensitizers, and effectors. Once effectors (e.g. Bax and Bak) are activated, their monomer form is converted to oligomers that form pores in the mitochondrial outer membrane, leading to membrane permeabilization, leading to the release of cytochrome c to the cytoplasm.[10] The activators are pro-apoptotic BH3-only proteins (e.g. Bim and Bid), which can directly induce the activation of effectors.[11] The sensitizer BH3-only pro-apoptotic proteins (e.g. Noxa, Bad, Hrk, Bik, Bmf and Puma) cannot directly induce the

activation of effectors, but they displace activators from binding to the anti-apoptotic proteins so they are considered the inhibitors of apoptosis inhibitors (Figure 4.1).[12]

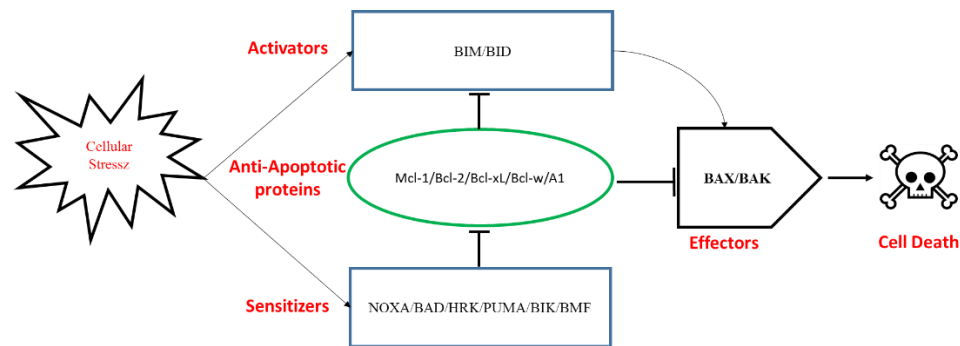


Figure 4.1. Bcl-2 family regulation of apoptosis. Cellular stress leads to the activation of BIM and BID leading to the activation of effectors and ultimately cell death.

BH3 profiling detects three classes of apoptotic evasion

In BH3 profiling, the mitochondria are exposed to a series of synthetic BH3 domain containing peptides that have different selectivity profiles towards anti-apoptotic proteins and detecting mitochondrial outer membrane permeabilization (MOMP). By pinpointing the pattern by which BH3 peptides induce MOMP, the method by which the cancer evades apoptosis can be determined.

There are majorly three distinct apoptosis evasion mechanisms that cancer cells use to evade the intrinsic apoptotic pathway (Figure 4.2). First, the elimination or reduction of effector proteins activation, which could be due to deletion of crucial pro-apoptotic BH3-only genes (class A), like in large cell lymphoma SU-DHL-8. Second, the elimination or reduction of the effector proteins, Bax and Bak, leading to a profound blockage of the apoptotic pathway due to the fact that Bax and Bak are crucial for the execution of pro-apoptotic function (class B). This can be detected in large cell lymphoma SU-DHL-10.[13] Finally, activation of Bax and Bak might be evaded through the expression of anti-apoptotic proteins like Bcl-2, Bcl-xL, and Mcl-1 (class C). The cells that adopt the class C evasion pathway are considered primed for death and can be determined by different levels of MOMP by sensitizer BH3 peptides.

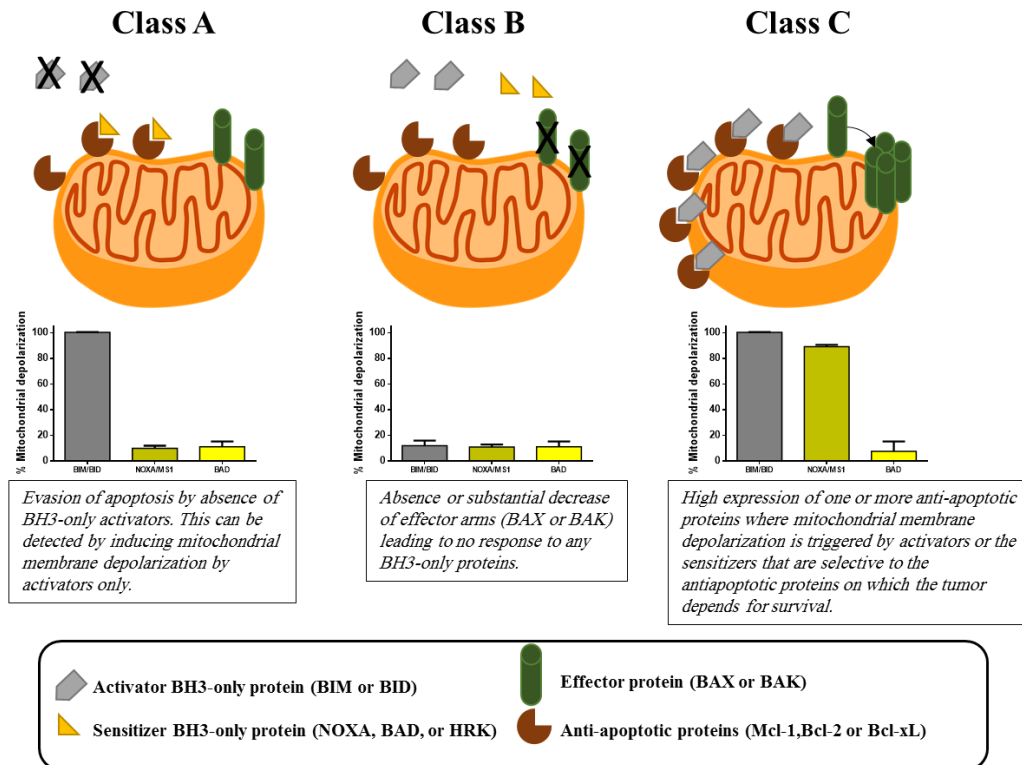


Figure 4.2. BH3 profiling distinguishes between three classes of apoptosis evasion.

Class C cell lines are the focus of the studies since they can be a promising target for Mcl-1 inhibitors, if they are Mcl-1 dependent. Based on the selectivity profile of the synthetic peptides used (Figure 4.3), the anti-apoptotic protein that is crucial for survival can be identified. If Noxa triggers a high mitochondrial depolarization but significantly less using Bad, then the tumor is most likely to be dependent on Mcl-1 for survival while the opposite will indicate dependence on Bcl-2 and/or Bcl-xL. MS1 is a synthetic peptide that was developed to be used in BH3 profiling due to its superior potency to Mcl-1 compared to Noxa.[14] Using MS1 is a better alternative to be used since its binding affinity to Mcl-1 is similar to the binding affinity of Bad to Bcl-2, Bcl-xL, and Bcl-w.

	Activator	Sensitizers			BH3 mimetics		
	Bim	Bad	Noxa	MS1	483	ABT 263	ABT 199
Mcl-1	Blue	White	Blue	Blue	Blue	White	White
Bcl-2	Blue	Blue	White	White	White	Blue	Blue
Bcl-xL	Blue	Blue	White	White	White	Blue	White

Figure 4.3. Selectivity profile of synthetic BH3 peptides and small-molecule BH3 mimetics.

Mitochondrial outer membrane permeabilization

Originally, BH3 profiling was performed by isolating mitochondria from cells and treating with various synthetic BH3 peptides derived from BH3-only domain proteins. The induction of MOMP was measured with western blotting or ELISA to detect cytochrome c release.[12, 15] This method required tens to hundreds of millions of cells to isolate enough mitochondria for various peptide treatments. A new technique for BH3 profiling was later developed to take advantage of the correlation between MOMP and change of the fluorescence of JC-1 (5,5',6,6'-tetrachloro-1,1',3,3'- tetraethylbenzimidazolylcarbocyanine iodide) from red to green. JC-1 is a lipophilic cation existing in a monomeric form and emits in the green region. It is widely used for microscopic and cytometric determination of mitochondrial membrane potential. In healthy mitochondria possessing high membrane potential, it accumulates in the mitochondria and forms J-aggregates and reversibly changes in fluorescence emission from green to red/orange. In cells with depolarized mitochondria (low mitochondrial membrane potential), JC-1 remains in cytoplasm as J-monomers, emitting green fluorescence. [16]

The use of JC-1 allowed the use of plate-based whole cells for BH3 profiling. Digitonin is used to permeabilize the cell membrane and allow introduction of synthetic peptides into the cells. The digitonin efficiency is directly proportional to membrane cholesterol, which is higher in the cell membrane compared to the mitochondrial membrane, so the concentration is only sufficient to permeabilize the cell membrane without harming the mitochondrial membrane.[17] A trehalose-based buffer is used in order to stabilize the mitochondria in permeabilized cells.[18] The advantage of this technique is that a few thousand cells are needed for the experiment and MOMP is followed for a maximum of 3 h at 30°C so the time of experiment is about 5 h (Figure 4.4).

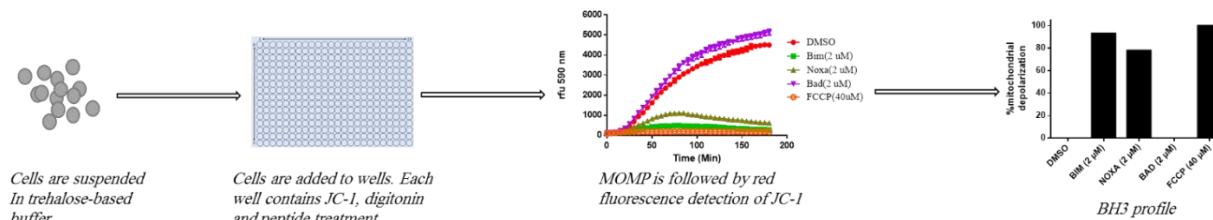


Figure 4.4. Whole cell BH3 profiling. The cells are suspended in trehalose based buffer and then transferred into wells containing JC-1, digitonin, and peptides. The JC-1 red fluorescence is measured in 5 minutes' intervals for 90 to 180 minutes. For ease of comparison, the kinetics data can be normalized and presented by selecting a fixed point at 90, 120, or 180 minutes, or calculating the area under the curve.

BH3 profiling can also be determined using flow cytometry. The advantage of flow cytometry is the ability to test specific cell populations in heterogeneous samples, especially if it is difficult to enrich the cell population to be used in the plate-based assay. In this method TMRE is usually the best choice.[19]

A new concept that is introduced lately is Dynamic BH3 profiling (DBP). This method measures the changes in priming induced through treatment with compounds prior to BH3 profiling. So if one tumor is resistant to a certain drug and another tumor is sensitive, the sensitive one will show more priming after treatment with sub-lethal dose of the drug while the resistant tumor will have no change in BH3 profile. Implementing DBP can aid in determining the best treatment that can be used to treat a certain type of cancer in a very short time, even if it takes several days for the drug to induce cell death. This method can be used on primary cancer cells where there is no need to wait for one or more days to determine the most effective treatment.[20]

4.1.3 Cancers that show dependence on the Bcl-2 family proteins for survival

In this study, the focus will be on four types of cancer: multiple myeloma and leukemia, as examples of hematologic tumors; as well as head and neck squamous cell carcinoma and pancreatic cancer, as examples of solid tumors.

Multiple myeloma (MM) is a hematologic malignancy and accounts for approximately 10% of all hematologic cancers.[21] Even though progress in the treatment of this disease has been

made, multiple myeloma remains largely incurable by current standard treatments and new therapeutic strategies are needed.[22] Recent advances in genomic and proteomic studies of MM have shown that the survival and resistance to chemotherapy of myeloma cells is dependent on defects in the programmed cell death pathway. Mcl-1 is highly upregulated in MM samples of patients at diagnosis, as well as in samples taken at relapse, and correlates with resistance to chemotherapy, relapse, and shorter survival times. [23-25] Downregulation of Mcl-1 significantly increased apoptosis in MM cell lines and plasma cells from MM patients [23].

Acute myeloid leukemia (AML) is a malignancy in which the bone marrow is replaced by immature myeloid cells. 70% of patients diagnosed with AML die from this malignancy. Mcl-1 is important for the survival of AML cells. This is confirmed by experiments based on the implementation of genetic methods to downregulate the expression of Mcl-1, in order to test its effect on survival of AML cells. [26] Knocking down the *mcl-1* gene has led to the spontaneous apoptosis of AML cells.

Head and neck squamous cell carcinoma (HNSCC) is composed of a heterogeneous group of tumors in the upper aero digestive tract, and is the sixth most common cancer in the world.[27] The 5-year survival rate is poor, with only small improvement in the past few years despite improvements in surgical procedures, radiotherapy, and chemotherapy.[28] The majority of head and neck carcinomas are highly resistant to various chemotherapy and radiotherapy regimens, highlighting the clinical need for alternate modalities of treatment for these cancers.[29] One of the HNSCC hallmarks is overexpression of the anti-apoptotic proteins of the Bcl-2 family. [30] Thus, new approaches are needed to identify key tumor-specific survival pathways, targeted therapeutics, and biomarkers to predict drug sensitivity in this disease.

Pancreatic cancer is among the most therapy resistant cancers, with a poor prognosis and high mortality rate. [31] The only possible curative treatment is surgical removal with five-year survival rate below 5%. [32] Although gemcitabine is the drug of choice in the treatment of pancreatic cancer, it produces a limited improvement in overall survival. [33] It has been shown that downregulation of Mcl-1 using siRNA approach enhances the induction of apoptosis and sensitivity of pancreatic cancer to gemcitabine and radiation, providing evidence that Mcl-1 might play an important role in pancreatic cancer biology.[34, 35]

Thus, Mcl-1 represents an attractive molecular target for designing a new class of agents for treatment of these types of cancer and overcoming resistance to chemotherapeutics. It is clear now that Mcl-1 is a validated target that can aid in the ongoing war against cancer.

Since BH3 profiling is important in determining the dependence on different anti-apoptotic proteins, this method is implemented in screening hematologic and solid tumors to determine the most sensitive cell lines to our novel and selective Mcl-1 inhibitors. This was further confirmed by the ability of Mcl-1 inhibitors to induce the hallmarks of apoptosis in cancer cell lines that depend on Mcl-1 for survival.

4.2 Results

4.2.1 BH3 profiling determines anti-apoptotic survival dependence

In this study, six established MM cell lines (H929, OPM-2, KMS-11, MM.1S, RPMI 8226 and U266) and three leukemia cell lines (ML2, THP-1 and K562) were obtained as representatives for hematologic tumors. For solid tumors, three pancreatic cell lines (PANC-1, MIA PaCa-2 and BxPC-3) and 12 HNSCC cell lines (UM47, UM97, UM23, UM59, UM104, UM110, UM69, UM14a, UM92, UM58, 93-VU-147 and UM49) were generously provided by Dr. Thomas Carey. BH3 profiling was performed to determine the anti-apoptotic proteins upon which these cell lines are dependent.

In MM cell lines three cell lines (H929, OPM2, and KMS-11) showed dependence on Mcl-1 for survival (Figure 4.5a). Although KMS-11 does not show Mcl-1 dependence at 8 μ M like OPM2, increasing peptide concentration to 16 and 32 μ M clearly showed a significantly increasing percentage of MOMP by MS1, the selective Mcl-1 peptide, indicating the dependence on Mcl-1 for survival. Bad but not MS1 induced around 60-80% mitochondrial depolarization when testing MM.1S, RPMI 8226, and U266, indicating the dependence on Bcl-2/Bcl-xL but not Mcl-1. The results for H929, OPM2, MM.1S, and RPMI 8226 were consistent with reported data regarding their anti-apoptotic proteins dependence.[36-38]

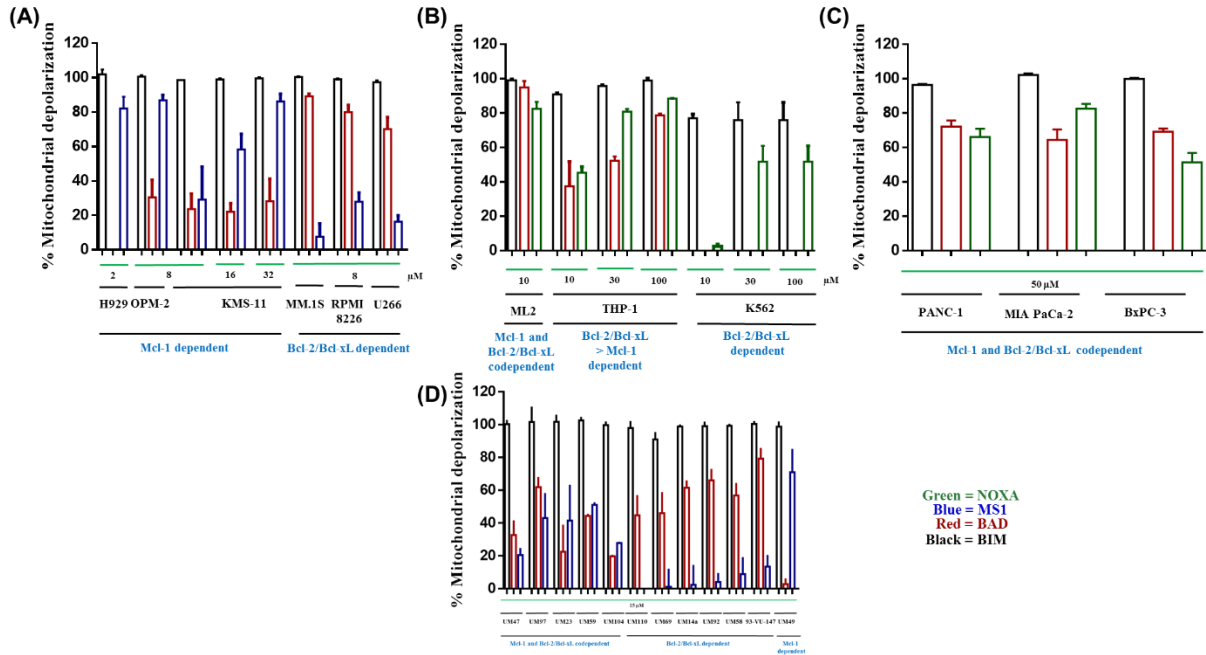


Figure 4.5. BH3 profiling distinguishes between Mcl-1 and Bcl-2/Bcl-xL dependence. BH3 profiling performed in (A) Multiple myeloma (B) Leukemia (C) Pancreatic cancer and (D) Head and neck cancer.

Tested leukemia cell lines, ML2 and THP1, showed Mcl-1 and Bcl-2/Bcl-xL co-dependence. However, THP1 showed a lower percentage of mitochondrial depolarization by Bad and MS1 compared to ML2 at the same peptide concentrations used (10 μ M). K562 showed no dependence on Mcl-1, confirmed by the diminished mitochondrial depolarization up to 100 μ M of MS1 (Figure 4.5b).

Interestingly, the three tested pancreatic cell lines showed co-dependence on Mcl-1 and Bcl-2/Bcl-xL (Figure 4.5c), which is consistent with data generated previously in our lab using siRNA studies as well as other labs. [34, 39]

Based on the BH3 profiling results, the HNSCC cell lines can be categorized into three groups: Mcl-1 and Bcl-2/Bcl-xL co-dependent (UM47, UM97, UM23, UM59, and UM104), Bcl-2/Bcl-xL dependent (UM110, UM69, UM14a, UM92, UM58, and 93-VU-147) and Mcl-1 dependent (UM-49) (Figure 4.5d). These results correlate with reported data indicating that Bcl-xL and less frequently Bcl-2 are major players in conferring resistance in HNSCC cell lines. [40-

42] The co-dependence of HNSCC cells on Bcl-2, Bcl-xL, and Mcl-1 was also confirmed in literature by treating the cells with ABT-737 and showing that this treatment was not enough in inducing cell death, but in combination with Noxa siRNA the cell death was promoted. [43]

To gain better understanding about the survival dependence of the cancer cell lines and predict their sensitivity, it is important to analyze the correlation between BH3 profiling data and the expression of anti-apoptotic genes. For this purpose, the Mcl-1, Bcl-2, and Bcl-xL gene expression data reported for the tested cell lines were obtained from Expression Atlas public repository (Table 4.1). [44]

Table 4.1.RPKM expression levels of anti-apoptotic proteins based on RNA-Seq data. RPKM in (A) Multiple myeloma (B) Leukemia and (C) Pancreatic cancer.[44]

(A)

	H929	OPM-2	KMS-11	MM.1S	RPMI 8226	U266
Mcl-1	434	131	150	109	62	189
Bcl-2	7	10	25	14	19	32
Bcl-xL	17	9	16	114	59	100

(B)

	ML2	THP1	K562
Mcl-1	50	71	48
Bcl-2	24	27	0.1
Bcl-xL	8	12	56

(C)

	PANC-1	MIA PaCa-2	BxPC-3
Mcl-1	48	80	85
Bcl-2	0	1	2
Bcl-xL	102	25	65

Using the expression data, the percentage of mitochondrial depolarization by 8 μ M MS1 peptide was plotted against the expression levels of anti-apoptotic proteins in MM cell lines. The data indicated that there was no correlation ($R^2 = 0.37$) between the percentage of mitochondrial depolarization and Mcl-1 expression (Figure 4.6a). However, there was an inverse correlation with Bcl-xL expression ($R^2 = 0.63$), which is consistent with expected mitochondrial depolarization. Higher expression of Bcl-xL will lead to less effect on the mitochondrial potential by MS1 peptide since it does not bind Bcl-xL protein (Figure 4.6b). With a Mcl-1/Bcl-xL expression ratio, a high positive correlation ($R^2 = 0.83$) has been confirmed, indicating the importance of Mcl-1 gene expression in regulating Mcl-1 dependence in MM (Figure 4.6c).

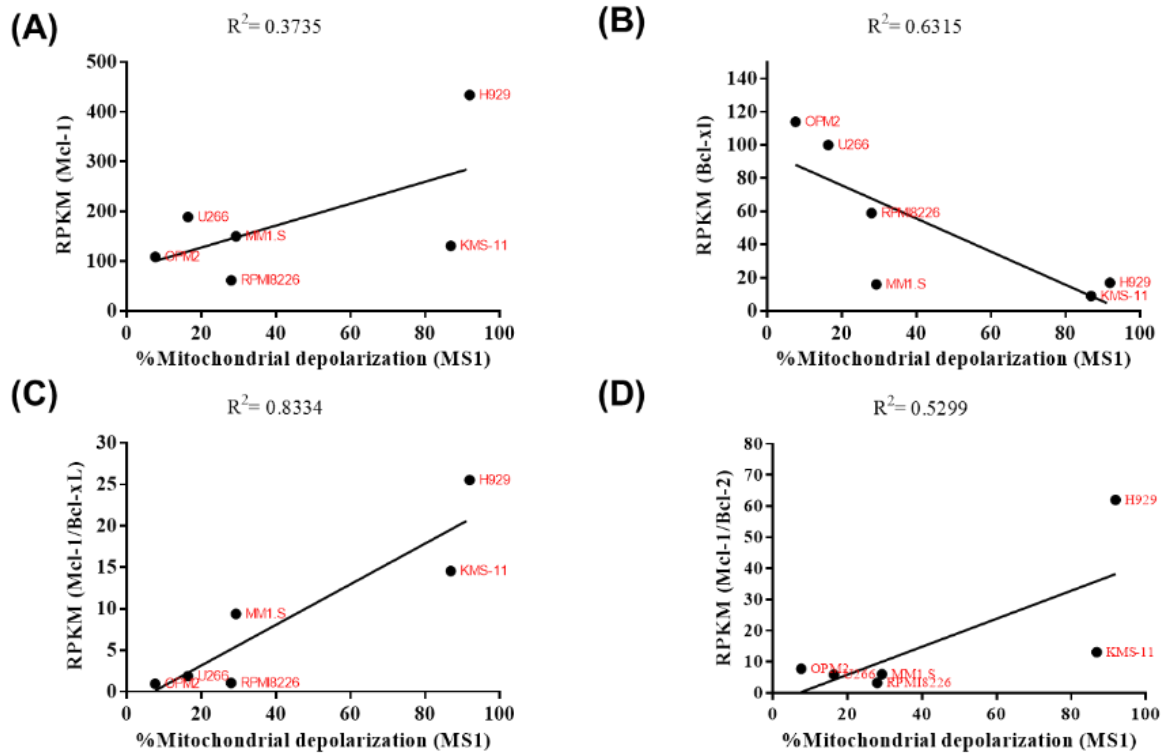


Figure 4.6. Plots between percentage of mitochondrial depolarization by MS1 in multiple myeloma cell lines and RPKM expression levels. The plot of (A) Mcl-1; (B) Bcl-xL; and ratio of expression levels (C) Mcl-1/Bcl-xL and (D) Mcl-1/Bcl-2.

We then determined the *in vitro* sensitivity of multiple myeloma cell lines to the Mcl-1 BH3 mimetic inhibitor, **483LM** through MTT cell proliferation assay. As expected based on the BH3 profiling, data cell lines which were identified to depend on Mcl-1 for survival were more sensitive to **483LM**. Plotting the IC₅₀ values of growth inhibition versus percentage of mitochondrial depolarization by MS1 showed high correlation ($R^2=0.75$) (Figure 4.7).

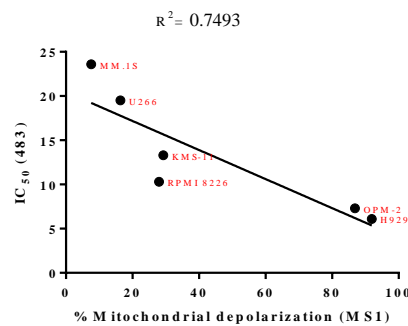


Figure 4.7. The sensitivity of MM cell lines correlates with percentage of mitochondrial depolarization by MS1.

4.2.2 Pharmacological approach for confirmation of cancer cell survival dependence

To further confirm the data obtained by BH3 profiling and cancer cell survival dependence, small-molecule BH3 mimetics with different binding selectivity were used as pharmacological tools. Selective Mcl-1 inhibitor **483LM** should mimic and behave in a similar manner as Noxa (and MS1), while ABT-263 is Bcl-2, Bcl-xL and Bcl-w inhibitor, as Bad BH3 mimetic. In addition, these studies will further confirm if these compounds act in an on-target mechanism.

Using the Mcl-1 dependent H929, **483LM** was able to induce dose dependent mitochondrial depolarization, similar to Noxa, while ABT-263 did not trigger the depolarization, similar to Bad. In contrast, **483LM** and Noxa did not show effect on the mitochondrial depolarization in the Bcl-2/Bcl-xL dependent MM.1S cell line, while ABT-263 and BAD induce almost 100% depolarization of the mitochondrial potential at tested concentrations (Figure 4.8).

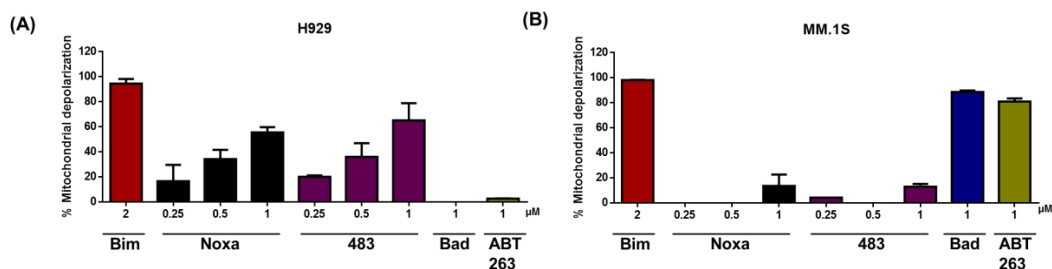


Figure 4.8. BH3 profiling using 483LM and ABT263 resembles the selectivity of NOXA and BAD respectively. (A) BH3 profiling of Mcl-1 dependent H929 (B) BH3 profiling of Bcl-2/Bcl-xL dependent MM.1S

This consistent data with the functional BH3 profiling assay were further confirmed with analyzing apoptosis induction in Mcl-1 dependent, H929, and non-dependent cells, MM.1S and U266. **483LM** induced apoptosis in H929 after a treatment of 4 h, while it has almost no effect on MM.1S and U266 after 24 h of treatment (Figure 4.9). In contrast, ABT-263 induced apoptosis only in MM1.S and U266 consistent with its binding selectivity profile.

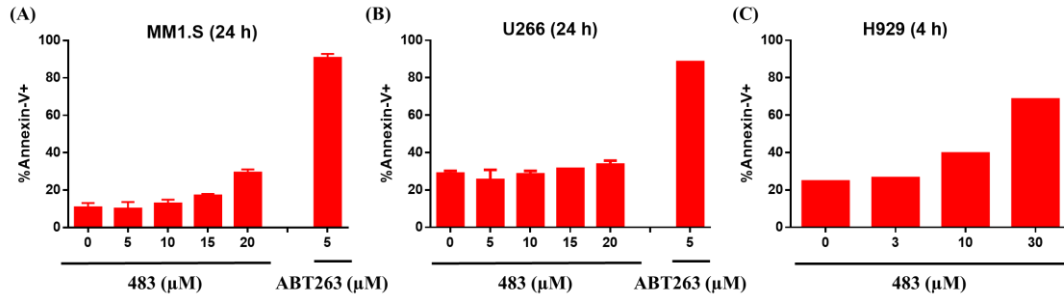


Figure 4.9. Detection of apoptosis induction after treatment with 483LM and ABT-263. Experiments are conducted in (A) MM1.S, (B) U266 and (C) H929 cell lines.

The same pattern was seen when HNSCC UM49 and UM110 were treated with **483LM**, **487LM**, ABT-199 (selective Bcl-2 inhibitor) and ABT-263. **483LM** induced dose-dependent apoptosis in UM-49 but not in UM-110 (Figure 4.10a).

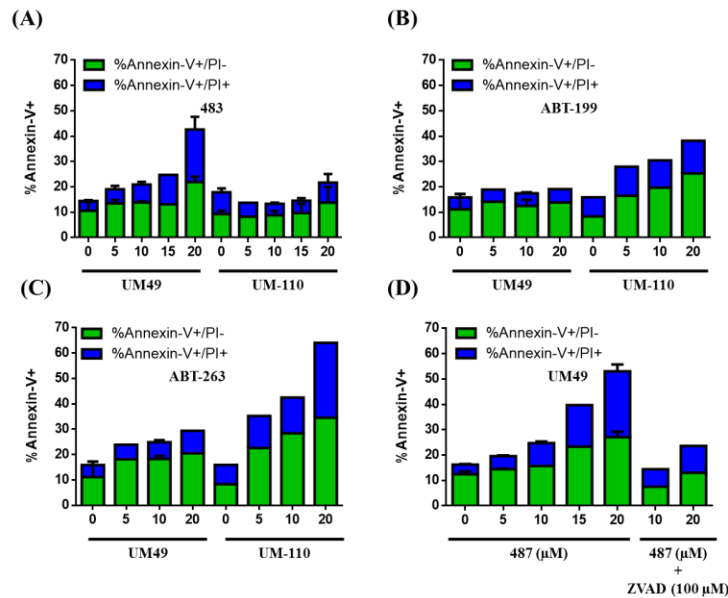


Figure 4.10. BH3 mimetics induce apoptosis in HNSCC UM-49 and UM-110 cell lines in 24 hours consistent with the predicted survival dependence on the anti-apoptotic proteins. (A) Mcl-1 inhibitor; (B) Bcl-2 inhibitor; (C) Bcl-2/Bcl-xL inhibitor; (D) Mcl-1 inhibitor induces caspase-dependent apoptosis in sensitive UM-49 cell line.

As expected, ABT-199 and ABT-263 induced apoptosis in UM-110 more than UM-49 (Figure 4.10b, c). It is worth noting that ABT-263 is more potent in inducing apoptosis in UM110, in comparison to ABT-199, indicating that the survival of this cell line depends more on Bcl-xL

than on Bcl-2. Further studies to probe the mechanism of apoptosis induction showed that **487LM** induces caspase-dependent apoptosis in UM-49 cells, which can be seen with the marked decrease in apoptosis when UM-49 cells were pretreated with the pan caspase inhibitors ZVAD (Figure 4.10d).

Identified Mcl-1 survival dependence of UM-49 cells was further confirmed by implementing a genetic approach. Mcl-1 gene expression in UM-49 and UM-110 was successfully knocked down using Mcl-1 siRNA. UM-49 cell viability was profoundly affected while UM110 was not significantly affected, further demonstrating that its survival does not depend on Mcl-1 (Figure 4.11).

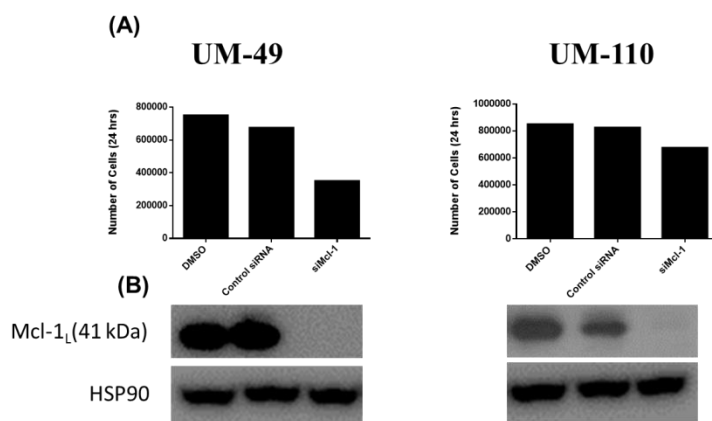


Figure 4.11. Mcl-1 siRNA knockdown induces cell death to UM-49 but not to UM110. (A) Number of live cells counted using trypan blue and **(B)** Corresponding western blots.

4.2.3 Selective Mcl-1 inhibitors activate the hallmarks of apoptosis in Mcl-1 dependent cancers

To confirm that these compounds act on-mechanism, we performed a series of assays designed to assess the sequential events that occur during activation of the intrinsic apoptosis pathway. For this purpose, H929 cell line was selected due to its Mcl-1 dependence. Using Co-Immunoprecipitation, **483LM** markedly disrupted the interaction between Mcl-1 and Bak, indicating the inhibition of Mcl-1 function as an anti-apoptotic protein (Figure 4.12a). Treating the cells with **483LM** for 4 h was enough to show mitochondrial depolarization, which was detected by the conversion of JC-1 fluorescence from red to green (Figure 4.12b). Mitochondrial depolarization is usually correlated with the oligomerization of effector proteins (Bax or Bak),

followed by the release of cytochrome c and Smac. [45, 46] The release of Smac from mitochondria to cytosol was detected after 6 h of treatment with **483LM** (Figure 4.12c).

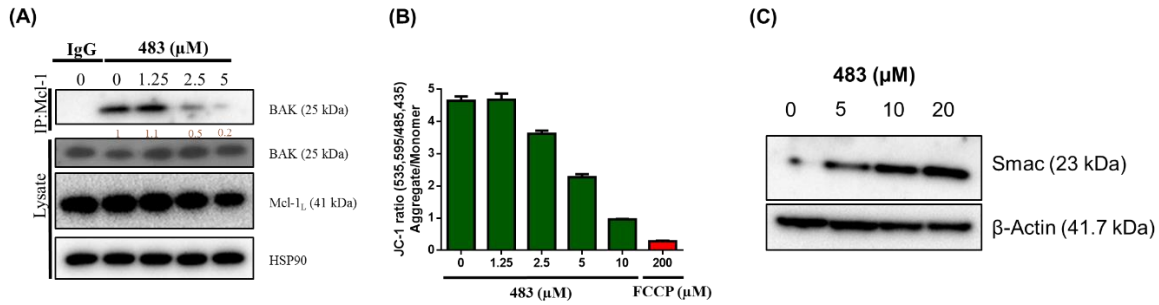


Figure 4.12.483LM disrupts the interaction between Mcl-1 and BAK inducing mitochondrial membrane depolarization and Smac release. (A) CoIP showing disruption of Mcl-1 and BAK interaction **(B)** Mitochondrial outer membrane depolarization detected using JC-1 **(C)** Cell fractionation assay indicating the release of Smac into the cytoplasm.

Smac release leads to the induction of cytochrome c-dependent caspase activation. [47] Caspase 3 activation was detected after 4 h of treatment with **483LM** (Figure 4.13a). The activation of caspases mediates PARP cleavage, which is detected after treatment with **483LM** (Figure 4.13b). Overall the obtained results demonstrated that **483LM** induces the hallmarks of apoptosis in the Mcl-1 dependent H929 cell line, including mitochondrial membrane depolarization, release of Smac, caspase-3 activation, and PARP cleavage.

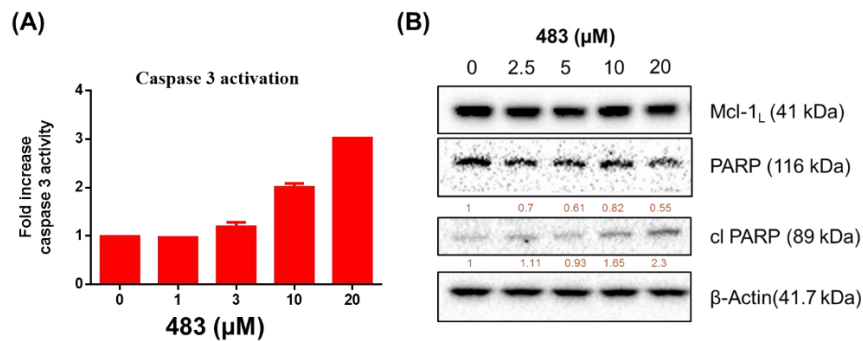


Figure 4.13.483LM induces caspase 3 activation and PARP cleavage. (A) Dose dependent caspase 3 activation after 4 h of treatment as well as **(B)** PARP cleavage.

4.2.4 *In Vivo* efficacy of 483LM in mouse xenograft models with Mcl-1 sensitive cell line

Based on the promising cellular activity of 483LM in H929 multiple myeloma cells and encouraged by the pharmacokinetic properties of 483LM (data not shown), we decided to test the *in vivo* activity of 483LM in the H929 xenograft tumor model. 483LM was administrated daily with IP injection at 30 and 60 mg/kg for 10 consecutive days. In this period 483LM did not cause any loss in the animal's weight, and there was no obvious sign of toxicity during the course of the injections. The treatment with 483LM resulted in statistically significant ($p < 0.001$) dose-dependent tumor growth inhibition in comparison with the control mice. A 60 mg/kg dose completely suppressed the tumor growth, an effect which lasted 7 days after the end of the treatment (Figure 4.14). This experiment confirms the ability of 483LM to distribute to the tumor and reduce its growth *in vivo*.

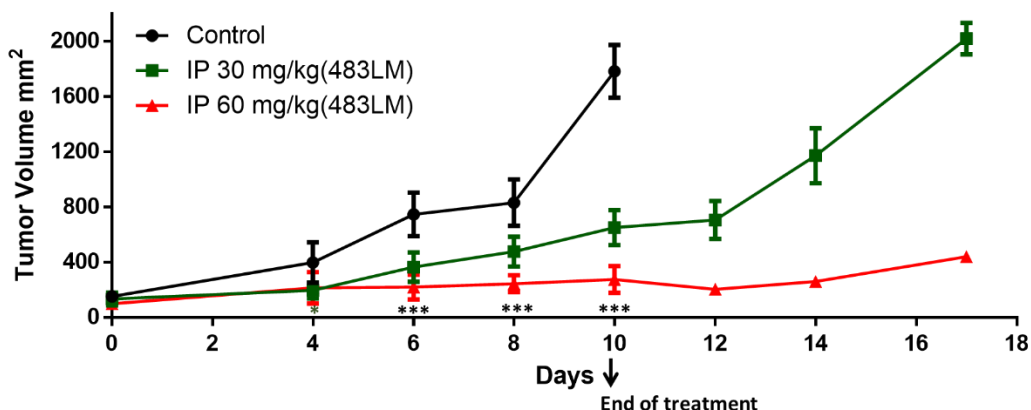


Figure 4.14. *In vivo* efficacy of 483LM in mouse xenograft model with Mcl-1 dependent H929. (*) $p < 0.05$ (***) $p < 0.001$, Columns, mean; bars, SEM. ANOVA, Bonferroni's post-hoc test

4.2.5 483LM causes cell death in Mcl-1 and Bcl-2/Bcl-xL codependent cell lines in combination with ABT 263.

Mcl-1 has been well characterized as a resistance factor for the Bcl-2/Bcl-xL inhibitors and many reports have demonstrated that siRNA-mediated knockdown of Mcl-1 sensitizes cancer cells to death by Bcl-2/Bcl-xL inhibitors, such as ABT-737. Using BH3 profiling, we also showed that

pancreatic cancer cell lines are co-dependent on Mcl-1 and Bcl-2/Bcl-xL for survival. Thus, we tested the combination of ABT-263 and **483LM** in PANC-1 and Mia PaCa2 cancer cell lines. As expected, ABT-263 had little effect on these cell lines (Figure 4.15). Combination treatment with **483LM** substantially shifted the dose–response curve of ABT-263 in both tested pancreatic cell lines, and IC₅₀ of cell growth inhibition was improved more than 600-fold, indicating an ability to potentiate the effect of Bcl-1/Bcl-xL inhibition. These data further demonstrate that **483LM** is indeed a cell-active Mcl-1 inhibitor that behaves as predicted in sensitizing cancer cells to the effects of Bcl-2/Bcl-xL inhibitors.

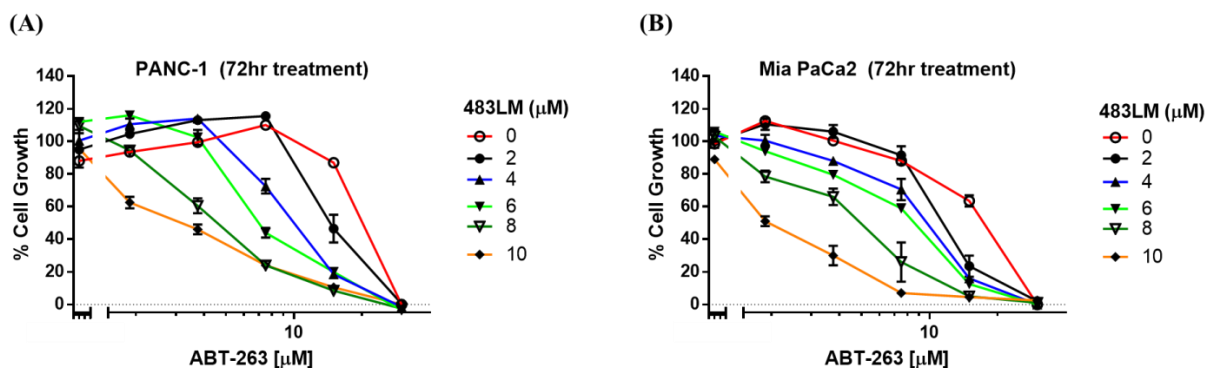


Figure 4.15.483LM exhibits synergism with ABT263 in PANC-1 and Mia Paca2 cell lines that depends on Mcl-1 and Bcl-2/Bcl-xL for survival. (A) Cell growth inhibition of ABT263 against PANC-1 and (B) Mia Paca2 in the presence of 483LM for 72 h determined by MTT assay.

4.3 Conclusions

BH3 profiling is a crucial tool in understanding the way cancer cells evade apoptosis. It can also be used to determine the sensitivity of cancer to cancer therapeutics as well as new drug candidates. It will be important to implement this method in clinical settings, to identify the types of cancer that can be effectively treated with Mcl-1 inhibitors that are introduced into the clinic, either as single agents or in combination with other therapeutics. Relying on levels of certain proteins or gene expressions might not be enough to identify the best candidate therapeutics to the type of tumor under investigation. In this study it was shown that Mcl-1 dependence, marked by a higher percentage of mitochondrial depolarization by Noxa or MS1 compared to Bad, might not necessarily correlate solely with the expression level of Mcl-1. Other anti-apoptotic gene expression levels could contribute to the overall Mcl-1 dependence. The implementation of BH3

profiling in a large panel of cell lines can help us understand the major players that add to the resistance or sensitivity of different types of cancer.

In this study, it was shown that Mcl-1 dependent cell lines showed the highest sensitivity to our developed inhibitors, while the Bcl-2/Bcl-xL dependent cell lines were the most resistant as determined by MTT cell viability assays. 483LM disrupted the interaction between Mcl-1 and Bak and induced apoptosis in 4 h as shown by annexin-V staining. Other hallmarks were activated, including Smac release from the mitochondria into the cytosol, activation of caspase 3, and PARP cleavage. Although cell lines such as PANC-1 and BxPC3 that are codependent on Mcl-1 as well as Bcl-2/Bcl-xL were not highly sensitive to **483LM**, the use of the Bcl-2/Bcl-xL inhibitor ABT-263 was able to aid in inducing synergistic cell death. This previous data, in addition to the *in vivo* efficacy, indicates that understanding the mechanism of cancer survival using functional assays such as BH3 profiling can help assess the response to drugs, which is a major progress in the field of personalized medicine.

4.4 Materials and Methods

BH3 profiling

Peptides; Bim (141-166) and Noxa (20-45) were purchased from Genbio synthetic peptide. BAD (102-128) and MS1 (RPEIWM TQGLRRLGDEINAYYAR-NH₂)[14] were synthesized on an ABI 433A peptide synthesizer, starting the synthesis with Rink amide resins. Cells were suspended in DTEB prepared as reported [19]. The cells were added into a 384 well plate (Corning #3573) in triplicates on wells containing peptides, 1 μ M JC-1 (Assay Biotech #Z0344), 40 μ g/ml oligomycin (Acros Organics #230350250), 5 mM 2-mercaptoethanol (Fisher Bioreagents #BP176) and digitonin (Sigma #D141). Digitonin concentration was 0.0025% for MM cell lines, Leukemia, HNSCC, and pancreatic cancer cell lines except 0.005% for PANC-1. 25,000 cells per sample were used for MM cell lines, 50,000 cells for Leukemia cell lines, and 10,000 for pancreatic and HNSCC cell lines. Fluorescence was continuously monitored at 490 nm excitation and at 590 nm emission every 5 min for 180 min on a Biotek synergy H4 plate reader, and data was analyzed using GraphPad Prism 6.01. Percent mitochondrial depolarization was calculated using the 90 minutes for BH3 profiling using **483LM** and ABT-263, and all others calculated at the 180 minutes

time point, except HNSCC where the AUC was measured as compared to the positive (Carbonyl cyanide-4-(trifluoromethoxy)phenylhydrazine) FCCP (Sigma #c2920) and negative (DMSO) controls.

Cell culture

HNSCC were provided by Dr. Chad Brenner and Dr. Thomas Carey. The cells were cultured in DMEM (Gibco #11965-092), supplemented with 1/100th volume of penicillin/streptomycin (Gibco #15140-122), 100 μ M (1x) of non-essential amino acids (Gibco #11140-050) and 10% heat inactivated fetal bovine serum (Corning #35-010-CF). Pancreatic cancer and leukemia cell lines were obtained from the American Type Culture Collection (ATCC) and cell cultured in DMEM (Gibco #11995-065) and RPMI 1640 (Gibco #11875093) respectively except BxPc3, which was cultured in RPMI 1640. In both cases, the media was supplemented with 1/100th volume of penicillin/streptomycin and 10% heat inactivated fetal bovine serum. MM cell lines were obtained from ATCC and cell cultured in RPMI 1640 media (Hyclone #SH30027.02) supplemented with 2 mM (1x) of L-Glutamine (Gibco #25030-081), (1x) of Anti-Anti (Gibco #15240-062), 10 mM of HEPES (Gibco #15630-080), 1 mM (1x) of sodium pyruvate (Gibco #11360-070) and 10% heat inactivated fetal bovine serum (Atlanta Biologicals).

MTT assay

MTT assay cell proliferation was assessed using the 3-(4,5- dimethylthiazol-2-yl)-2,5-diphenyltetrazolium bromide (MTT) assay. Cells were seeded at 20,000 cells/well (MM cell lines) except MM.1S (30,000 cells/well), 15,000 cells/well (Leukemia cell lines), and 5,000 cells/well (pancreatic cell lines) in transparent 96-well plates and treated for 72 h, after which 10 μ L of MTT (5 mg/mL in PBS) was added to each well (Amresco #0793). The wells were incubated for an additional 4 h at 37°C. The MTT formazan precipitate was dissolved using 100 μ L SDS 1 g per 10 ml of 0.01M HCl and incubated overnight. The mitochondrial activity, reflecting cell growth and viability, was evaluated by measuring optical density at 570 nm with plate reader.

siRNA silencing of Mcl-1

500,000 cells /well/2.25ml of UM49 and UM110 were plated in 6-well plates in their growth media on day 0. On day 1, siRNA was complexed with Lipofectamine™ 2000 (Life Technologies) according to manufacturer's instructions and the cells were incubated with 44nM Mcl1 siRNA (Dharmacon # J-004501-15) and scrambled control (Dharmacon #D-001810-10-05) in Opti-MEM medium (Invitrogen) for 24 h.

Determination of caspase activity

H929 cells were seeded in 12-well plates at 0.5×10^6 cells/well. After 4 h of treatment with different concentrations of the compounds, caspase 3 activity was determined using the fluorometric substrates DEVD-AFC, according to the manufacturer's protocol of Caspase-3 fluorometric assay kit (BioVision). The calculation of caspase 3 activity is presented as the fold change relative to DMSO treated cells.

Analysis of apoptosis

To determine the induction of apoptosis, MM cells were plated in 12-well plates at 0.2×10^6 cells/well and treated with various concentrations of tested compounds. After 4 or 24 h, cells were harvested, washed two times with PBS, and treated with APC-Annexin-V (Biolegend #640941) according to manufacturer's protocol. HNSCC cells were plated in 12-well plates at 0.2×10^6 cells/well overnight at day 0. On day 1, the cells are treated with various concentrations of compounds for 24 h. The cells are then stained with APC-Annexin-V (Biolegend), according to protocol and propidium iodide (MP Biomedicals #0219545810), to final concentration of 25 $\mu\text{g/ml}$. The percentage of cells undergoing apoptosis was assessed by flow cytometry within 1 h and analyzed using WinList 8.0. Apoptosis was also determined in the presence of Z-VAD-FMK (Bachem # N15100005), pan caspase-inhibitor. For this purpose, cells were pretreated with 100 μM Z-VAD-FMK for 1 h before adding tested compounds.

Smac release assay

4x10⁶ of H929 cells were treated with compound (100 mm cell culture dish). After 4 h treatment, cells were washed with PBS, and re-suspended in digitonin buffer (20 mM HEPES [pH 7.4], 10 mM KCl, 2.5 mM MgCl₂, 1 mM EDTA, 700 µg/ml digitonin, 250 mM sucrose, and 1 mM DTT) supplemented with protease inhibitors cocktail (Biotool #B14002), and incubated for 90 seconds. Cytosolic fractions were separated by centrifugation at 13,200 rpm, 4°C for 10 min. Levels of cytosolic Smac were measured using a Smac/DIABLO antibody (GenLantis # ABI248).

JC-1 mitochondrial membrane potential assay

The mitochondrial membrane potential ($\Delta\Psi_m$) was determined by using JC-1 (Assay Biotech # Z0344). 0.1 x 10⁶ Cells/100 µL were plated and treated with compounds for 4 h, with one sample treated with FCCP (Sigma #c2920) as a positive control. 100 µg/ml JC-1 was prepared using 37°C PBS and 10% DMSO. 10 µL of JC-1 was added to the 100 µL of cells to have 10 µg/ml final concentration and was incubated for 30 minutes. Cells were transferred into 1.5 microcentrifuge tubes and washed twice with 37°C PBS (0.6 rcf, 5min, room temp.). Pellets were resuspended in 100 µL of PBS and transferred to black round bottom 96 well plate (Corning #3792). Fluorescence was detected at Ex.535/Em.595 (aggregate) and Ex.485/Em.435 (monomer). Data was analyzed using GraphPad Prism 6.01 and presented as ratio of aggregate/monomer fluorescence.

Immunoprecipitation

4 x 10⁶ of H929 cells/10 ml of growth media were treated with different concentrations of compound for 24 h. Cells were washed with PBS then lysed using NP-40 lysis buffer (50 mM Tris [pH 7.4], 150 mM NaCl, 1 mM EDTA, 0.5% [v/v] NP-40 and 1 mM DTT) and protease inhibitors cocktail (Biotool #B14002). Cell lysates (500 µg) were precleared and then subjected to immunoprecipitation by adding 3 µg of anti-Mcl-1 antibody or IgG antibody (Santa Cruz #sc-2025) and incubated overnight at 4°C. 20 µL of A/G sepharose beads (Santa Cruz #sc-2003) were added and incubated for 2 h at 4°C, followed by centrifugation of samples. The beads were washed, resuspended in 40 µL of 4x Laemmli buffer, boiled, and supernatant was used for western blot

analysis. The primary antibodies used are: Anti-Mcl-1 Ab-1 (Clone RC13) (ThermoFisher Scientific #MS681P1), Anti-BAK (ThermoFisher Scientific # PA1-31513), and Anti-HSP90 (Santa Cruz # sc-7947).

Western blot analysis

0.1x10⁶/100 µL of H929 cells in 12 replicates in a 96-well plate were treated with compounds and harvested after 4 h. Cells were lysed using RIPA buffer (ThermoFisher Scientific #89900) and protease inhibitors cocktail (Biotool #B14002). Total cell lysates were subjected to electrophoresis, then transferred to PVDF membranes, followed by incubation with primary antibody. Visualization of blots was performed using the chemiluminescent reagent Amersham ECL Prime (GE Healthcare Life Sciences # RPN2232). The primary antibodies used are: Mcl-1 Ab-1 (Clone RC13) (ThermoFisher Scientific #MS681P1), PARP (Cell Signaling #9542), and β-Actin (GenScript #A00702).

In vivo efficacy studies

Twelve Severe Combined Immunodeficiency (SCID) mice were xenografted with 1.2 million human H929 cells. After one week, four mice were treated daily with one IP injection dose of 483LMLM at 30 mg/kg and the other four mice are treated at 60 mg/kg. Four control mice were injected with the IP vehicle. Treatment ended at day 10 and four control mice, two 30 mg/kg, and three 60 mg/kg. The two remaining 30 mg/kg mice and the 60 mg/kg mouse were sacrificed after 7 and 14 days of stopping the treatment, respectively.

4.5 Contributions

Ahmed Mady performed all experiments reported in this chapter except the *in vivo* efficacy study which was performed by Dr. Luke Peterson in Dr. Moshe Talpaz's lab at the Department of Hematology and Oncology.

4.6 References

- [1] van't Veer LJ, Bernards R. Enabling personalized cancer medicine through analysis of gene-expression patterns. *Nature*. 2008;452:564-70.
- [2] Yu M, Bardia A, Aceto N, Bersani F, Madden MW, Donaldson MC, et al. Cancer therapy. Ex vivo culture of circulating breast tumor cells for individualized testing of drug susceptibility. *Science*. 2014;345:216-20.
- [3] Rookmaaker MB, Schutgens F, Verhaar MC, Clevers H. Development and application of human adult stem or progenitor cell organoids. *Nat Rev Nephrol*. 2015;11:546-54.
- [4] Vorsmann H, Groeber F, Walles H, Busch S, Beissert S, Walczak H, et al. Development of a human three-dimensional organotypic skin-melanoma spheroid model for in vitro drug testing. *Cell death & disease*. 2013;4:e719.
- [5] Aparicio S, Hidalgo M, Kung AL. Examining the utility of patient-derived xenograft mouse models. *Nat Rev Cancer*. 2015;15:311-6.
- [6] Letai AG. Diagnosing and exploiting cancer's addiction to blocks in apoptosis. *Nat Rev Cancer*. 2008;8:121-32.
- [7] Cojohari O, Burrer CM, Peppenelli MA, Abulwerdi FA, Nikolovska-Coleska Z, Chan GC. BH3 Profiling Reveals Selectivity by Herpesviruses for Specific Bcl-2 Proteins To Mediate Survival of Latently Infected Cells. *J Virol*. 2015;89:5739-46.
- [8] Ishizawa J, Kojima K, McQueen T, Ruvolo V, Chachad D, Nogueras-Gonzalez GM, et al. Mitochondrial Profiling of Acute Myeloid Leukemia in the Assessment of Response to Apoptosis Modulating Drugs. *PLoS One*. 2015;10:e0138377.
- [9] Czabotar PE, Lessene G, Strasser A, Adams JM. Control of apoptosis by the BCL-2 protein family: implications for physiology and therapy. *Nat Rev Mol Cell Biol*. 2014;15:49-63.
- [10] Westphal D, Kluck RM, Dewson G. Building blocks of the apoptotic pore: how Bax and Bak are activated and oligomerize during apoptosis. *Cell death and differentiation*. 2014;21:196-205.
- [11] Kim H, Rafiuddin-Shah M, Tu HC, Jeffers JR, Zambetti GP, Hsieh JJ, et al. Hierarchical regulation of mitochondrion-dependent apoptosis by BCL-2 subfamilies. *Nat Cell Biol*. 2006;8:1348-58.
- [12] Deng J, Carlson N, Takeyama K, Dal Cin P, Shipp M, Letai A. BH3 profiling identifies three distinct classes of apoptotic blocks to predict response to ABT-737 and conventional chemotherapeutic agents. *Cancer Cell*. 2007;12:171-85.
- [13] Wei MC, Zong WX, Cheng EH, Lindsten T, Panoutsakopoulou V, Ross AJ, et al. Proapoptotic BAX and BAK: a requisite gateway to mitochondrial dysfunction and death. *Science*. 2001;292:727-30.
- [14] Foight GW, Ryan JA, Gulla SV, Letai A, Keating AE. Designed BH3 peptides with high affinity and specificity for targeting Mcl-1 in cells. *ACS Chem Biol*. 2014;9:1962-8.
- [15] Certo M, Del Gaizo Moore V, Nishino M, Wei G, Korsmeyer S, Armstrong SA, et al. Mitochondria primed by death signals determine cellular addiction to antiapoptotic BCL-2 family members. *Cancer Cell*. 2006;9:351-65.
- [16] Perelman A, Wachtel C, Cohen M, Haupt S, Shapiro H, Tzur A. JC-1: alternative excitation wavelengths facilitate mitochondrial membrane potential cytometry. *Cell death & disease*. 2012;3:e430.
- [17] Sudji IR, Subburaj Y, Frenkel N, Garcia-Saez AJ, Wink M. Membrane Disintegration Caused by the Steroid Saponin Digitonin Is Related to the Presence of Cholesterol. *Molecules*. 2015;20:20146-60.

- [18] Ryan JA, Brunelle JK, Letai A. Heightened mitochondrial priming is the basis for apoptotic hypersensitivity of CD4+ CD8+ thymocytes. *Proc Natl Acad Sci U S A*. 2010;107:12895-900.
- [19] Ryan J, Letai A. BH3 profiling in whole cells by fluorimeter or FACS. *Methods*. 2013;61:156-64.
- [20] Ryan J, Montero J, Rocco J, Letai A. iBH3: simple, fixable BH3 profiling to determine apoptotic priming in primary tissue by flow cytometry. *Biol Chem*. 2016;397:671-8.
- [21] Jemal A, Siegel R, Xu J, Ward E. Cancer statistics, 2010. *CA Cancer J Clin*. 2010;60:277-300.
- [22] Mahindra A, Laubach J, Raje N, Munshi N, Richardson PG, Anderson K. Latest advances and current challenges in the treatment of multiple myeloma. *Nat Rev Clin Oncol*. 2012;9:135-43.
- [23] Zhang B, Gojo I, Fenton RG. Myeloid cell factor-1 is a critical survival factor for multiple myeloma. *Blood*. 2002;99:1885-93.
- [24] Derenne S, Monia B, Dean NM, Taylor JK, Rapp MJ, Housseau JL, et al. Antisense strategy shows that Mcl-1 rather than Bcl-2 or Bcl-x(L) is an essential survival protein of human myeloma cells. *Blood*. 2002;100:194-9.
- [25] Wulleme-Toumi S, Robillard N, Gomez P, Moreau P, Le Gouill S, Avet-Loiseau H, et al. Mcl-1 is overexpressed in multiple myeloma and associated with relapse and shorter survival. *Leukemia*. 2005;19:1248-52.
- [26] Glaser SP, Lee EF, Trounson E, Bouillet P, Wei A, Fairlie WD, et al. Anti-apoptotic Mcl-1 is essential for the development and sustained growth of acute myeloid leukemia. *Genes Dev*. 2012;26:120-5.
- [27] Haddad RI, Shin DM. Recent advances in head and neck cancer. *The New England journal of medicine*. 2008;359:1143-54.
- [28] Riaz N, Morris LG, Lee W, Chan TA. Unraveling the molecular genetics of head and neck cancer through genome-wide approaches. *Genes & Diseases*. 2014;1:75-86.
- [29] Shin DM, Khuri FR. Advances in the management of recurrent or metastatic squamous cell carcinoma of the head and neck. *Head & neck*. 2013;35:443-53.
- [30] Gallo O, Chiarelli I, Boddi V, Bocciolini C, Bruschini L, Porfirio B. Cumulative prognostic value of p53 mutations and bcl-2 protein expression in head-and-neck cancer treated by radiotherapy. *Int J Cancer*. 1999;84:573-9.
- [31] Bardeesy N, DePinho RA. Pancreatic cancer biology and genetics. *Nat Rev Cancer*. 2002;2:897-909.
- [32] Hochster HS, Haller DG, de Gramont A, Berlin JD, Philip PA, Moore MJ, et al. Consensus report of the international society of gastrointestinal oncology on therapeutic progress in advanced pancreatic cancer. *Cancer*. 2006;107:676-85.
- [33] Quinn BA, Wang S, Barile E, Das SK, Emdad L, Sarkar D, et al. Therapy of pancreatic cancer via an EphA2 receptor-targeted delivery of gemcitabine. *Oncotarget*. 2016;7:17103-10.
- [34] Abulwerdi F, Liao C, Liu M, Azmi AS, Aboukameel A, Mady AS, et al. A novel small-molecule inhibitor of mcl-1 blocks pancreatic cancer growth in vitro and in vivo. *Mol Cancer Ther*. 2014;13:565-75.
- [35] Wei D, Zhang Q, Schreiber JS, Parsels LA, Abulwerdi FA, Kausar T, et al. Targeting mcl-1 for radiosensitization of pancreatic cancers. *Transl Oncol*. 2015;8:47-54.
- [36] Touzeau C, Ryan J, Guerriero J, Moreau P, Chonghaile TN, Le Gouill S, et al. BH3 profiling identifies heterogeneous dependency on Bcl-2 family members in multiple myeloma and predicts sensitivity to BH3 mimetics. *Leukemia*. 2016;30:761-4.

- [37] Punnoose EA, Levenson JD, Peale F, Boghaert ER, Belmont LD, Tan N, et al. Expression Profile of BCL-2, BCL-XL, and MCL-1 Predicts Pharmacological Response to the BCL-2 Selective Antagonist Venetoclax in Multiple Myeloma Models. *Mol Cancer Ther.* 2016;15:1132-44.
- [38] Morales AA, Kurtoglu M, Matulis SM, Liu J, Siefker D, Gutman DM, et al. Distribution of Bim determines Mcl-1 dependence or codependence with Bcl-xL/Bcl-2 in Mcl-1-expressing myeloma cells. *Blood.* 2011;118:1329-39.
- [39] Takahashi H, Chen MC, Pham H, Matsuo Y, Ishiguro H, Reber HA, et al. Simultaneous knock-down of Bcl-xL and Mcl-1 induces apoptosis through Bax activation in pancreatic cancer cells. *Biochim Biophys Acta.* 2013;1833:2980-7.
- [40] Sharma H, Sen S, Lo Muzio L, Mariggio A, Singh N. Antisense-mediated downregulation of anti-apoptotic proteins induces apoptosis and sensitizes head and neck squamous cell carcinoma cells to chemotherapy. *Cancer Biol Ther.* 2005;4:720-7.
- [41] Pena JC, Thompson CB, Recant W, Vokes EE, Rudin CM. Bcl-xL and Bcl-2 expression in squamous cell carcinoma of the head and neck. *Cancer.* 1999;85:164-70.
- [42] Li R, Boehm AL, Miranda MB, Shangary S, Grandis JR, Johnson DE. Targeting antiapoptotic Bcl-2 family members with cell-permeable BH3 peptides induces apoptosis signaling and death in head and neck squamous cell carcinoma cells. *Neoplasia.* 2007;9:801-11.
- [43] Li R, Zang Y, Li C, Patel NS, Grandis JR, Johnson DE. ABT-737 synergizes with chemotherapy to kill head and neck squamous cell carcinoma cells via a Noxa-mediated pathway. *Mol Pharmacol.* 2009;75:1231-9.
- [44] Klijn C, Durinck S, Stawiski EW, Haverty PM, Jiang Z, Liu H, et al. A comprehensive transcriptional portrait of human cancer cell lines. *Nature biotechnology.* 2015;33:306-12.
- [45] Kroemer G, Galluzzi L, Brenner C. Mitochondrial membrane permeabilization in cell death. *Physiol Rev.* 2007;87:99-163.
- [46] Sharpe JC, Arnoult D, Youle RJ. Control of mitochondrial permeability by Bcl-2 family members. *Biochim Biophys Acta.* 2004;1644:107-13.
- [47] Du C, Fang M, Li Y, Li L, Wang X. Smac, a mitochondrial protein that promotes cytochrome c-dependent caspase activation by eliminating IAP inhibition. *Cell.* 2000;102:33-42.

CHAPTER 5

Summary and future directions

5.1 Summary

There has been a marked progress in cancer research, especially with significant understanding of traits that are acquired by normal cells in order to transform to cancer. This has led to the initiation of a vast number of drug discovery campaigns to develop drugs that modulate these traits. One of the hallmarks of cancer is resistance to apoptosis. Evading apoptosis contributes to tumor proliferation and progression, as well as resistance to therapeutic interventions that act by triggering the activation of the apoptotic pathway. Thus, it is important to understand the mechanisms that contribute to apoptosis resistance in cancer cells. Apoptosis regulates various conserved physiological and pathological processes. The Bcl-2 family of proteins regulates the intrinsic apoptotic pathway through a network of protein-protein interactions between pro-apoptotic and anti-apoptotic proteins. Cell fate is tightly controlled by these interactions. The upregulation of anti-apoptotic proteins and/or downregulation of pro-apoptotic proteins are mechanisms activated by cancers to block the induction of apoptosis. The tumorigenic potential of Bcl-2 family proteins was observed in combination with overexpressed Bcl-2 and c-Myc, promoting proliferation and immortalization of pre-B cells.[1, 2] Another anti-apoptotic protein is Mcl-1, which was identified when the *MCL-1* gene was isolated from maturing ML-1 myeloid cell leukemia.[3] Overexpression of Mcl-1 has been associated with poor prognosis of human cancers as well as resistance to chemotherapeutics.[4-8] Consequently, there are efforts to develop drugs that could block the function of Mcl-1, either indirectly by inhibiting its expression or inducing its degradation, or directly by targeting its interaction with pro-apoptotic partner proteins by developing BH3 mimetics.[9]

In Chapter 2, we employed an integrated screening approach, combining high throughput and virtual screening to identify novel chemical classes as inhibitors of myeloid cell leukemia-1 (Mcl-1), a potent anti-apoptotic protein. For this purpose, we used the PubChem BioAssay Database to further study 1214 positive hits that were identified from our previously reported dual-readout HTS assay that combined two assay technologies, FP and FRET, into one system using Mcl-1 either with labeled Noxa or Bid BH3 derived peptides.[10] A high hit rate in HTS campaigns can make the identification of the most promising hits a challenging task, and novel strategies to simplify this process are desired. Therefore, to further improve the output and the quality of the identified inhibitors, as well as to incorporate the structure-based knowledge of the interactions between Mcl-1 and number of BH3 peptides, we have integrated in silico target-based screening for selection of the most promising hits for further validation. 37 compounds were purchased and evaluated in a complementary set of biochemical and biophysical assays to determine the binding potency against Mcl-1. 20 hits were confirmed to have activity against Mcl-1 with different chemical scaffolds. We further studied one of the hits, **E238**, by synthesizing and testing a small library of triazine-based analogs and reaching 10-fold improvement in binding compared to the original hit compound. We also demonstrated Bax/Bak dependent cellular activity with **E305** as well as Mcl-1 selectivity.

In Chapter 3, we used the knowledge gained from the previously synthesized small library and analyzed the established SAR through various biochemical assays. Consequently, we performed a structural-based design of a new class Mcl-1 inhibitors. The utilization of molecular modeling supported by HSQC-NMR led to designing the new inhibitor **368LM** with a new chemical scaffold. Several analogs were synthesized to explore the interactions with the BH3 binding pocket of Mcl-1. Three of the compounds developed (**396LM**, **382LM**, and **462LM**) were successfully co-crystallized with Mcl-1. These X-ray crystal structures significantly enhanced our understanding of the binding interactions between the inhibitors and Mcl-1, and guided us to optimize their binding affinities. Further drug design efforts led to the development of **483LM**, **487LM** and **491LM** as potent and selective Mcl-1 inhibitors confirmed by FP, TR-FRET, and SPR competitive assays. **483LM** disrupted the interaction between biotinylated Noxa and endogenous Mcl-1 protein in 2LMP cell lysate and also inhibited the function of Mcl-1 in a cell-free functional assay, disrupting its interaction with introduced Bim BH3 peptide. Treating PANC-1 with **483LM** for 6 h disrupted Mcl-1/Bak interaction in a co-immunoprecipitation assay.

Furthermore, compound **483LM** selectively sensitizes E μ -myc lymphomas overexpressing Mcl-1, but not E μ -myc lymphomas overexpressing Bcl-2 or Bcl-xL, correlating with the selectivity profile generated via FP assay. Using MEFs model cell lines, 483LM demonstrated Bax/Bak dependent induction of cell death.

In Chapter 4, we demonstrated the importance of developing functional assays that can aid in predicting the best chemotherapeutic to benefit cancer patients. One of these functional assays is BH3 profiling, where the mitochondria is interrogated by various BH3 pro-apoptotic peptides with different selectivity profiles against anti-apoptotic proteins. With this method, the anti-apoptotic protein on which a certain type of cancer depends can be determined. Using BH3 profiling, we screened a panel of solid and hematological tumors. We detected different dependence profiles in the tested cell lines. Using **483LM** and ABT-263 in BH3 profiling exhibited a similar effect to Noxa and Bad BH3 peptides, respectively. A correlation between mitochondrial depolarization induced by MS1 and Noxa with expression ratio of Mcl-1/Bcl-xL was established in the investigated multiple myeloma and leukemia cell lines, respectively, indicating that these two proteins play a major role in controlling their cell fate. Cell viability and synergistic studies with **483LM** and ABT-263 recapitulated the BH3 profiling data generated. We further investigated the mechanism by which compound **483LM** induces cell death in the Mcl-1 sensitive cell line H929. We demonstrated the ability of the compound to disrupt Mcl-1/Bak interaction, induce mitochondrial membrane depolarization, and trigger the release of Smac from mitochondria to the cytosol. Consequently, caspase 3 is activated and PARP is cleaved, indicating the induction of the apoptotic pathway. This data was encouraging to proceed with in vivo efficacy studies, where 483LM demonstrated, in H929 mouse xenograft model, dose-dependent inhibition of tumor growth. The inhibition of tumor growth was sustained for more than 7 days after stopping the 60 mg/kg treatment.

5.2 Impact and significance of the dissertation studies

The research presented in the dissertation reports discovery and development of potent and selective small-molecule Mcl-1 inhibitors as disruptors of anti- and pro-apoptotic protein-protein challenging interactions. The most important scientific contributions are:

- The use of integrated approach combining high-throughput screening results (deposited in PubChem database) and computational structure-based docking, allowed identification of diverse and novel chemical scaffolds as potential lead compounds for further development.
- Applying structure-based design, followed by medicinal chemistry campaign and SAR studies, novel chemical class of Mcl-1 inhibitors with 2,4,5-substituted benzoic acid scaffold was developed.
- Potent and selective inhibitors exhibit on-target Mcl-1 cellular activity and *in vivo* activity in human multiple myeloma xenograft model as single agents. These compounds, used as chemical tools, will have significant impact on further understanding and validating Mcl-1 as therapeutic target.
- Established BH3 profiling functional assay and understanding the survival dependence of human cancers will allow further implementation of this assay towards personalized medicine, to screen patient samples, and determine the population which will benefit the most of the treatment with Mcl-1 inhibitors or other apoptosis inducers, as single agents or in combination with standard chemotherapy.

5.3 Future directions

Optimization of physicochemical properties of inhibitors

As stated previously, development of PPI inhibitors is a challenging process due to the hydrophobic nature of the PPI interfaces. Several groups have developed highly potent indole-based Mcl-1 inhibitors with limited cell permeability [11-13], and none of these compounds were shown to have *in vivo* efficacy. [14] There is a necessity to develop Mcl-1 inhibitors with enhanced physicochemical properties to develop drug-like molecules that can be taken further to clinical studies. Our most potent Mcl-1 inhibitor, **483LM**, demonstrated encouraging *in vivo* efficacy through intra-peritoneal (IP) injections. However, the physicochemical properties of **483LM** (logP = 9.37 and solubility is up to 15 μ M in PBS buffer with 6% DMSO) require further chemical optimizations in order to improve the oral bioavailability. This will be a significant step towards initiating clinical trials of this class of Mcl-1 inhibitors.

Implementing novel functional methods for precision medicine

The use of functional assays to monitor tumor response in patients is the future of precision medicine. This can guide clinicians to design the most optimum intervention protocol that is most beneficial to cancer patients. We performed BH3 profiling on established cancer cell lines. It is important to extend the assay to primary cells in order to correlate the results of the assay with the predicted outcome of patient treatment. The use of recent dynamic BH3 profiling techniques will be important to determine the best chemotherapeutics to treat a patient's cancer in a matter of hours, instead of waiting for one or more days to determine the best treatment. [15]

Using Mcl-1 inhibitors in single or combination therapy

We have demonstrated the *in vivo* efficacy of an Mcl-1 inhibitor as a single agent on H929 xenograft mouse model. Based on BH3 profiling, H929 is dependent on Mcl-1 for survival. Various types of cancer develop resistance to certain chemotherapeutics, due to upregulation of Mcl-1. As a result, it will be important to determine the *in vivo* efficacy of Mcl-1 inhibitors in these resistant types of cancer, as single agents or as combination therapy to the already used chemotherapeutics. It is yet to be determined if the use of Mcl-1 inhibitors can shift the apoptotic balance of these resistant cancers to induce elimination by a combined chemotherapeutic agent.

Overall, the studies presented in this dissertation will open the door for further research efforts to develop Mcl-1 inhibitors that can be used to treat various types of cancer, either as single agents or in combination with other therapeutics.

5.4 References

- [1] Fanidi A, Harrington EA, Evan GI. Cooperative interaction between c-myc and bcl-2 proto-oncogenes. *Nature*. 1992;359:554-6.
- [2] Vaux DL, Cory S, Adams JM. Bcl-2 gene promotes haemopoietic cell survival and cooperates with c-myc to immortalize pre-B cells. *Nature*. 1988;335:440-2.
- [3] Kozopas KM, Yang T, Buchan HL, Zhou P, Craig RW. MCL1, a gene expressed in programmed myeloid cell differentiation, has sequence similarity to BCL2. *Proc Natl Acad Sci U S A*. 1993;90:3516-20.
- [4] Aichberger KJ, Mayerhofer M, Krauth MT, Skvara H, Florian S, Sonneck K, et al. Identification of mcl-1 as a BCR/ABL-dependent target in chronic myeloid leukemia (CML):

evidence for cooperative antileukemic effects of imatinib and mcl-1 antisense oligonucleotides. *Blood*. 2005;105:3303-11.

[5] Derenne S, Monia B, Dean NM, Taylor JK, Rapp MJ, Harousseau JL, et al. Antisense strategy shows that Mcl-1 rather than Bcl-2 or Bcl-x(L) is an essential survival protein of human myeloma cells. *Blood*. 2002;100:194-9.

[6] Cho-Vega JH, Rassidakis GZ, Admirand JH, Oyarzo M, Ramalingam P, Paraguya A, et al. MCL-1 expression in B-cell non-Hodgkin's lymphomas. *Hum Pathol*. 2004;35:1095-100.

[7] Sieghart W, Losert D, Strommer S, Cejka D, Schmid K, Rasoul-Rockenschaub S, et al. Mcl-1 overexpression in hepatocellular carcinoma: a potential target for antisense therapy. *J Hepatol*. 2006;44:151-7.

[8] Hussain SR, Cheney CM, Johnson AJ, Lin TS, Grever MR, Caligiuri MA, et al. Mcl-1 is a relevant therapeutic target in acute and chronic lymphoid malignancies: down-regulation enhances rituximab-mediated apoptosis and complement-dependent cytotoxicity. *Clin Cancer Res*. 2007;13:2144-50.

[9] Quinn BA, Dash R, Azab B, Sarkar S, Das SK, Kumar S, et al. Targeting Mcl-1 for the therapy of cancer. *Expert Opin Investig Drugs*. 2011;20:1397-411.

[10] Du Y, Nikolovska-Coleska Z, Qui M, Li L, Lewis I, Dingledine R, et al. A dual-readout F2 assay that combines fluorescence resonance energy transfer and fluorescence polarization for monitoring bimolecular interactions. *Assay Drug Dev Technol*. 2011;9:382-93.

[11] Burke JP, Bian Z, Shaw S, Zhao B, Goodwin CM, Belmar J, et al. Discovery of tricyclic indoles that potently inhibit Mcl-1 using fragment-based methods and structure-based design. *J Med Chem*. 2015;58:3794-805.

[12] Friberg A, Vigil D, Zhao B, Daniels RN, Burke JP, Garcia-Barrantes PM, et al. Discovery of potent myeloid cell leukemia 1 (Mcl-1) inhibitors using fragment-based methods and structure-based design. *J Med Chem*. 2013;56:15-30.

[13] Pelz NF, Bian Z, Zhao B, Shaw S, Tarr JC, Belmar J, et al. Discovery of 2-Indole-acylsulfonamide Myeloid Cell Leukemia 1 (Mcl-1) Inhibitors Using Fragment-Based Methods. *J Med Chem*. 2016;59:2054-66.

[14] Bruncko M, Wang L, Sheppard GS, Phillips DC, Tahir SK, Xue J, et al. Structure-guided design of a series of MCL-1 inhibitors with high affinity and selectivity. *J Med Chem*. 2015;58:2180-94.

[15] Khan M, DiNardo CD. Great expectations in acute myeloid leukemia. *Future Oncol*. 2016;12:289-92.